Table of Contents

Materials

All the amino acids (Gly, L-tryptophan, L-aspartic acid and L-lysine, β-Ala), adenosine 5' monophosphate monohydrate (AMP), adenosine, adenine, adenosine 5' triphosphate (ATP), adenosine 2', 3'-cyclic monophosphate (2',3'-cAMP), 1-ethyl-3-(3-dimethylaminopropyl) carbodiimide hydrochloride (EDC) and magnesium chloride ($MgCl_2$) were procured from Sigma Aldrich. Standard Gly oligopeptide controls [diglycine (Cat No.: G1002); triglycine (Cat No.: G1377); tetraglycine (Cat No.: G3882); pentaglycine (Cat No.: G5755); hexaglycine Cat No.: G5630)], the HPLC buffer salts including sodium perchlorate and tris salts were also procured from Sigma Aldrich. (S)-3-Amino-4-methoxy-oxobutanoic acid, Boc-N-t-Gly and Methyl-Gly, tri-n-butylamine, tri-n-octylamine and Sec-butyl chloroformate obtained from BLD Pharma. 1,4 dioxane and Dichloromethane, DMF was obtained from Finar. Standard AMP oligonucleotide controls including dimer to tetramer of AMP i.e. AMP-AMP, AMP-AMP-AMP, AMP-AMP-AMP-AMP) were custom synthesised from Dharmacon™ siRNA solutions. The LCMS solvents, acetonitrile (ACN) and water, were purchased from J.T.Baker® while N,N-Dimethylformamide (DMF), triethyl amine (TEA) and glacial acetic were obtained from Finar. All reagents were used without further purification.

Methods

A. **Dehydration-Rehydration (DH-RH) reaction setup (with ATP):** In a typical DH-RH reaction mixture of 300 uL volume, ATP/cAMP was added to a final concentration of 25 mM. The amino acids (L-Gly/L-tryptophan/L-aspartic acid/L-lysine) were added to a final concentration of 25 mM or 75 mM (for only Gly). $MgCl_2$ was added to a final concentration of 10 mM in case of all reactions that comprised it. The pH was set to 7 (in all the reactions studied case of Gly and lysine) with 1 M NaOH or 1.5N HCl, as need be. After setting the pH to 7, 0 time point sample (Cycle 0) was taken out. The rest of the reaction mix was transferred to 20 mL glass vials with their caps fitted with PTFE septa purchased from Chemglass. These were placed on a heating block set at elevated temperatures (90°C/ 130°C, depending on the experiment) to simulate early Earth geological conditions (S1). Predetermined time points were taken at 1hr (Cycle 1), 2hrs (Cycle 2), 5hrs (Cycle 5), 10hrs (Cycle 10) and 24hr (Cycle 24), after rehydration the dry sample with pH adjusted Milli Q water (pH 7).

   The overall reactions undertaken were as follows (tabulated in **Table 1**): ATP + Gly + $MgCl_2$ (25 mM:25 mM:10 mM), abbreviated as AGM 90L or AGM 130L, depending on the temperature used (90°C or 130°C). Higher concentration of Gly-based reactions contained ATP + Gly + $MgCl_2$ in 25 mM:75 mM:10 mM concentration, which is abbreviated as AGM 90H or AGM 130H depending on the temperature of the reaction. Reactions without $MgCl_2$ contained ATP + Gly in 25 mM:25 mM concentration, abbreviated AG 90L or AG 130L, and ATP + Gly in 25 mM:75 mM concentration, abbreviated AG 90H or AG 130H. Control reactions contained 25mM and 75mM Gly, with or without $MgCl_2$ and the following variations of the reactions were performed: Gly+ $MgCl_2$ (25 mM:10 mM), abbreviated GM 90L or GM 130L; Gly + $MgCl_2$ (75 mM:10 mM), abbreviated GM 90H or GM 130H; Gly at 25mM, abbreviated G 90L or G 130L and Gly at 75mM, abbreviated G 90H or G 130H (**Table 2**).

Dehydration-Rehydration (DH-RH) reaction setup (with cAMP): In a parallel iteration of the main reaction, the ATP was replaced with cAMP and these reactions contained 25mM of 2'-3' cAMP and 75mM of Gly, which were subjected to wet-dry cycles at elevated temperatures of 90°C and 130°C, at neutral pH conditions (**Table 1**)., abbreviated as cAG 90 or cAG 130, respectively. Control reactions were carried involving 25mM ATP with $MgCl_2$ (abbreviated AM 90 or AM 130) and 25 mM ATP alone (abbreviated A 90 or A 130, **Table 2**). For cAMP-based reactions, a mixture of 25mM 2', 3'-cAMP with 75mM Gly (pH 7) was subjected to wet-dry cycling at 90°C and 130°C (abbreviated cAG90 and cAG130, respectively) (**Table 1**). The control reaction contained just 25 mM 2',3'-cAMP (abbreviated cAMP), which was then subjected to similar conditions as the main reaction setup (**Table 2**).

Dehydration-Rehydration (DH-RH) reaction setup (with AMP-Gly intermediates): Reactions with 10 mM of AMP-Gly (P-N)/ AMP-Gly (P-O-C) with or without 10 mM Gly was subjected to wet-dry cycles at 130°C for 5 hours and time points were taken after rehydration at 0 hr (Cycle 0), 1hr (Cycle 1), 2hrs (Cycle 2) and 5hrs (Cycle 5).

B. Anion Exchange-HPLC analysis: HPLC analysis was carried out using an Agilent Technologies Infinity Series 1260 HPLC instrument. The time points from the DH-RH reaction were loaded onto the HPLC system after filtering them with 0.22µm Costar Spin-X filter centrifugation tubes to separate any solid impurities. Separation of molecules was achieved through the DNAPac PA 200 anion-exchange column from Thermo Scientific. This column separates the molecules based on the column matrix's interaction with the negatively charged phosphate groups. Samples were analyzed using 20 mM Tris, pH 8 (Solvent A) and 400 mM NaClO4 in 20 mM Tris buffer, pH 8 (Solvent B) with a step gradient [0% Solvent B, 3 mins; 30% Solvent B, 10 mins; 100% Solvent B, 13 mins; 100% Solvent B, 16 mins; 0% Solvent B, 18 mins; 0% Solvent B, 21 mins] at a flow rate of 1.2 mL/min. Detection of analytes was carried out at 260 nm using a photo diode-array detector (DAD), using a highly sensitive 60 mm flow cell. A typical HPLC chromatogram revealed the presence of adenine, adenosine, cAMP monomer, linear AMP monomer, ATP, and oligomers. To semi-quantify the analytes, the area under the respective peaks was measured. It is worth noting that while the semi-quantified area could comprise of various species carrying the same charge (for example adenosine 5'-dihosphate and AMP-AMP molecules), it still provided insights into the distribution of species following a specific DH-RH cycle in the reaction.

C. Ion pair exchange HPLC: Ion pair exchange HPLC chromatography was performed on Luna Phenomenex C18 reverse phase column according to the protocol described by Rodriguez-Garcia, M. *et* al[1]. We also spiked the reaction run of AGM 130H Cy24 with purified Gly peptides which were commercially available (Digycine to Hexaglycine) to identify the peptides in the reaction.

D. Liquid Chromatography Mass Spectrometry (LCMS): The mass analysis of the filtered samples was achieved utilizing a Sciex X500R QTOF mass spectrometer (MS), coupled with an Exion-LC series UHPLC system from Sciex. The scanning approach employed was information-dependent acquisition (IDA). The initial reaction mixture was subjected to separation on a Zorbax C8 column [Dimensions: 4.6 × 150 mm, particle size: 3.6 µm] supplied by Agilent

technologies. A gradient of mixture of LCMS grade water containing 0.1% formic acid and acetonitrile containing 0.1% formic acid was employed for the separation of the oligomers. Each run time was of 25 mins with a flow rate of 0.5 ml/mins. For TOF-MS analysis, Electron spray ionization (ESI) was used for all mass acquisitions, using the following specific instrument parameters; ion source gas 1 & 2 was kept at 40 and 50 psi respectively, curtain gas 30 L/min, CAD gas 7 psi, ion spray voltage set at 5500 V (in positive mode) and an operating temperature of 500°C. The acquisition for Time-of-Flight Mass Spectrometry (TOF-MS) was conducted at an 80 V declustering potential, with a spread of 20 V, and a collision energy of 10 V. An internal standard of 1.4 uL (alanine, stock concentration of 20mg/ml) was injected with 6 µl of samples to obtain the relative response of resultant products, which were then summed up to get the overall oligomer yield. All quantitation experiments were performed in at least 6 replicates. Analysis of the acquired data was done using Sciex OS software, from University of Florida. The confirmation of a specific species or molecule's presence involved verifying the precursor mass within a 5-ppm error range. For TOF MS–MS analysis, a collision energy of 50 V with a spread of 20 V was employed. Since mass acquisition was conducted in the positive mode, the observed masses corresponded to the mass of the H+ adduct of the parent molecule. The confirmation of a specific molecule was identified using its signature fragmentation pattern mass within a 20-ppm error range.

For low intensity peaks of compounds, for e.g., AMP tetramer (AMP) 4, Agilent MS Q-TOF Dual AJS ESI (component model, G6545B) was utilized for TOF MS-MS spectra. 10 µl (5nmoles) of filtered samples was subjected to separation on a Phenomenex Luna C18 Column [Dimension: 250 * 4.6 mm, particle size: 5 µm and pore size: 100 Å] with column oven temperature set at 40°C. Mass spectra were acquired in the positive ion polarity using solvents containing gradient mixture of LCMS grade water containing 0.1% formic acid and methanol containing 0.1% formic acid (again, gradient details in brief along with run time and flow rate). For the separation of the oligomers with specific instrument parameters [Gas Temp 320°C, Gas Flow 11 L/min, Nebulizer 45 psig, Sheath Gas Temperature 320°C and Sheath Gas Flow 11] and scanning parameters [VCap 3000, Nozzle Voltage 1000 V, Fragmentor voltage 80 and collision energy formula set with slope 2 and offset of 5] was standardized. For analysis, Agilent Mass Hunter Qualitative analysis software [Version 10.0] was used and molecule specific spectra were acquired using a Find by Formula approach.

D. Chemical synthesis of AMP-Gly linked via a phosphoramidate (P-N) linkage: The AMP-Gly [P-N linkage] was synthesized with a previous protocol [S2]. The mixture was purified using HPLC [Shimadzu HPLC system CBM-20 A, quaternary pump LC-20AD; Shimadzu Corporations, Kyoto, Japan)] and an analytical C18 Phenomenex Luna column (dimension: 250 * 4.6 mm, particle size: 5 µm and pore size: 100 Å) to obtain pure product [**Fig S20**]. Multiple batches of reaction were run and the obtained fractions were then evaporated to acquire pure compound in sufficient amounts for further characterization.

Chemical synthesis of AMP-Gly linked via an anhydride bond (P-O-C) linkage: The protocol for synthesizing the anhydride bond-linked AMP-G was followed as reported in Armstrong, D. W. et al (1977) [S2].

E. HRMS analysis of Methyl-Gly-Amp and Boc-Gly-AMP: Mass analysis was performed using an ESI-MS Waters Synapt G2-Si Mass Spectrometry instrument. HPLC analysis was done using Prominence UFLC Next Generation High-Throughput- Shimadzu HPLC using reverse phase shim-pack GIST C18 column (250 mm × 4.6 mm, 5 µm).

F. NMR analysis of AMP-Gly: NMR samples were prepared by dissolving the compound obtained from the above referenced protocol in deuterium oxide, which was then subjected to ^{1}H analysis for characterizing the AMP-G (P-N) AMP-G (P-O-C) bond, using a 400 MHz Jeol ECS-400 and Bruker AVANCE III HD ASCEND 400 MHz at IISER Pune NMR facility. The corresponding NMR spectra were analysed using Mnova software from Mestrelab [**Fig S20a, b**]. The synthetic standard of AMP-G (P-N) was dissolved in D_2O whereas the AMP-G (P-O-C) was dissolved in $DMSO_{d6}$. The DH-RH reaction runs were dissolved in D_2O before analysis.

G. TOF MS-MS analysis comparison of chemically synthesized AMP-Gly (both P-N and P-O-C linkages) with the TOF MS-MS spectra of AMP-Gly that resulted in the AGM 130°C reaction: For the TOF MS-MS analysis of AMP-Gly with P-N linkage, multiple reaction mode (MRM) approach was employed. The source gas parameters and TOF MS parameters remain similar to the IDA acquisition method outlined in previous section. For TOF MS-MS, 9 groups of fragment ion mass groups were used, which were earlier obtained from IDA acquisition method [97.0020 Da, 136.0600 Da, 158.0400 Da, 193.0000 Da, 238.9500 Da, 256.0300 Da, 284.0600 Da, 284.8500 Da, 405.1000 Da]. After obtaining the fragmentation spectra of chemically synthesized AMP-Gly, we visually matched with the MRM acquired TOF MS-MS spectra of AMP-Gly that resulted in the AGM 130°C reaction.

H. Percentage yield quantification was performed by integrating the area under the curve (AUC) for each product across six independent replicates. For each replicate, the analyte-to-internal standard (Analyte/IS) ratio was calculated using the corresponding AUC values, and this ratio was multiplied by 100 to obtain the percentage yield and averaged value was obtained. The resulting dataset was then used to construct the heat map representation.

I. ^{31}P NMR acquisition: Dissolved the samples in deuterated water. Set the VT unit to 0 °C and equilibrate 10–15 min before inserting the sample. Tune/match the ^{31}P, lock, and shim. Acquire ^{1}H-decoupled ^{31}P NMR using WALTZ-16 decoupling, a 30° pulse, 2–5 s relaxation delay, 32–128 scans, and ~400 ppm spectral width — JEOL ECS-400 (Delta, *single_pulse_dec*) or Bruker AVANCE III HD ASCEND (TopSpin, *zgpg30*). Process with 1–5 Hz line broadening and reference to H_3PO_4 at 0.00 ppm. The corresponding NMR spectra were analysed using Mnova software from Mestrelab.

Supplementary Table S1: Reactions performed with their concentration and abbreviations:

Reaction No.	Nucleotide	Amino acid	$MgCl_2$	Temperature	Abbreviations
1	ATP	Gly (25 mM)	+	90 °C	AGM 90L
2	ATP	Gly (75 mM)	+	90 °C	AGM 90H
3	ATP	Gly (25 mM)	+	130 °C	AGM 130L
4	ATP	Gly (75 mM)	+	130 °C	AGM 130H
5	ATP	Gly (25 mM)	-	90 °C	AG 90L
6	ATP	Gly (75 mM)	-	90 °C	AG 90H
7	ATP	Gly (25 mM)	-	130 °C	AG 130L
8	ATP	Gly (75 mM)	-	130 °C	AG 130H
9	2',3'-cAMP	Gly (75 mM)	-	90 °C	cAG 90
10	2',3'-cAMP	Gly (75 mM)	-	130 °C	cAG 130
11	ATP	Lys (25 mM)	+	90 °C	AKM 90
12	ATP	Lys (25 mM)	+	130 °C	AKM 130
13	ATP	Lys (25 mM)	-	90 °C	AK 90
14	ATP	Lys (25 mM)	-	130 °C	AK 130
15	ATP	Asp (25 mM)	+	90 °C	ADM 90
16	ATP	Asp (25 mM)	+	130 °C	ADM 130
17	ATP	Trp (25 mM)	+	90 °C	AWM 90
18	ATP	Trp (25 mM)	+	130 °C	AWM 130
19	ATP	β-alanine (75 mM)	+	90 °C	AAM 90
20	ATP	β-alanine (75 mM)	+	130 °C	AAM 130
21	ATP	(S)-3-Amino-4-methoxy-oxobutanoic acid (25 mM)	+	90 °C	ABM 90
22	ATP	(S)-3-Amino-4-methoxy-oxobutanoic acid (25 mM)	+	130 °C	ABM 130

Supplementary Table S1: Reaction experiments performed with the starting reactants and reaction parameters. The nucleotides used were either ATP or 2',3' cAMP. The concentration of all nucleotides used was kept constant at 25 mM. The different amino acids used, along with their respective concentrations within brackets, are denoted. The concentration of $MgCl_2$, wherever used, was kept constant at 10 mM. The two temperatures evaluated were 90°C or 130°C. The abbreviations used correspond to the specific reactions conducted and has been kept constant throughout the article.

Supplementary Table S2: Details of the various control experiments conducted with concentrations and abbreviations

Reaction No.	Nucleotide	Amino acid	$MgCl_2$	Temperature	Abbreviations
1	ATP	-	+	90 °C	AM 90
2	ATP	-	-	90 °C	A 90
3	ATP	-	-	130 °C	AM 130
4	ATP	-	-	130 °C	A 130
5	-	Gly (25 mM)	+	90 °C	GM 90L
6	-	Gly (25 mM)	-	90 °C	G 90L
7	-	Gly (75 mM)	+	90 °C	GM 90H
8	-	Gly (75 mM)	-	90 °C	G 90H
9	-	Gly (25 mM)	+	130 °C	GM 130L
10	-	Gly (25 mM)	-	130 °C	G 130L
11	-	Gly (75 mM)	+	130 °C	GM 130H
12	-	Gly (75 mM)	-	130 °C	G 130H
13	2',3'-cAMP	-	-	90 °C	cAMP 90
14	2',3'-cAMP	-	-	130 °C	cAMP 130
15	-	Lys (25 mM)	-	130 °C	K 130
16	-	Asp (25 mM)	-	130 °C	D 130
17	-	Trp (25 mM)	-	130 °C	W 130

Supplementary Table S2: Details of the various control experiments performed along with the starting reactants and reaction parameters used. The nucleotides used were either ATP or 2',3' cAMP. The concentration of all the nucleotides used was kept constant at 25 mM. The different amino acids used, along with their respective concentrations within brackets, are denoted. The concentration of MgCl2, wherever used, was kept constant at 10 mM. The temperatures used are 90°C or 130°C. The abbreviations mentioned corresponds to the specific reactions that were conducted, which has been kept constant throughout the article.

Different amino acids and nucleotides that were used in the study.

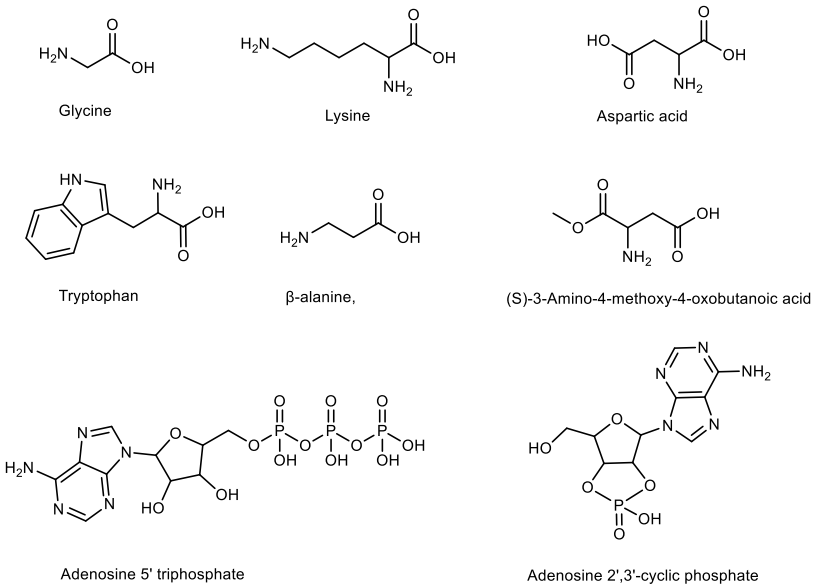

Figure S1: Different amino acids and nucleotides that were used in the study. The structures were derived using ChemDraw Version 21.0.0.

TOF MS-MS spectra of various control Gly peptides

a.

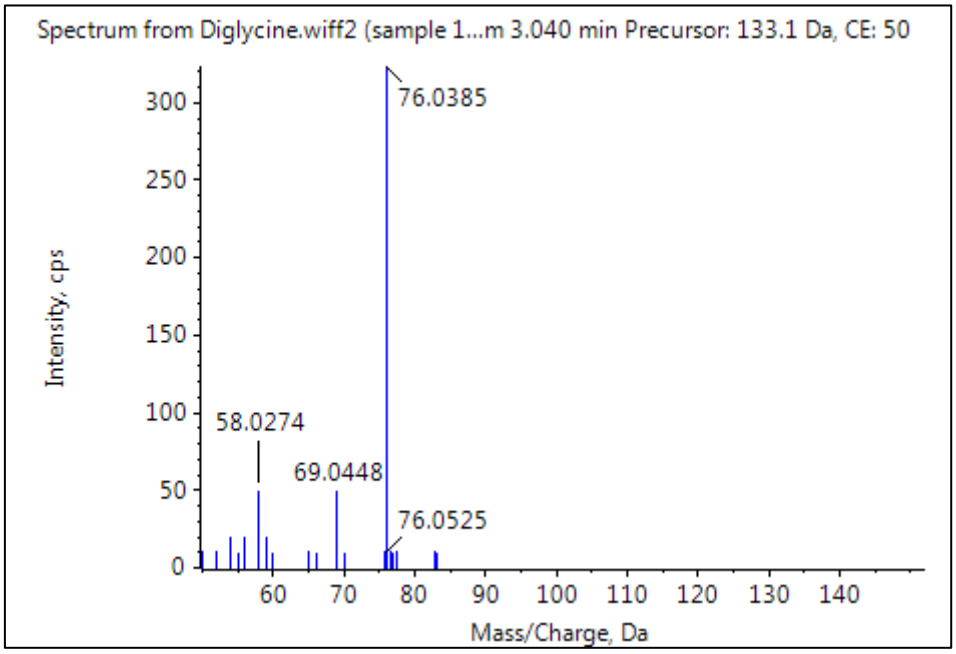

b.

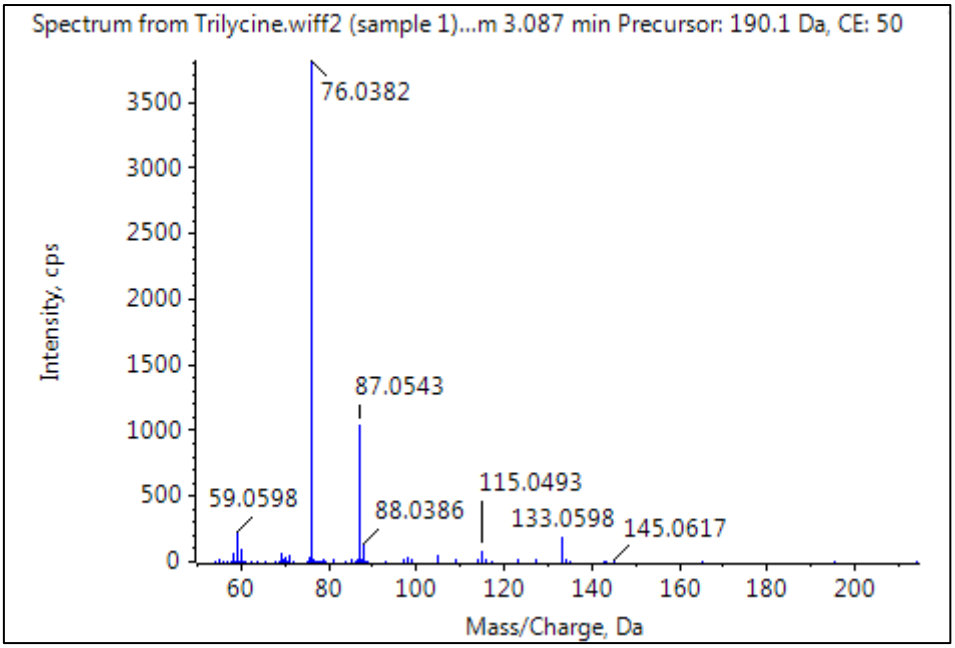
Spectrum from Trilycine.wiff2 (sample 1)...m 3.087 min Precursor: 190.1 Da, CE: 50
Intensity, cps
Mass/Charge, Da
76.0382
87.0543
59.0598
88.0386
115.0493
133.0598
145.0617
0
500
1000
1500
2000
2500
3000
3500
60
80
100
120
140
160
180
200

c.

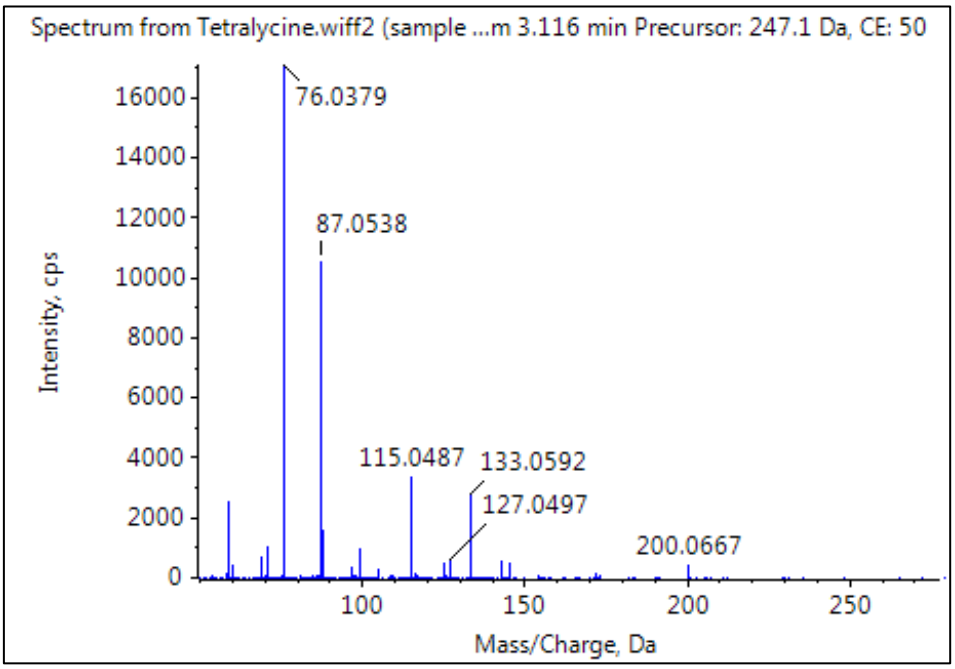
Spectrum from Tetralycine.wiff2 (sample ...m 3.116 min Precursor: 247.1 Da, CE: 50
Intensity, cps
Mass/Charge, Da
76.0379
87.0538
115.0487
133.0592
127.0497
200.0667
0
2000
4000
6000
8000
10000
12000
14000
16000
100
150
200
250

d.

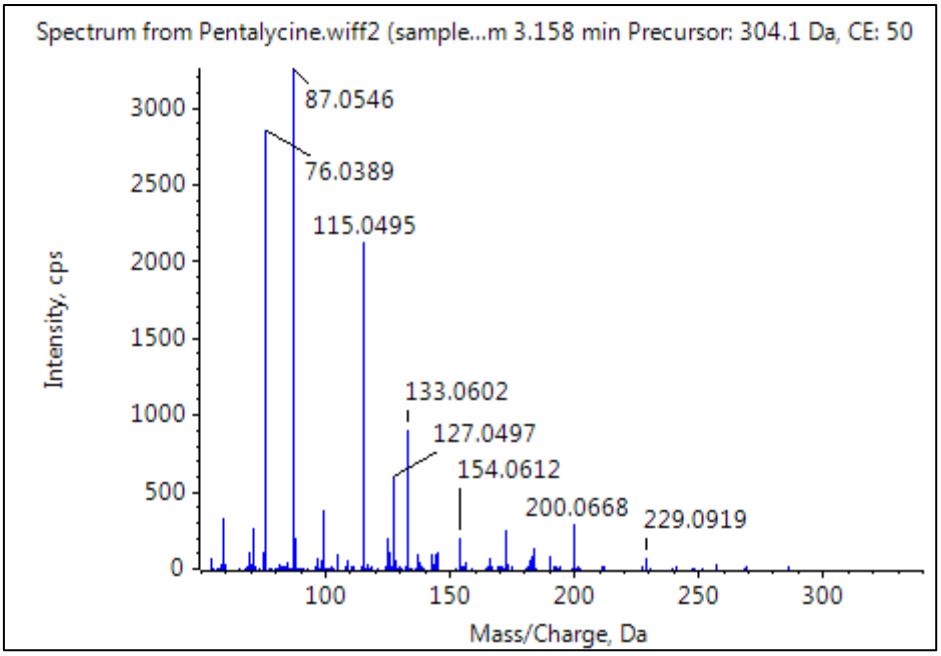

e.

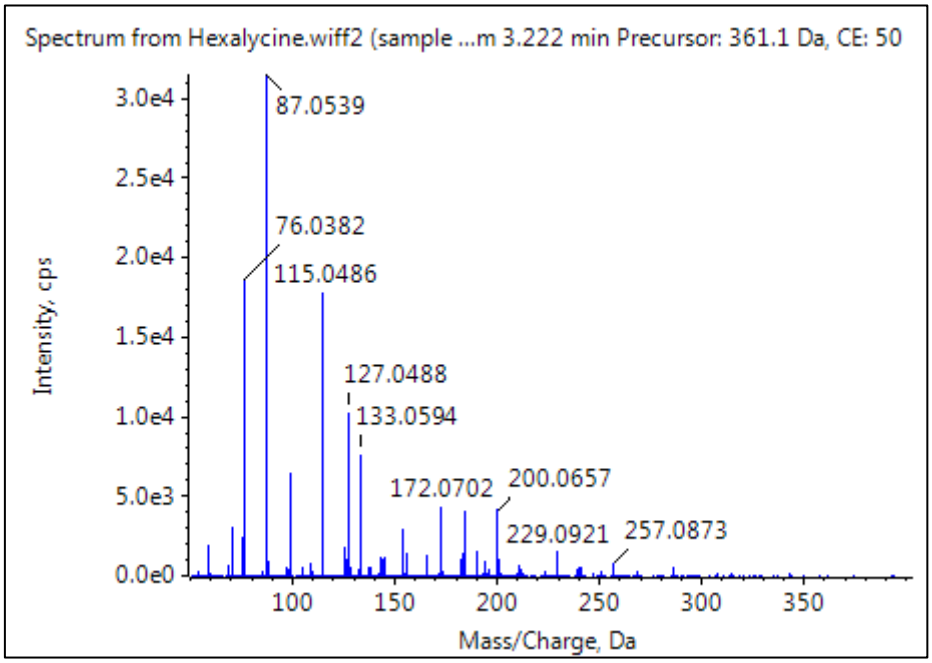

Figure S2: TOF MS-MS fragmentation spectra of purified control Gly peptides **a. Diglycine** [Precursor mass: 133.0608 (M+H)+], **b. Triglycine** [Precursor mass: 190.0823 (M+H)+], **c. Tetraglycine** [Precursor mass: 247.1037 (M+H)+], **d. Pentaglycine** [Precursor mass: 304.1252 (M+H)+], **e. Hexaglycine** [Precursor mass: 361.1467 (M+H)+]. CE used was 50 eV.

TOF MS-MS spectra of Gly peptides obtained in the reactions

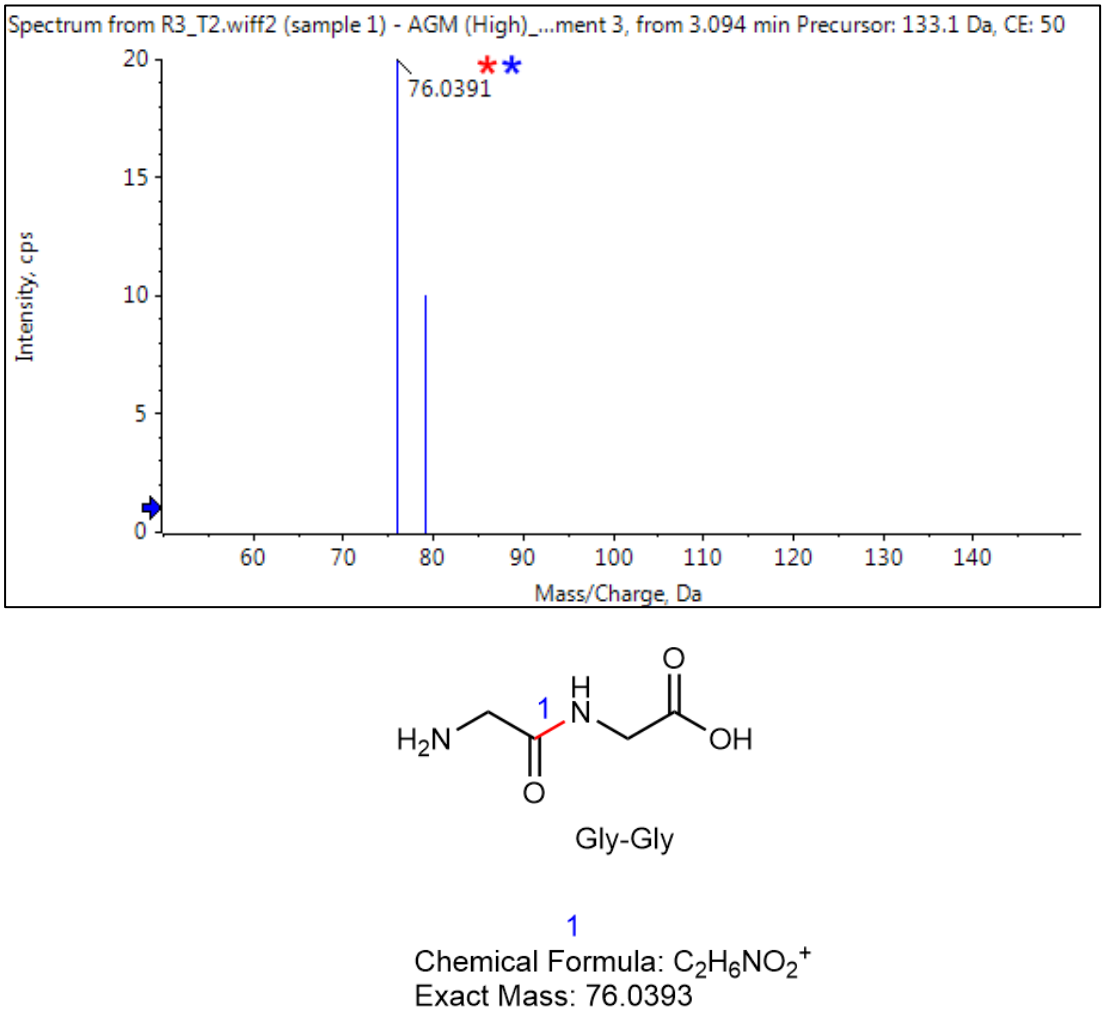

Figure S3a: TOF MS-MS spectra and fragmentation pattern of diglycine [Precursor mass: 133.0608 (M+H)+] formed in the AGM and AG reaction. Expected masses corresponding to the fragmented ions of diglycine are observed in the spectra. Experimental data matches with the predicted fragmentation pattern of Gly-Gly sequence. The theoretically calculated masses and structures of molecules obtained post fragmentation were derived using ChemDraw Version 21.0.0. The fragmented bonds are highlighted in red. CE used was 50 eV. The red asterisk denotes the observed masses within 20 ppm error of the calculated fragmented mass. The blue asterisk denotes the observed masses within 20 ppm error of the observed fragmented masses from the control runs.

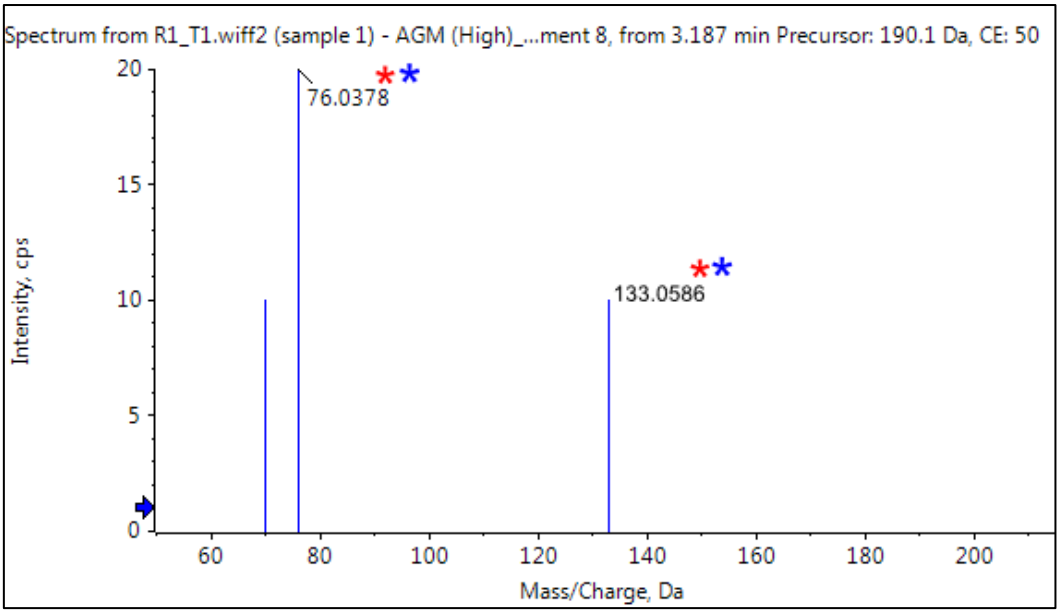

Figure S3b: TOF MS-MS spectra and fragmentation pattern of triglycine [Precursor mass: 190.0823 (M+H)+] formed in the AGM and AG reaction. Expected masses corresponding to the fragmented ions of triglycine are observed in the spectra. Experimental data matches with the predicted fragmentation pattern of Gly-Gly-Gly sequence. The theoretically calculated masses and structures of molecules obtained post fragmentation were derived using ChemDraw Version 21.0.0. The fragmented bonds are highlighted in red. CE used was 50 eV. The red asterisk denotes the observed masses within 20 ppm error of the calculated fragmented mass. The blue asterisk denotes the observed masses within 20 ppm error of the observed fragmented masses from the control runs.

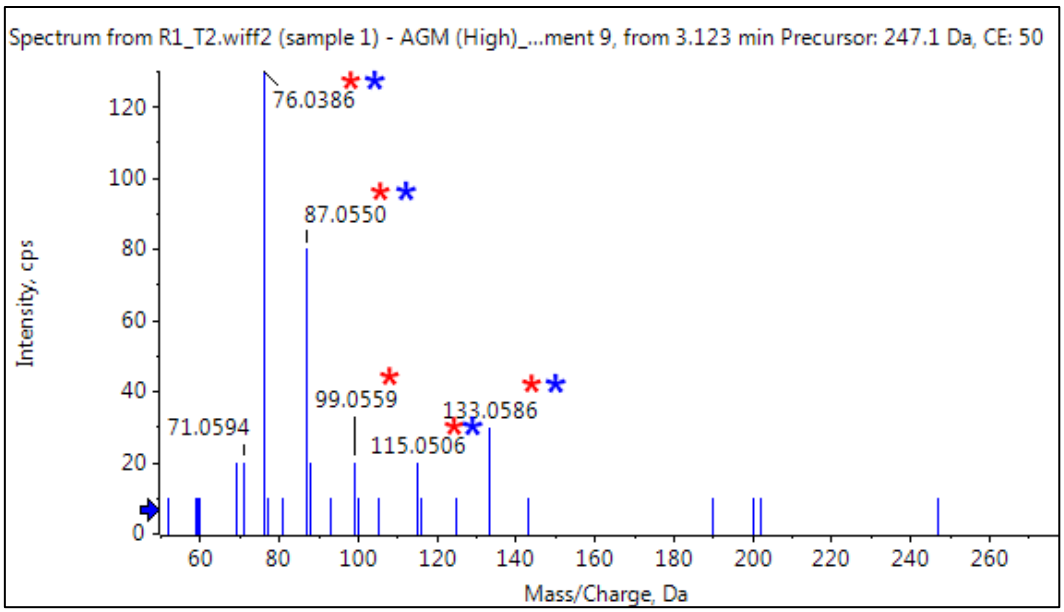

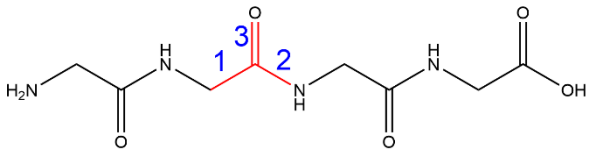

Gly-Gly-Gly-Gly

1	2	2 & 3
Chemical Formula: $C_3H_7N_2O^{\bullet}$	Chemical Formula: $C_4H_7N_2O_2^{\bullet}$	Chemical Formula: $C_4H_7N_2O^{\bullet 2+}$
Exact Mass: 87.0558	Exact Mass: 115.0508	Exact Mass: 99.0547

Figure S3c: TOF MS-MS spectra and fragmentation pattern of tetraglycine [Precursor mass: 247.1037 (M+H)+] formed in the AGM and AG reaction. Expected masses corresponding to the fragmented ions of tetraglycine are observed in the spectra. Experimental data matches with the predicted fragmentation pattern of Gly-Gly-Gly-Gly sequence. The theoretically calculated masses and structures of molecules obtained post fragmentation were derived using ChemDraw Version 21.0.0. The fragmented bonds are highlighted in red. The fragmented masses which have appeared in earlier images have not been shown for the sake of brevity. CE used was 50 eV. The red asterisk denotes the observed masses within 20 ppm error of the calculated fragmented mass. The blue asterisk denotes the observed masses within 20 ppm error of the observed fragmented masses from the control runs.

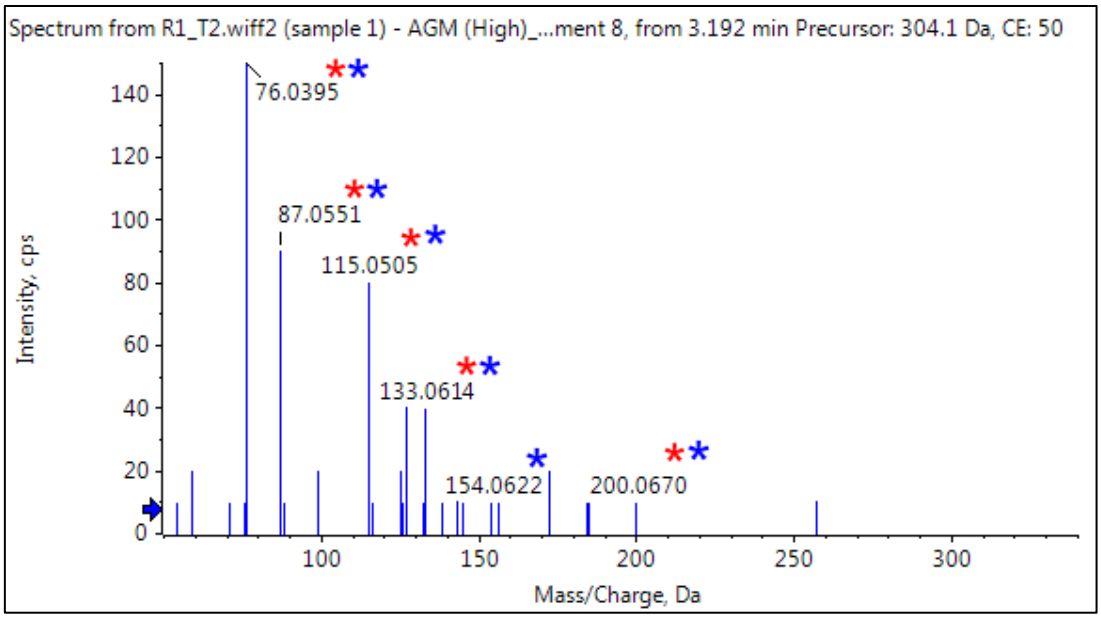

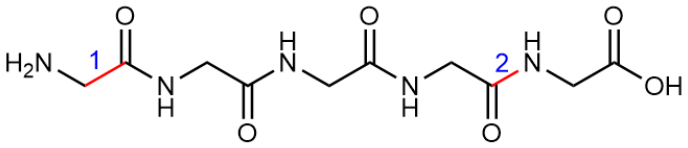

Gly-Gly-Gly-Gly-Gly

1 & 2

Chemical Formula: $C_7H_{10}N_3O_4^{\bullet}$
Exact Mass: 200.0671

Figure S3d: TOF MS-MS spectra and fragmentation pattern of pentaglycine [Precursor mass: 304.1252 (M+H)+(M+H)+] formed in the AGM and AG reaction. Expected masses corresponding to the fragmented ions of pentaglycine are observed in the spectra. Experimental data matches with the predicted fragmentation pattern of Gly-Gly-Gly-Gly-Gly sequence. The theoretically calculated masses and structures of molecules obtained post fragmentation were derived using ChemDraw Version 21.0.0. The fragmented bonds are highlighted in red. The fragmented masses which have appeared in earlier images have not been shown for the sake of brevity. CE used was 50 eV. The red asterisk denotes the observed masses within 20 ppm error of the calculated fragmented mass. The blue asterisk denotes the observed masses within 20 ppm error of the observed fragmented masses from the control runs.

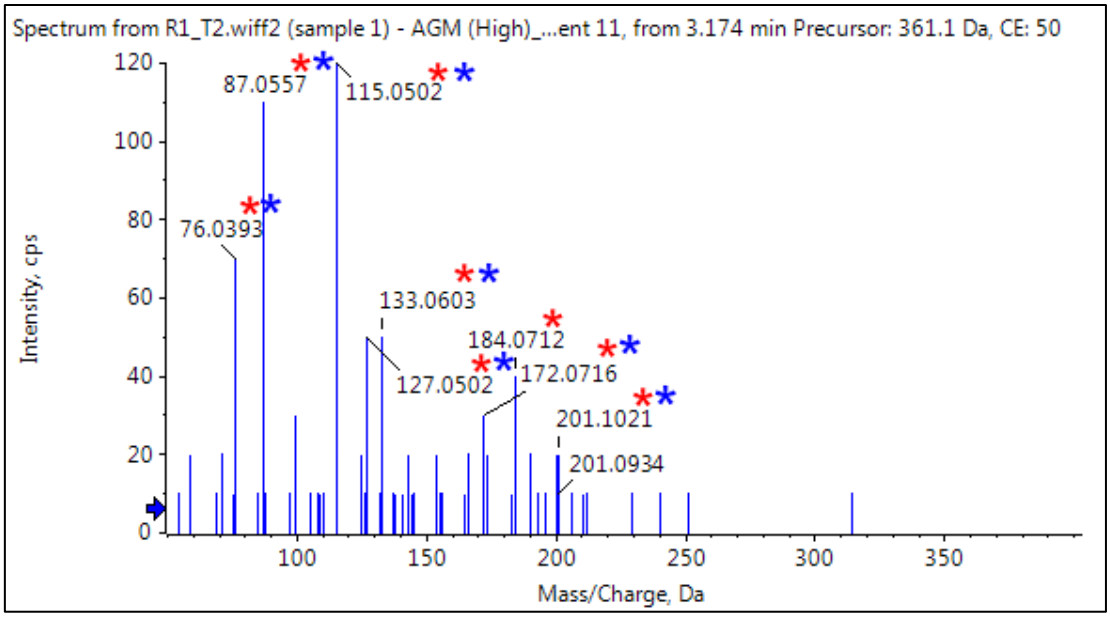

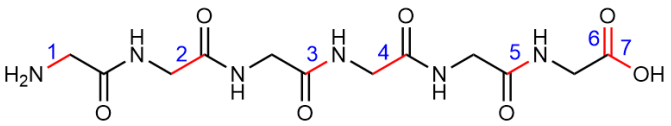

Gly-Gly-Gly-Gly-Gly-Gly

1 & 4
Chemical Formula: $C_7H_{10}N_3O_{32}^{\bullet+}$
Exact Mass: 184.0717

3
Chemical Formula: $C_6H_{10}N_3O_3^{\bullet}$
Exact Mass: 172.0722

2 & 5
Chemical Formula: $C_7H_{11}N_3O_4$
Exact Mass: 201.0750

4, 6 & 7
Chemical Formula: $C_5H_7N_2O_{22}^{\bullet+}$
Exact Mass: 127.0502

Figure S3e: TOF MS-MS spectra and fragmentation pattern of hexaglycine [Precursor mass: 361.1467 (M+H)+] formed in the AGM and AG reaction. Expected masses corresponding to the fragmented ions of hexaglycine are observed in the spectra. Experimental data matches with the predicted fragmentation pattern of Gly-Gly-Gly-Gly-Gly-Gly sequence. The theoretically calculated masses and structures of molecules obtained post fragmentation were derived using ChemDraw Version 21.0.0. The fragmented bonds are highlighted in red. The fragmented masses which have appeared in earlier images have not been shown for the sake of brevity. CE used was 50 eV. The red asterisk denotes the observed masses within 20 ppm error of the calculated fragmented mass. The blue asterisk denotes the observed masses within 20 ppm error of the observed fragmented masses from the control runs.

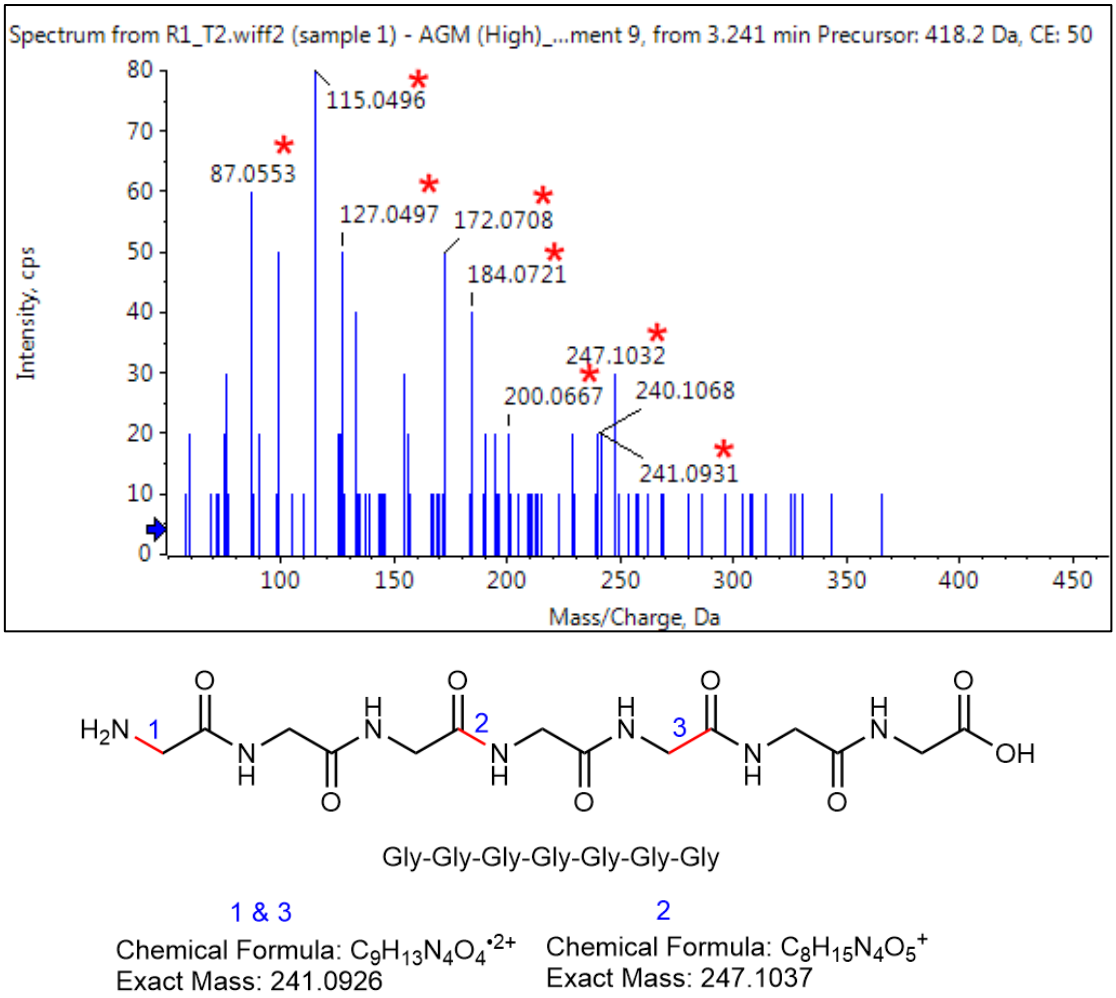

Figure S3f: TOF MS-MS spectra and fragmentation pattern of heptaglycine [Precursor mass: 418.1681 (M+H)+] formed in the AGM and AG reaction. Expected masses corresponding to the fragmented ions of Heptaglycine are observed in the spectra. Experimental data matches with the predicted fragmentation pattern of Gly-Gly-Gly-Gly-Gly-Gly-Gly sequence. The theoretically calculated masses and structures of molecules obtained post fragmentation were derived using ChemDraw Version 21.0.0. The fragmented bonds are highlighted in red. The fragmented masses which have appeared in earlier images have not been shown for the sake of brevity. CE used was 50 eV. The red asterisk denotes the observed masses within 20 ppm error of the calculated fragmented mass.

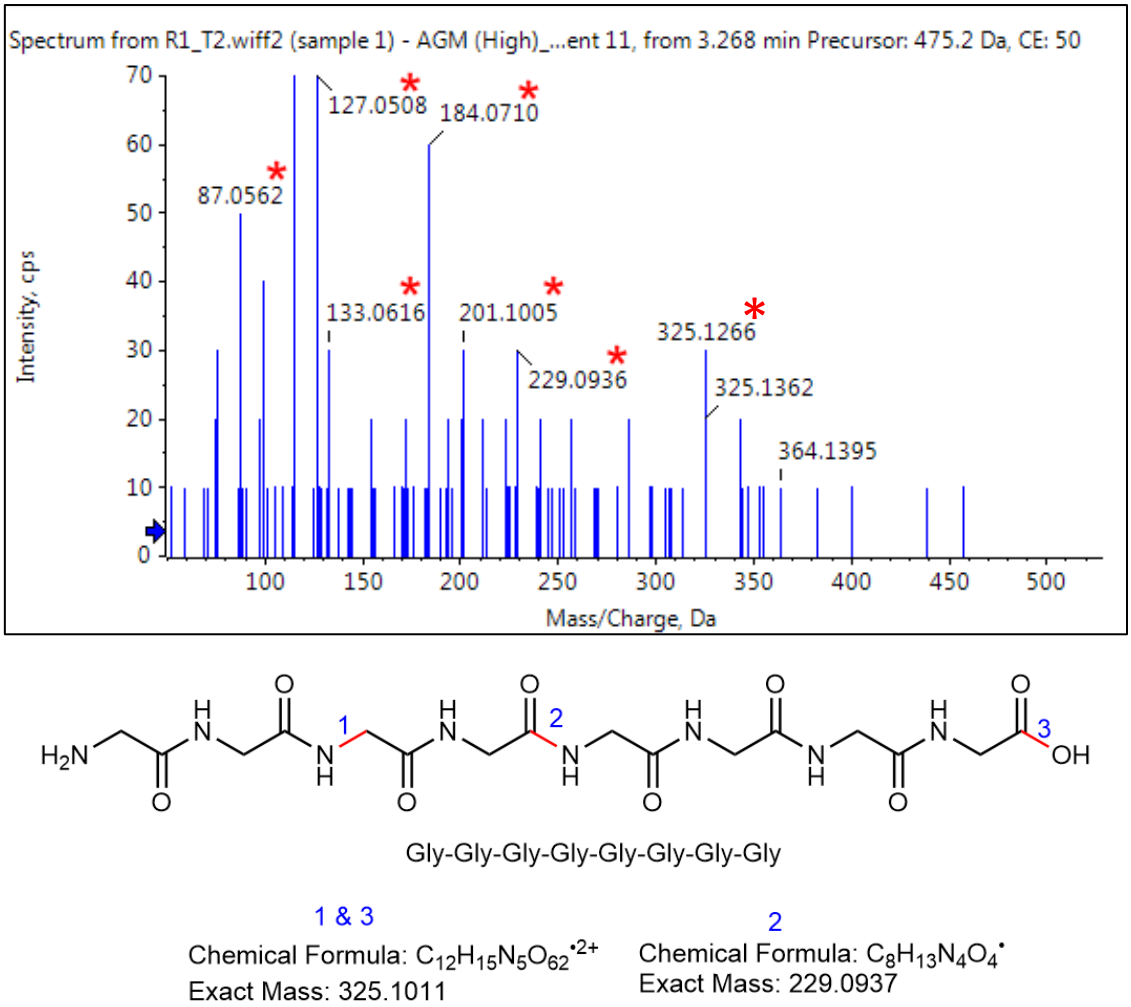

Figure S3g: TOF MS-MS spectra and fragmentation pattern of octaglycine [Precursor mass: 475.1896 (M+H)+] formed in the AGM and AG reaction. Expected masses corresponding to the fragmented ions of octaglycine are observed in the spectra. Experimental data matches with the predicted fragmentation pattern of Gly-Gly-Gly-Gly-Gly-Gly-Gly-Gly sequence. The theoretically calculated masses and structures of molecules obtained post fragmentation were derived using ChemDraw Version 21.0.0. The fragmented bonds are highlighted in red. The fragmented masses which have appeared in earlier images have not been shown for the sake of brevity. CE used was 50 eV. The red asterisk denotes the observed masses within 20 ppm error of the calculated fragmented mass.

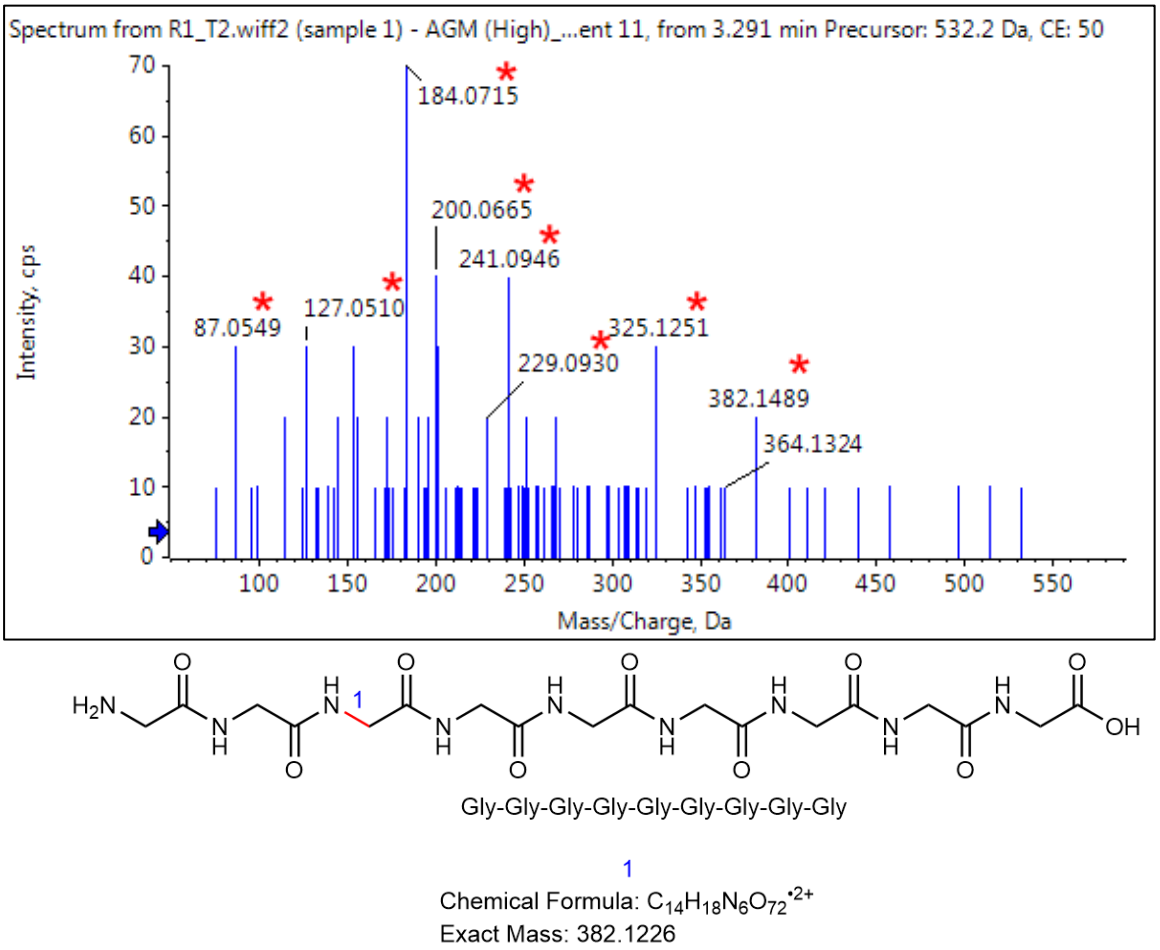

Figure S3h: TOF MS-MS spectra and fragmentation pattern of nonaglycine [Precursor mass: 532.2111 (M+H)+] formed in the AGM and AG reaction. Expected masses corresponding to the fragmented ions of nonaglycine are observed in the spectra. Experimental data matches with the predicted fragmentation pattern of Gly-Gly-Gly-Gly-Gly-Gly-Gly-Gly-Gly sequence The theoretically calculated masses and structures of molecules obtained post fragmentation were derived using ChemDraw Version 21.0.0. The fragmented bonds are highlighted in red. The fragmented masses which have appeared in earlier images have not been shown for the sake of brevity. CE used was 50 eV. The red asterisk denotes the observed masses within 20 ppm error of the calculated fragmented mass.

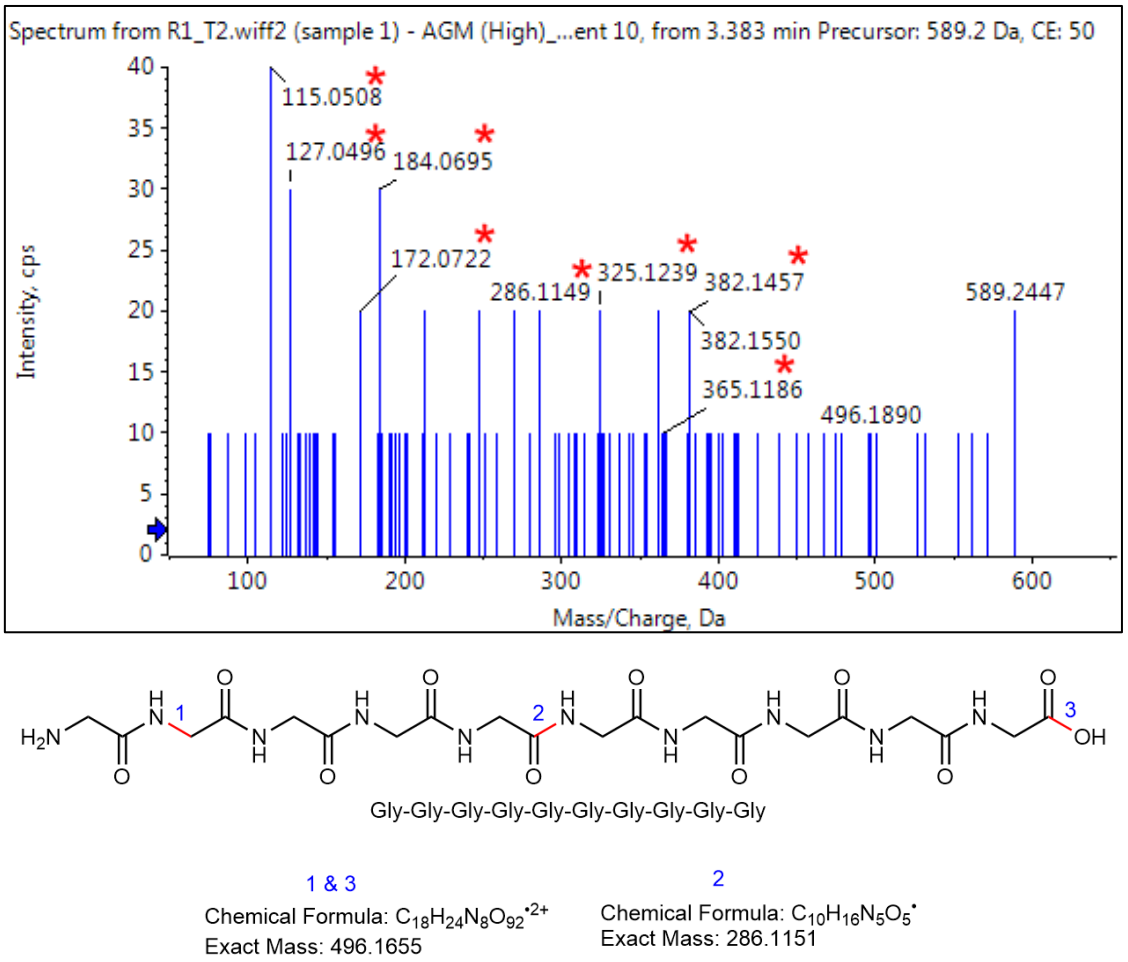

Figure S3i: TOF MS-MS spectra and fragmentation pattern of decaglycine [Precursor mass: 589.2325 (M+H)+] formed in the AGM and AG reactions. Expected masses corresponding to the fragmented ions of decaglycine are observed in the spectra. Experimental data matches with the predicted fragmentation pattern of Gly-Gly-Gly-Gly-Gly-Gly-Gly-Gly-Gly-Gly sequence. The theoretically calculated masses and structures of molecules obtained post fragmentation were derived using ChemDraw Version 21.0.0. The fragmented bonds are highlighted in red. The fragmented masses which have appeared in earlier images have not been shown for the sake of brevity. CE used was 50 eV. The red asterisk denotes the observed masses within 20 ppm error of the calculated fragmented mass.

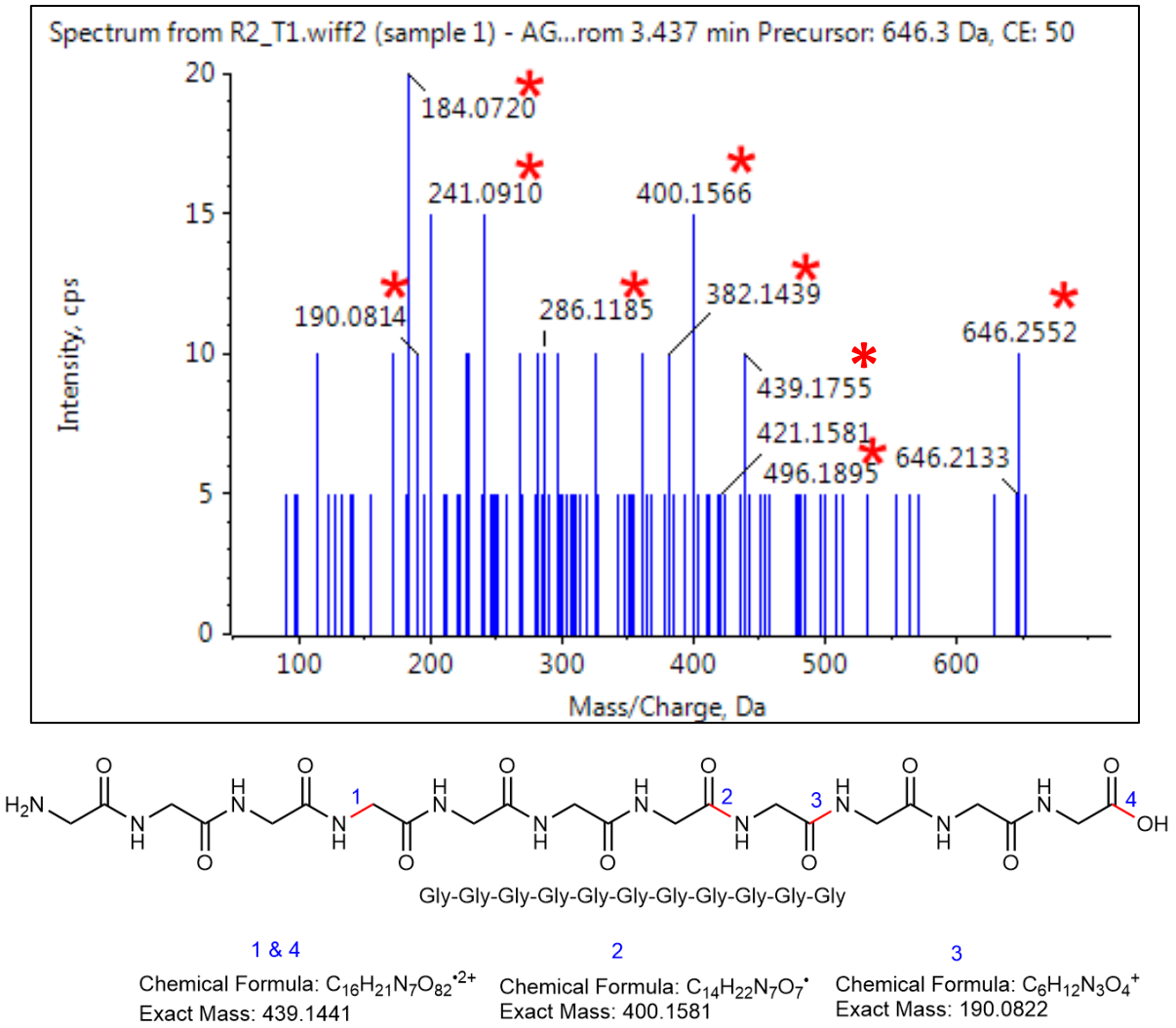

Figure S3j: TOF MS-MS spectra and fragmentation pattern of undecaglycine [Precursor mass: 646.2540 (M+H)+] formed in the AGM and AG reactions. Expected masses corresponding to the fragmented ions of undecaglycine are observed in the spectra. Experimental data matches with the predicted fragmentation pattern of Gly-Gly-Gly-Gly-Gly-Gly-Gly-Gly-Gly-Gly-Gly sequence. The theoretically calculated masses and structures of molecules obtained post fragmentation were derived using ChemDraw Version 21.0.0. The fragmented bonds are highlighted in red. The fragmented masses which have appeared in earlier images have not been shown for the sake of brevity. CE used was 50 eV. The red asterisk denotes the observed masses within 20 ppm error of the calculated fragmented mass.

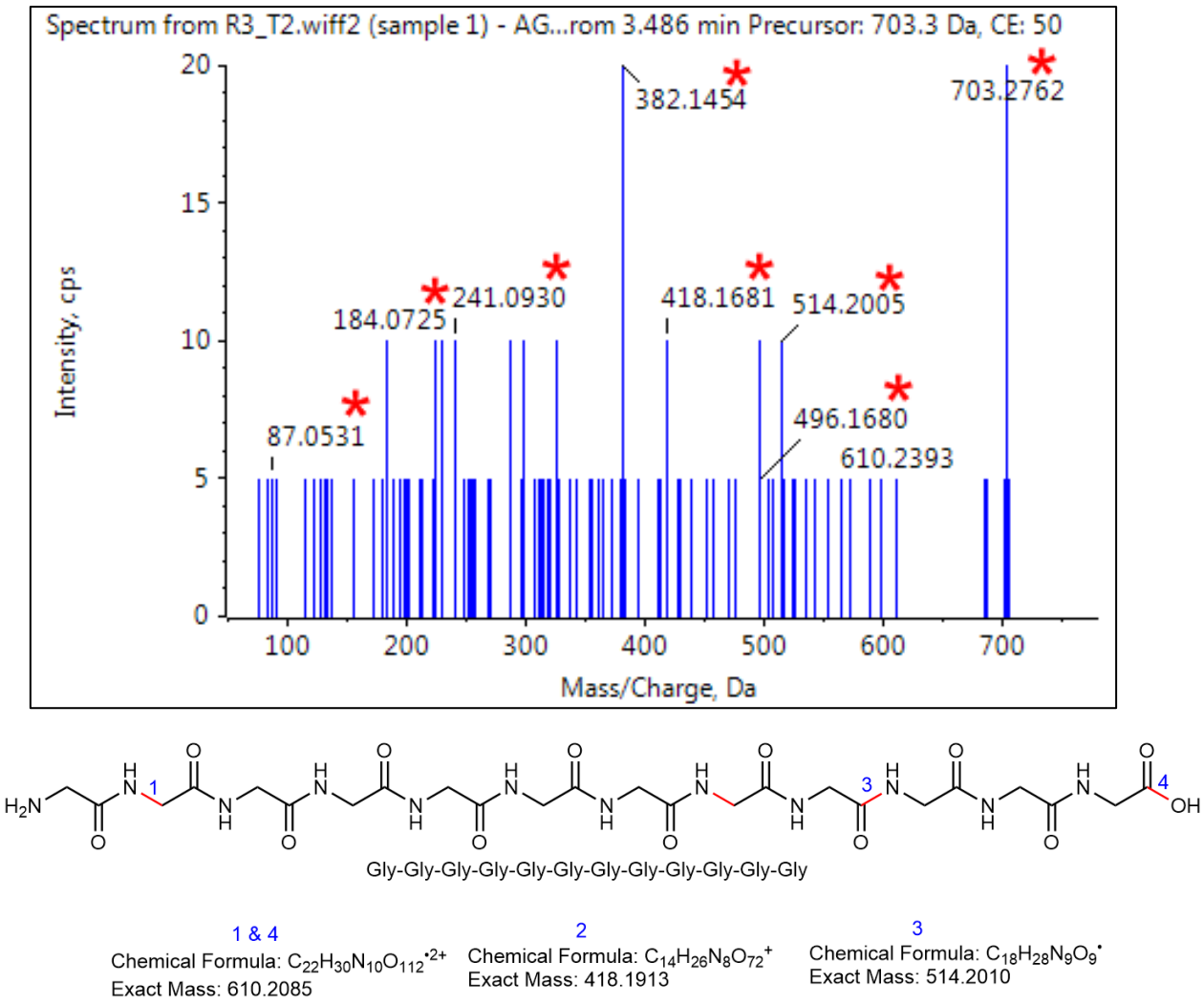

Figure S3k: TOF MS-MS spectra and fragmentation pattern of dodecaglycine [Precursor mass: 703.2755 (M+H)+] formed in the AGM and AG reactions. Expected masses corresponding to the fragmented ions of dodecaglycine are observed in the spectra. Experimental data matches with the predicted fragmentation pattern of Gly-Gly-Gly-Gly-Gly-Gly-Gly-Gly-Gly-Gly-Gly-Gly sequence. The theoretically calculated masses and structures of molecules obtained post fragmentation were derived using ChemDraw Version 21.0.0. The fragmented bonds are highlighted in red. The fragmented masses which have appeared in earlier images have not been shown for the sake of brevity. CE used was 50 eV. The red asterisk denotes the observed masses within 20 ppm error of the calculated fragmented mass.

TOF MS spectra and TOF MS-MS spectra obtained for peptides in AGM and G-based reactions

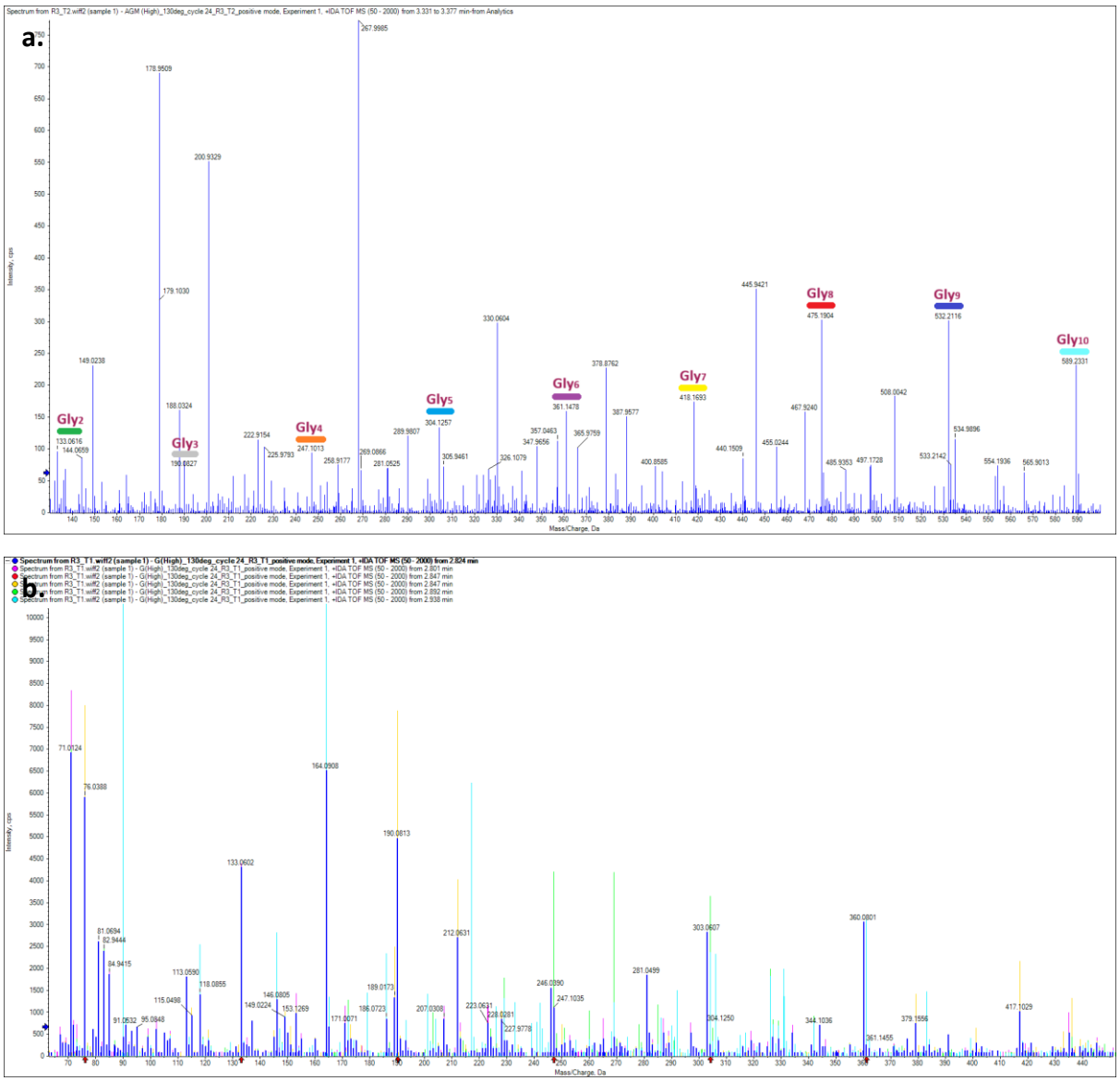

Figure S4a: TOF MS spectra of AGM 130H reaction at cycle 24. The spectra shows the masses for diglycine [Precursor mass: 133.0608 (M+H)+], triglycine [Precursor mass: 190.0823 (M+H)+], tetraglycine [Precursor mass: 247.1037 (M+H)+], of pentaglycine [Precursor mass: 304.1252 (M+H)+], hexaglycine [Precursor mass: 361.1467 (M+H)+], heptaglycine [Precursor mass: 418.1681 (M+H)+], octaglycine [Precursor mass: 475.1896 (M+H)+], nonaglycine [Precursor mass: 532.2111 (M+H)+] and decaglycine [Precursor mass: 589.2325 (M+H)+]. **b.** TOF MS spectra of G 130H reaction at cycle 24. The spectra shows the masses for diglycine [Precursor mass: 133.0608 (M+H)+], triglycine [Precursor mass: 190.0823 (M+H)+], tetraglycine [Precursor mass: 247.1037 (M+H)+], of pentaglycine [Precursor mass: 304.1252 (M+H)+] and hexaglycine [Precursor mass: 361.1467 (M+H)+].

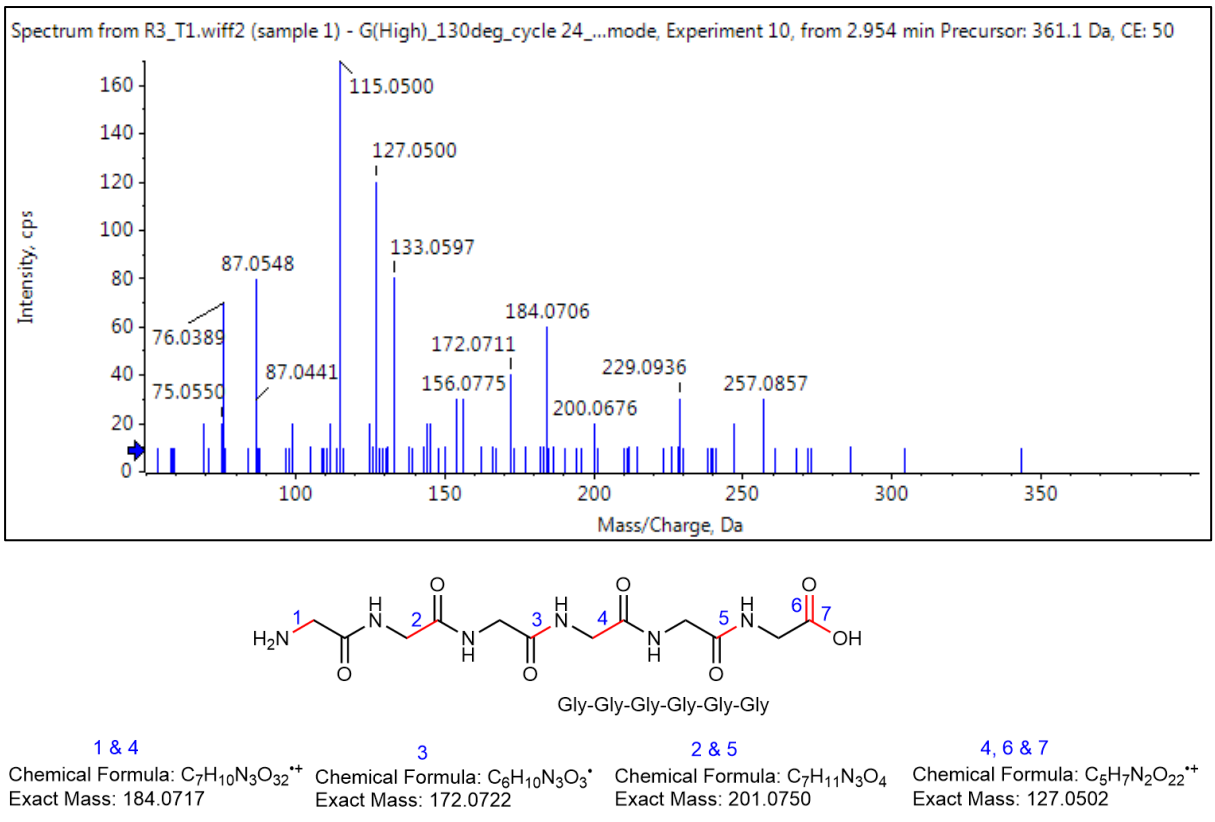

Figure S4c: TOF MS-MS spectra and fragmentation pattern of hexaglycine [Precursor mass: 361.1467 (M+H)+] formed in the G 130H reaction. Expected masses corresponding to the fragmented ions of hexaglycine are observed in the spectra. Experimental data matches with the predicted fragmentation pattern of Gly-Gly-Gly-Gly-Gly-Gly sequence. The theoretically calculated masses and structures of molecules obtained post fragmentation were derived using ChemDraw Version 21.0.0. CE used was 50 eV.

Longest peptide observed across various reactions

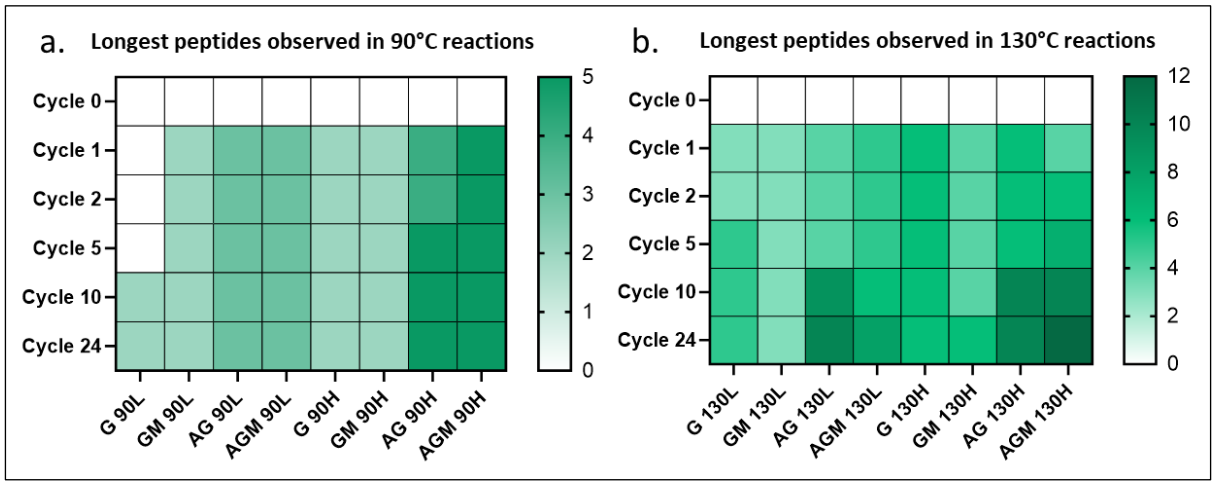

Figure S5: Heat map representation of formation of glycine oligomers under wet–dry cycling conditions demonstrating the effect of two temperature conditions (90 °C and 130 °C) at 25 mM and 75 mM glycine concentrations across multiple reaction cycles. (a) Longest glycine peptides observed in reactions performed at 90 °C. (b) Longest glycine peptides observed in reactions performed at 130 °C.

HPLC chromatograms of AGM-based reactions

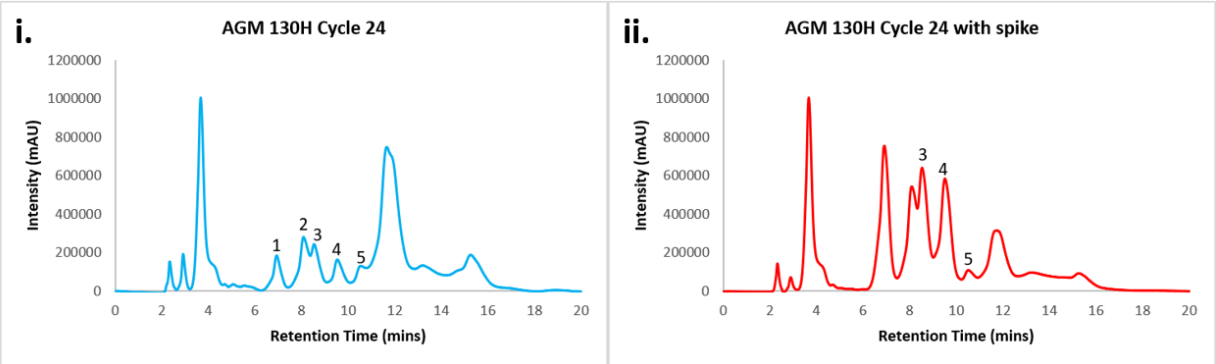

Figure S6 i-ii: HPLC chromatograms obtained from ion pair exchange chromatogram in reverse phase column (C18) for identification of peptides. **a.** HPLC chromatogram of AGM 130H Cycle 24. **b.** HPLC chromatogram of AGM 130H cycle 24 with spiking of purified controls. the chromatograms shown above, the following glycine oligomers were identified by spiking: diglycine (1), triglycine (2), tetraglycine (3), pentaglycine (4), and hexaglycine (5). As noted previously, heptaglycine and higher glycine oligomers co-elute with AMP, adenosine, and other compounds at retention times greater than approximately 11 minutes. Consequently, these higher oligomers cannot be resolved using the present chromatographic method. This is evident in the first chromatogram, where the hexaglycine peak, particularly at lower concentrations, nearly co-elutes with the AMP peak observed at approximately 12 minutes.

a.

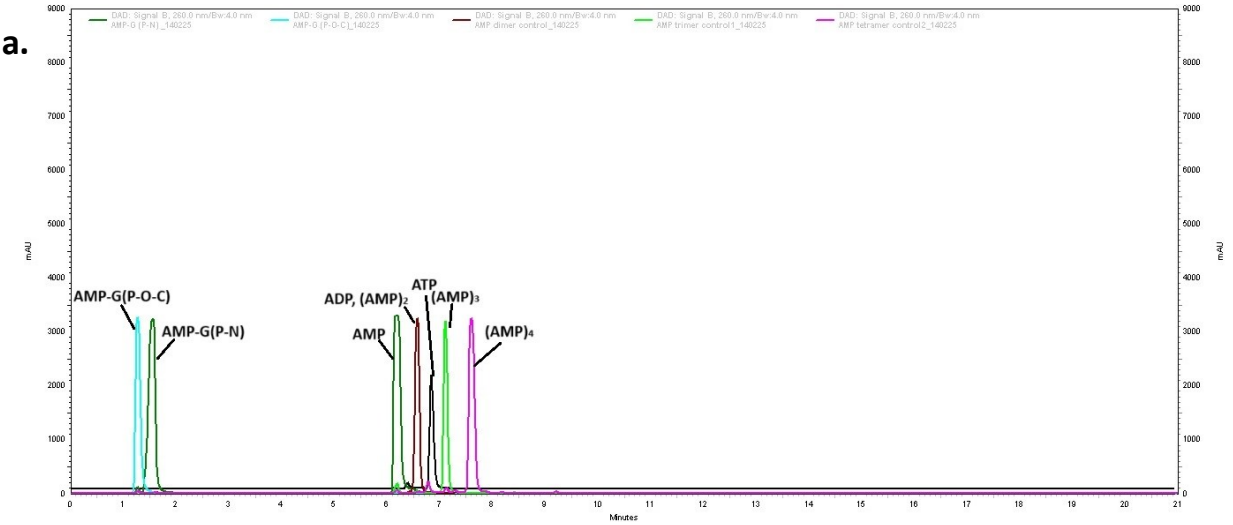
AMP-G(P-O-C)
AMP-G(P-N)
AMP
ADP, (AMP)2
ATP
(AMP)3
(AMP)4
mAU
Minutes

b.

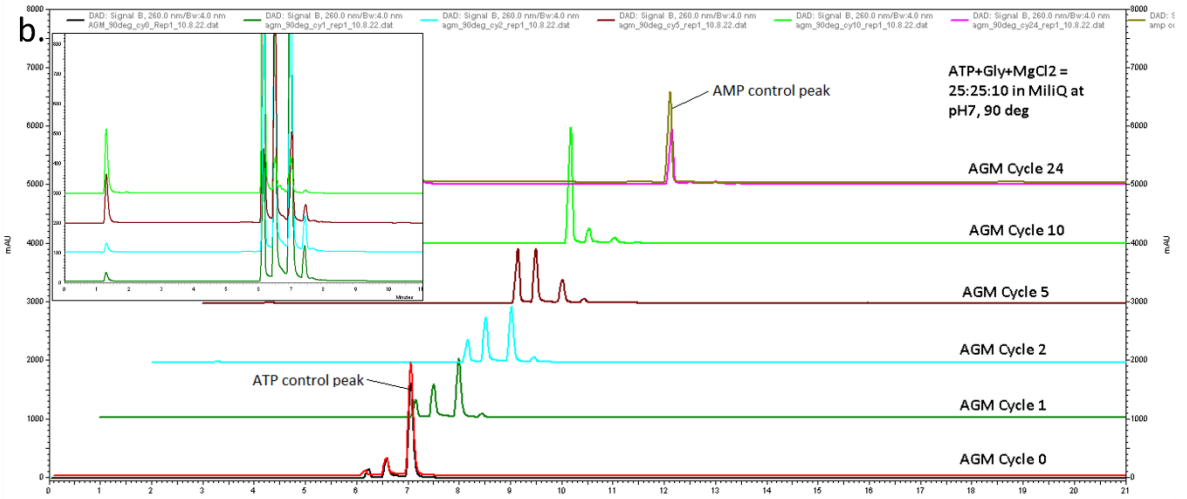
AMP control peak
ATP+Gly+MgCl2 = 25:25:10 in MiliQ at pH7, 90 deg
AGM Cycle 24
AGM Cycle 10
AGM Cycle 5
AGM Cycle 2
ATP control peak
AGM Cycle 1
AGM Cycle 0
mAU

C.

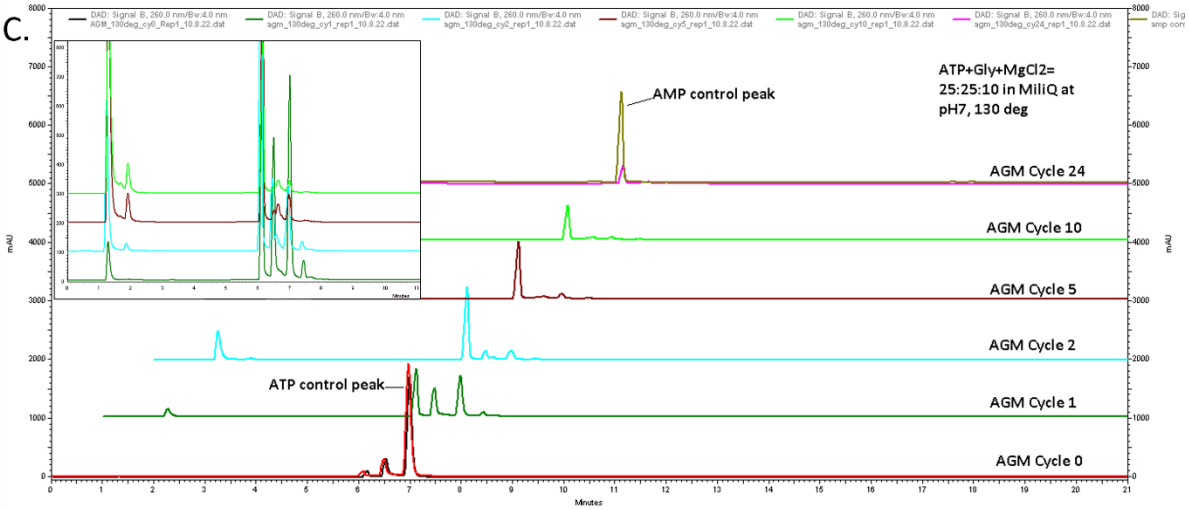
AMP control peak
ATP+Gly+MgCl2= 25:25:10 in MiliQ at pH7, 130 deg
AGM Cycle 24
AGM Cycle 10
AGM Cycle 5
AGM Cycle 2
ATP control peak
AGM Cycle 1
AGM Cycle 0
mAU
Minutes

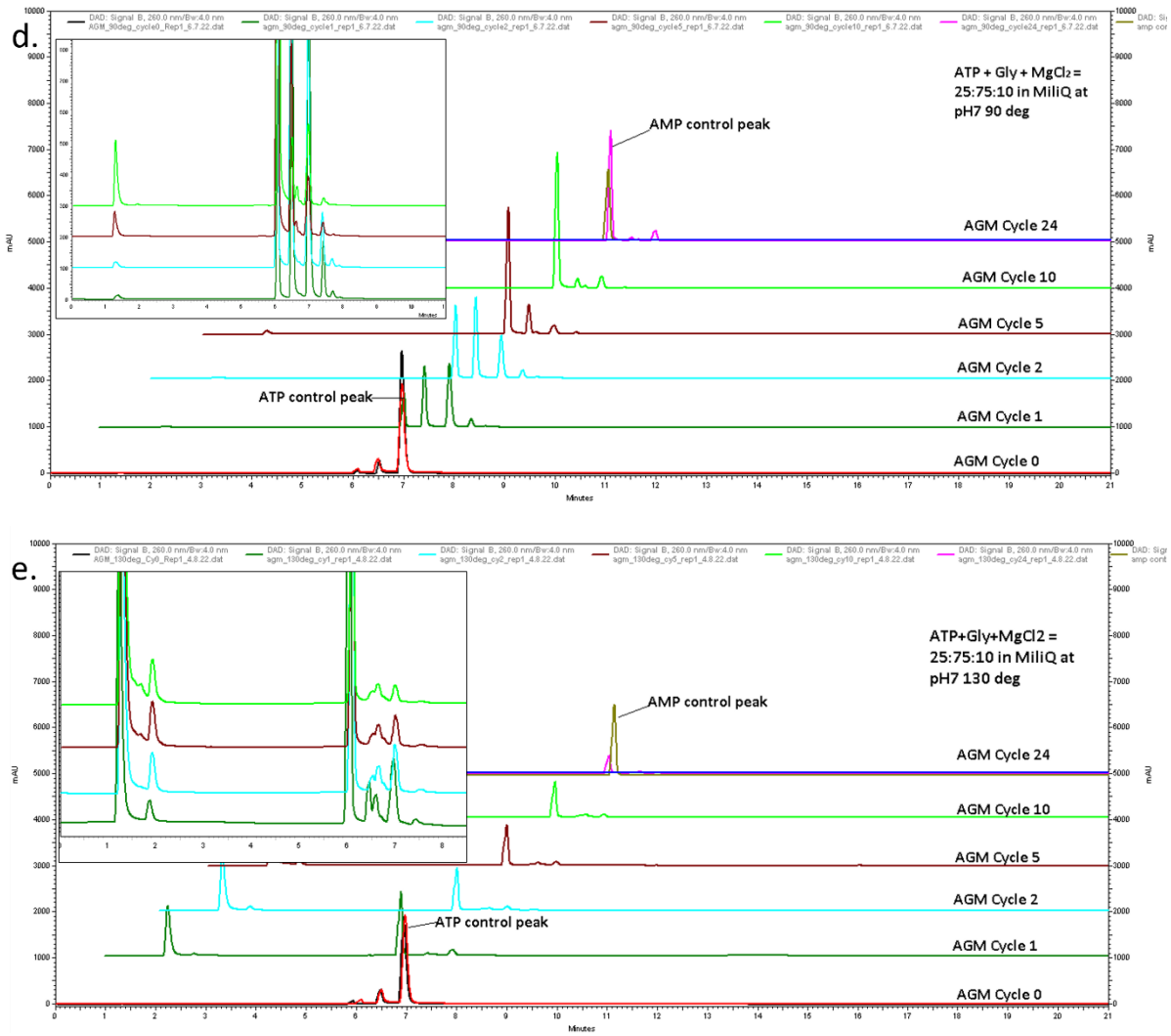

Figure S6 a-e: Overlays of HPLC chromatograms of **a.** purified controls [AMP-G (P-O-C); AMP-G(P-N); AMP; ADP, $(AMP)_2$; ATP; $(AMP)_3$; $(AMP)_4$] and of different time points obtained in **b.** AGM 90L, **c.** AGM 130L, **d.** AGM 90H and **e.** AGM 130 H, reactions. Y- axes (left and right) represent absorbance in mAU while X-axis represents retention time (RT) in minutes. An offset of 1 minute has been used from Cycle 1 onwards for better visualization. The staggered overlays of Cycle 1, 2, 5 and 10 hrs have been zoomed in as insets (on the left) from RT 0 to 11 mins for better visualization.

HPLC chromatograms of AG-based reactions

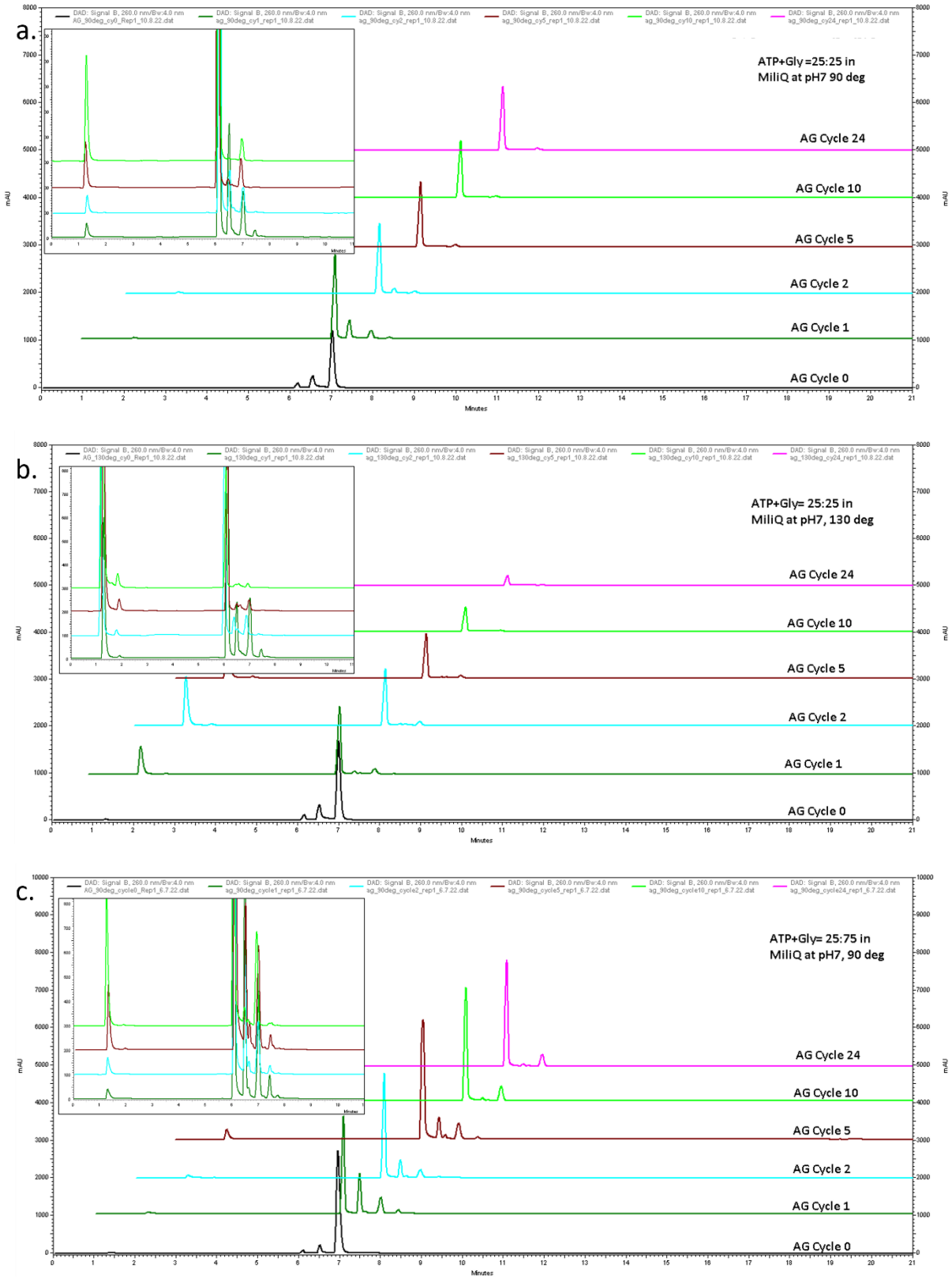

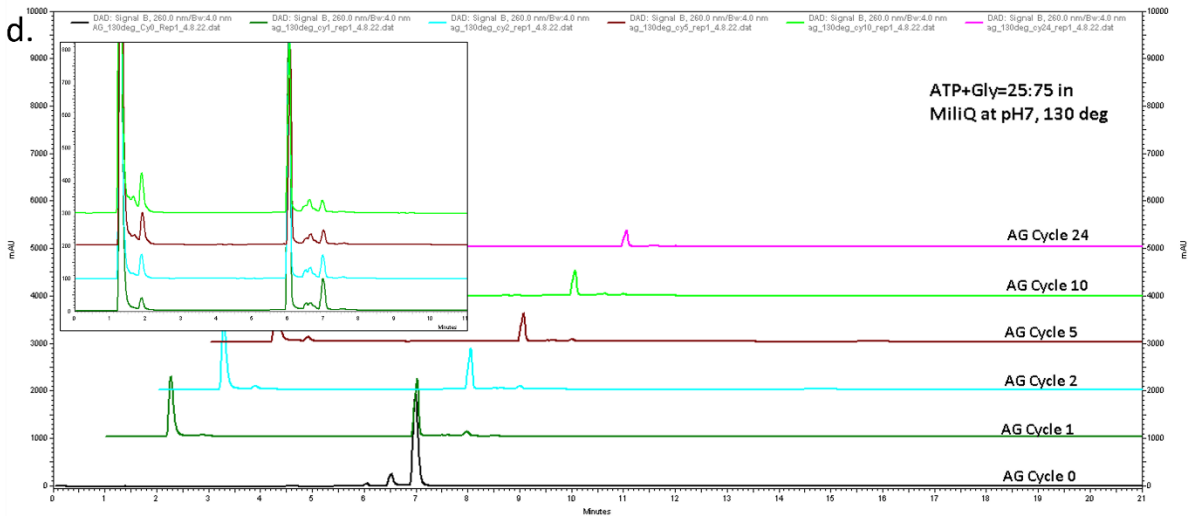

Figure S7: Overlays of HPLC chromatograms of different time points in **a.** AG 90L, **b.** AG 130L, **c.** AG 90H and **d.** AG 130H reactions. Y- axes (left and right) represent absorbance in mAU while X-axis represents retention time (RT) in minutes. An offset of 1 minute has been used from Cycle 1 onwards for better visualization. The staggered overlays of Cycle 1, 2, 5 and 10 hrs have been zoomed in as insets (on the left) from RT 0 to 11 mins for better visualization.

HPLC chromatograms of AM-based reactions

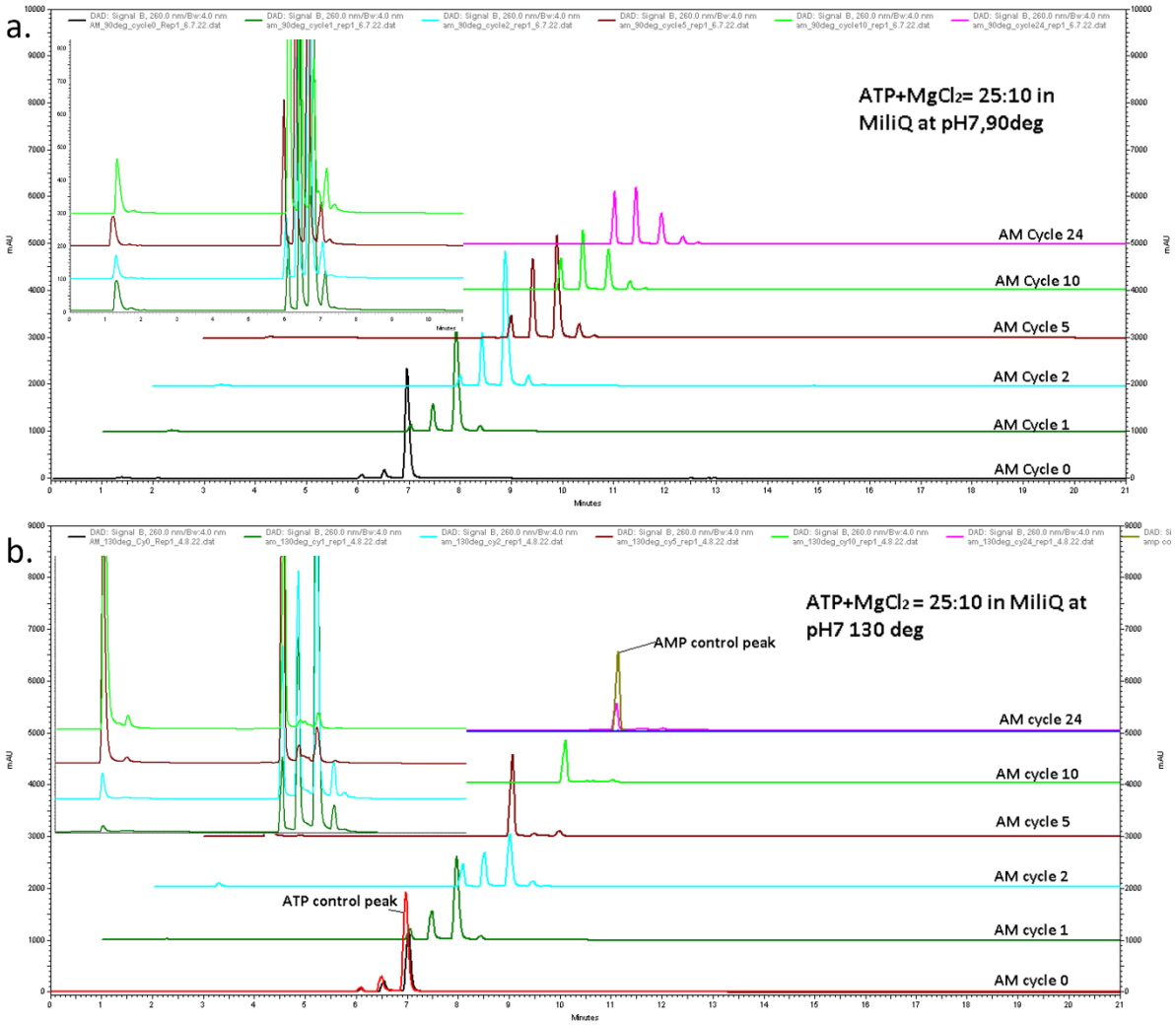

Figure S8: Overlays of HPLC chromatograms of different time points in **a.** AM 90, **b.** AM 130 reactions. Y- axes (left and right) represent absorbance in mAU while X-axis represents retention time (RT) in minutes. An offset of 1 minute has been used from Cycle 1 onwards for better visualization. The staggered overlays of Cycle 1, 2, 5 and 10 hrs have been zoomed in as insets (on the left) from RT 0 to 11 mins for better visualization.

HPLC chromatograms of A-based reactions

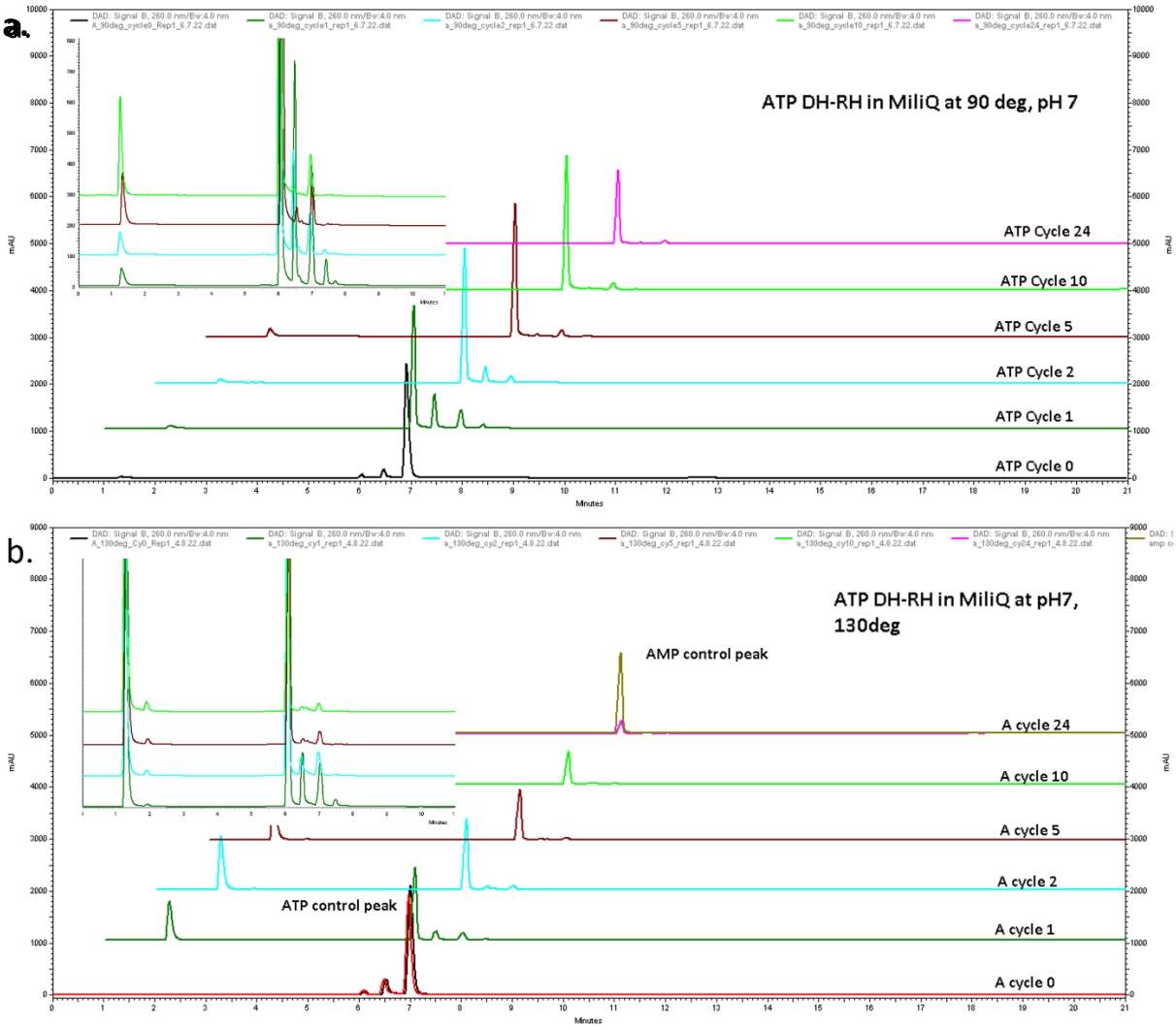

Figure S9: Overlays of HPLC chromatograms through different time points in **a.** A 90°C, **b.** 130 reactions. Y- axes (left and right) represent absorbance in mAU while X-axis represents retention time (RT) in minutes. An offset of 1 minute has been used from Cycle 1 onwards for better visualization. The staggered overlays of Cycle 1, 2, 5 and 10 hrs have been zoomed in as insets (on the left) from RT 0 to 11 mins for better visualization.

TOF MS-MS spectra of control oligonucleotides

a.

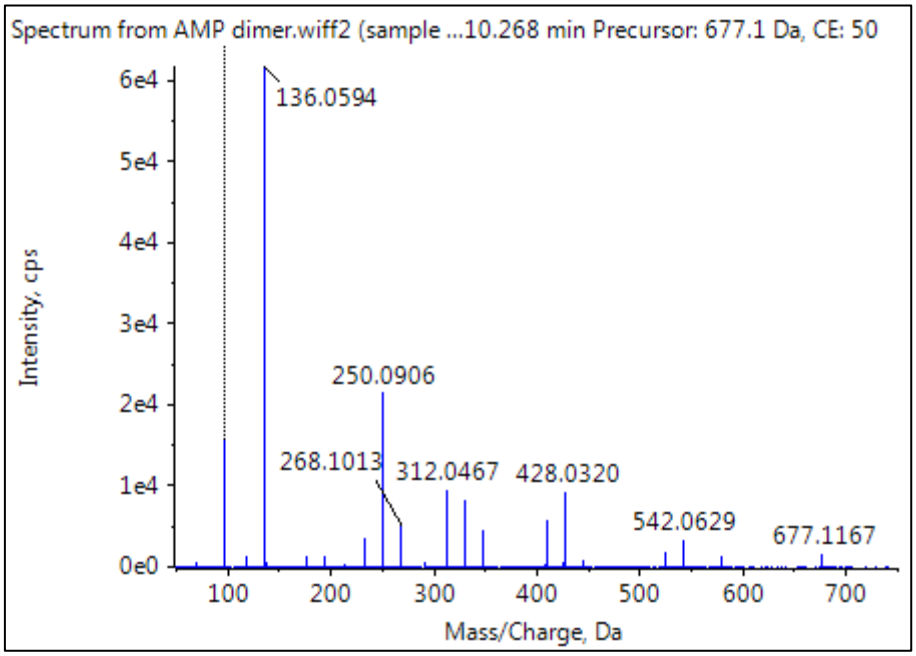

b.

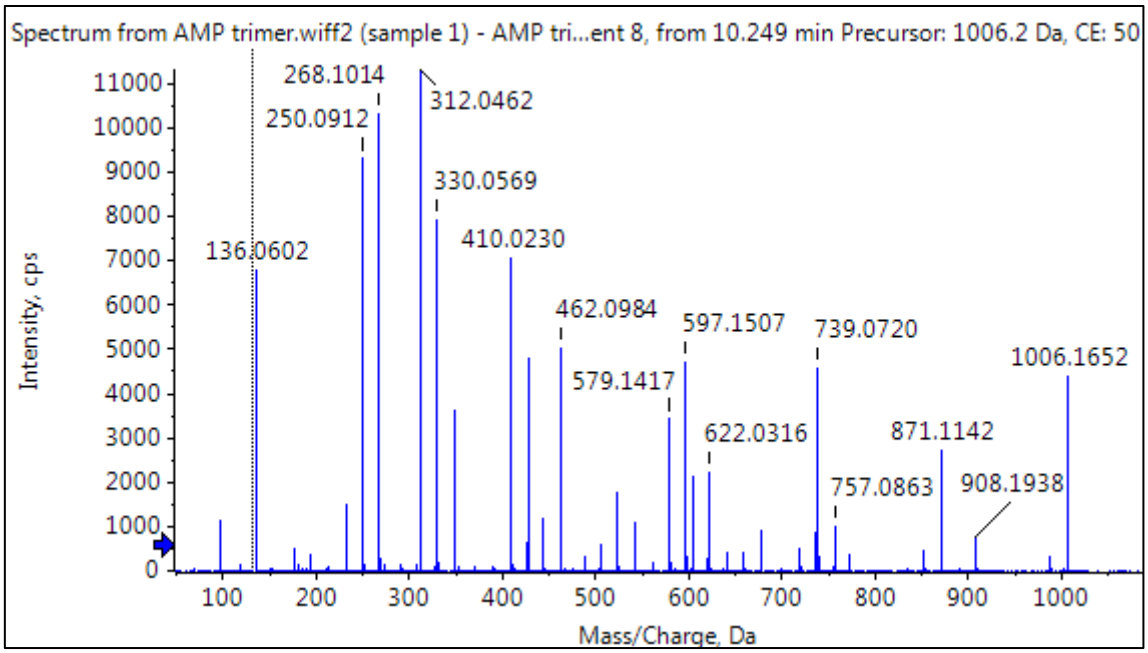

c.

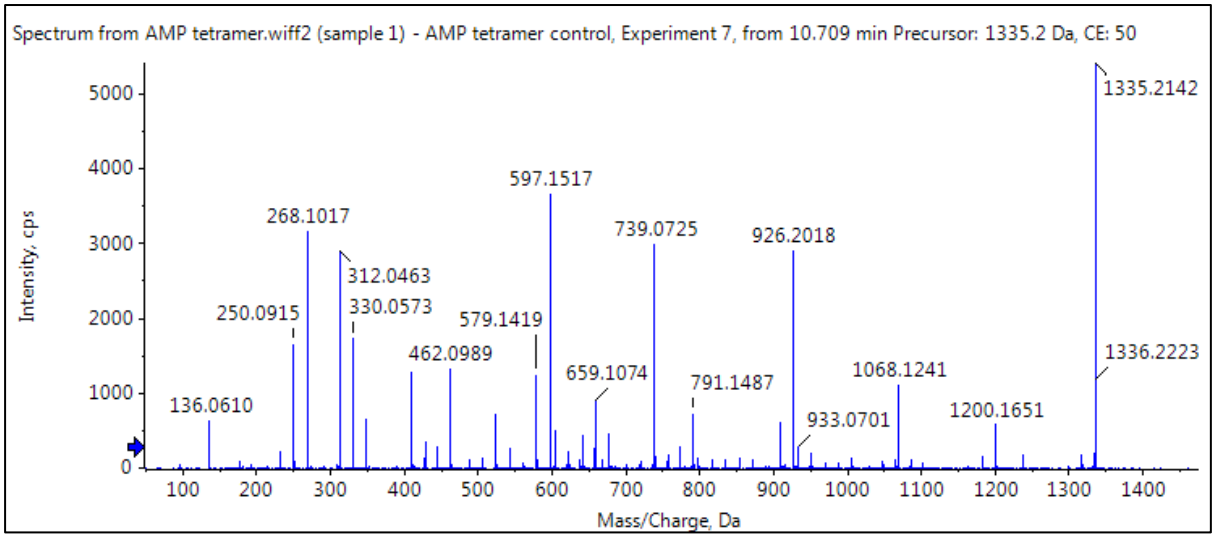

Figure S10: TOF MS-MS spectra and fragmentation pattern of purified control **a.** AMP oligonucleotides **a.** AMP-AMP [Precursor mass: 677.1229 (M+H)+], **b.** AMP-AMP-AMP [Precursor mass: 1006.1754 (M+H)+] and **c.** AMP-AMP-AMP-AMP [Precursor mass: 1335.2280 (M+H)+]. Expected masses corresponding to the fragmented ions of AMP oligonucleotides are observed in the spectra. CE used was 50 eV.

TOF MS-MS spectra of oligonucleotides found in the AGM reactions

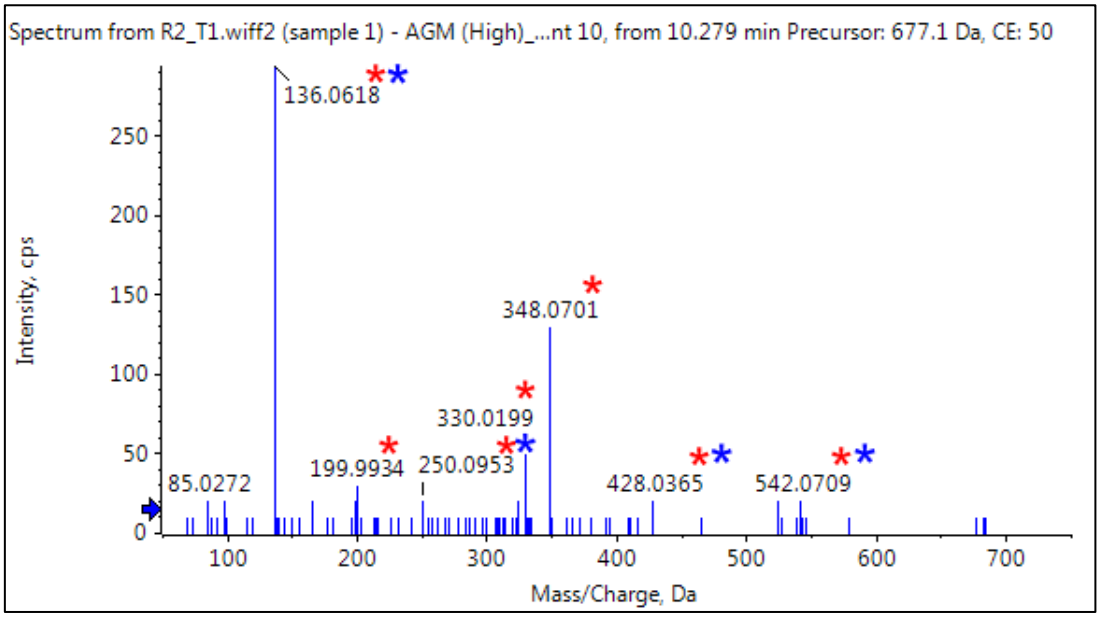

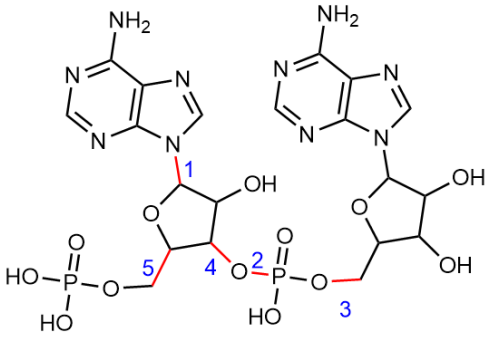

1
Chemical Formula: $C_5H_6N_5^+$
Exact Mass: 136.0618

1
Chemical Formula: $C_{15}H_{22}N_5O_{13}P_2^{\bullet}$
Exact Mass: 542.0689

2
Chemical Formula: $C_{10}H_{13}N_5O_6P$
Exact Mass: 330.0603

2
Chemical Formula: $C_{10}H_{15}N_5O_7P^{\bullet+}$
Exact Mass: 348.0704

3
Chemical Formula: $C_{10}H_{12}N_5O_3^{\bullet}$
Exact Mass: 250.0940

3
Chemical Formula: $C_{10}H_{16}N_5O_{10}P_2^+$
Exact Mass: 428.0367

1, 4 & 5
Chemical Formula: $C_4H_5O_{23}^{\bullet}$
Exact Mass: 85.0290

1 & 4
Chemical Formula: $C_5H_{12}O_6P^{\bullet+}$
Exact Mass: 199.0366

Figure S11a: TOF MS-MS spectra and fragmentation pattern of AMP dimer [Precursor mass: 677.1229 (M+H)+] formed in the AGM and AG reactions. Expected masses corresponding to the fragmented ions of AMP dimer are observed in the spectra. Experimental data matches with the predicted fragmentation pattern of AMP-AMP sequence The theoretically calculated masses and structures of molecules obtained post fragmentation were derived using ChemDraw Version 21.0.0. The fragmented bonds are highlighted in red. CE used was 50 eV. The red asterisk denotes the observed masses within 20 ppm error of the calculated fragmented mass. The blue asterisk denotes the observed masses within 20 ppm error of the observed fragmented masses from the control runs.

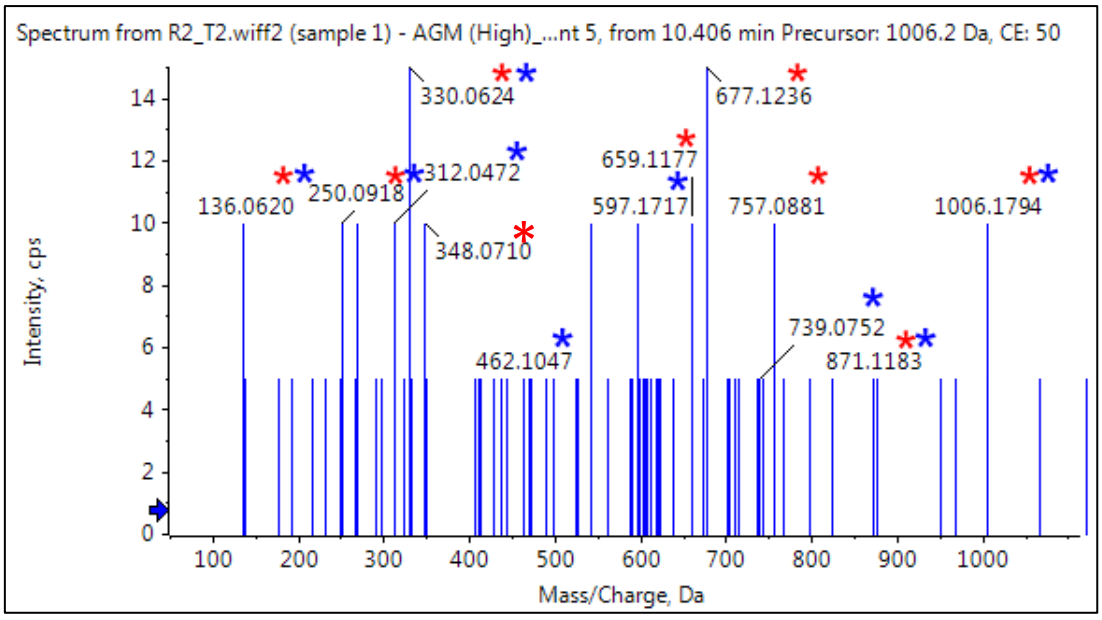

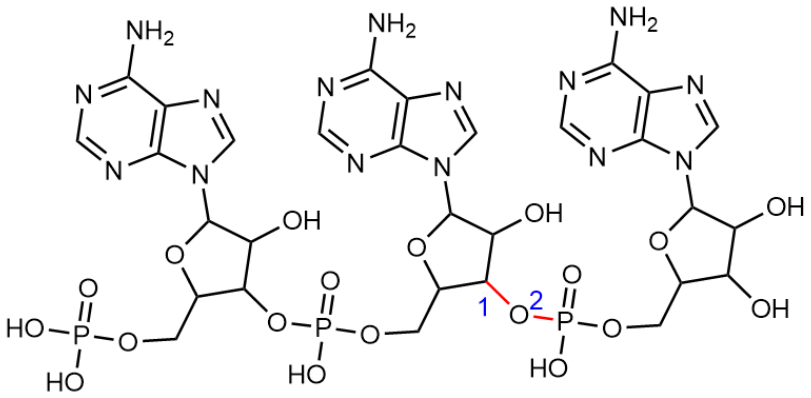

1

Chemical Formula: $C_{20}H_{25}N_{10}O_{12}P_2^{\bullet}$
Exact Mass: 659.1129

2

Chemical Formula: $C_{20}H_{27}N_{10}O_{13}P_2^{+}$
Exact Mass: 677.1229

Figure S11b: TOF MS-MS spectra and fragmentation pattern of AMP trimer [Precursor mass: 1006.1754 (M+H)+] formed in the AGM. Expected masses corresponding to the fragmented ions of AMP trimer are observed in the spectra. Experimental data matches with the predicted fragmentation pattern of AMP-AMP-AMP sequence. The theoretically calculated masses and structures of molecules obtained post fragmentation were derived using ChemDraw Version 21.0.0. The fragmented bonds are highlighted in red. The fragmented masses which have appeared in earlier images have not been shown for the sake of brevity. CE used was 50 eV. The red asterisk denotes the observed masses within 20 ppm error of the calculated fragmented mass. The blue asterisk denotes the observed masses within 20 ppm error of the observed fragmented masses from the control runs.

Relative abundance of oligonucleotides formed at 90°C and 130°C reactions

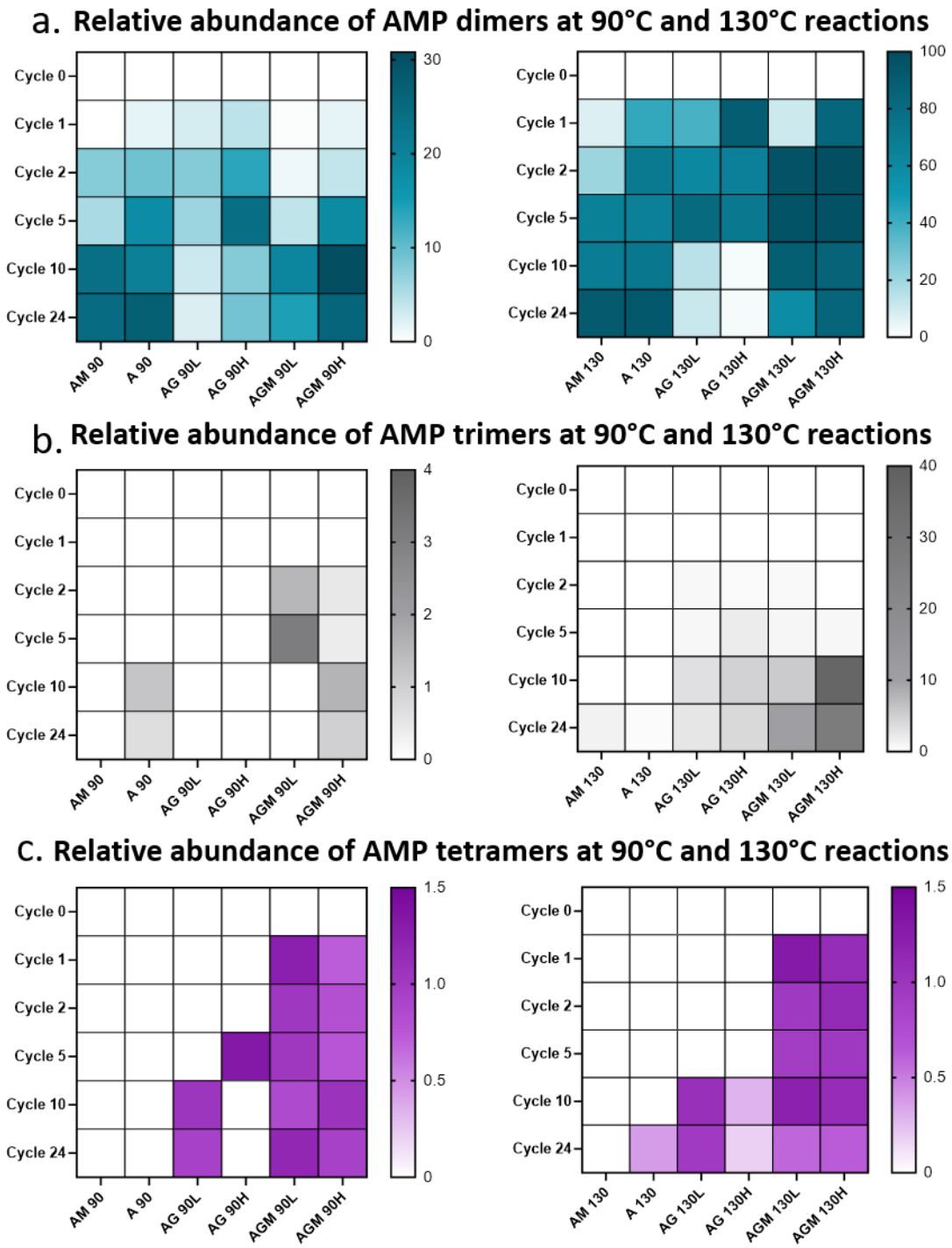

Figure S12: Relative abundance of **a.** AMP dimers, **b.** AMP trimers and **c.** AMP tetramers formed under wet-dry cycling conditions at 90°C and 130°C at different concentrations of Gly (25 mM, abbreviated as L or 75 mM, abbreviated as H) through different cycles in the various reactions studied. Relative oligonucleotide response in reactions involving ATP + Gly+ Mg^{2+} (AGM), ATP + Gly (AG), ATP+ Mg^{2+} (AM) and ATP (A) mixtures are demonstrated. The Y-axis indicates the wet-dry cycle timepoints at which samples were analyzed. The Xaxis indicates the percentage response of oligonucleotide relative to the internal standard used of different length oligonucleotide compounds formedfor N = 6 replicates.

HPLC Chromatograms of cAG and cAMP control reactions

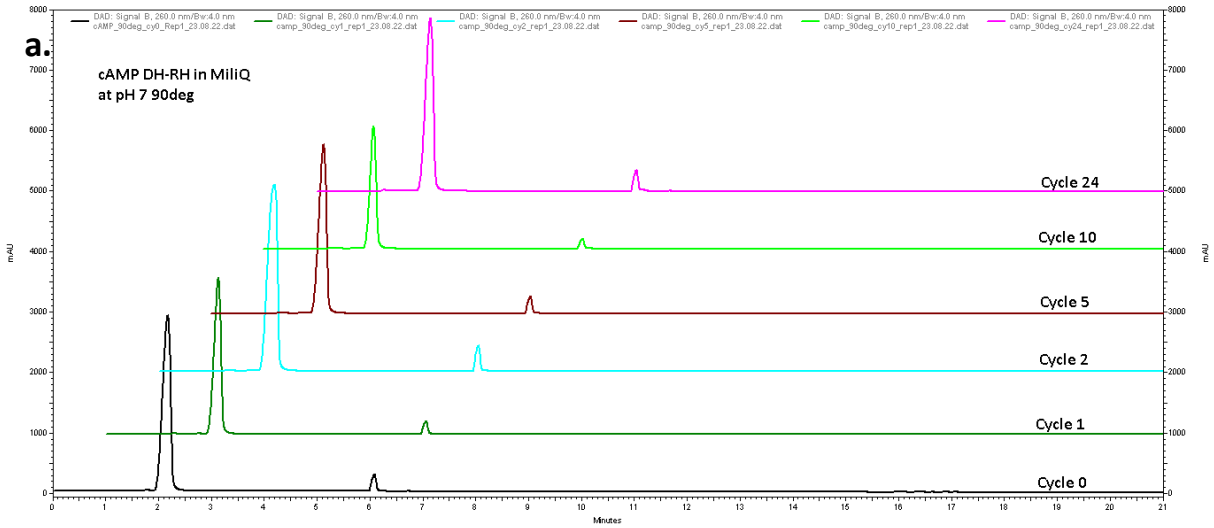

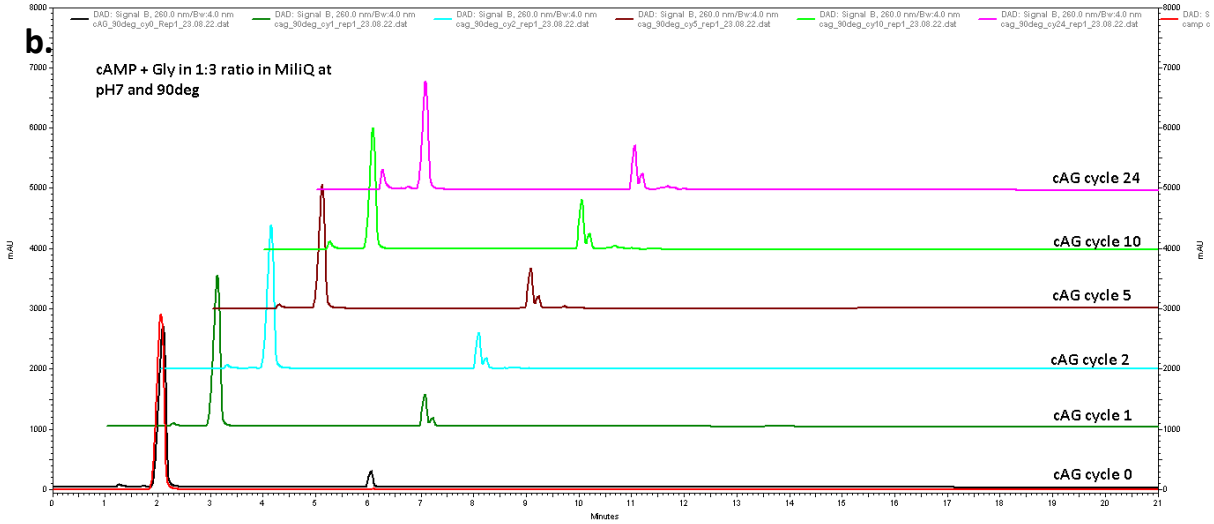

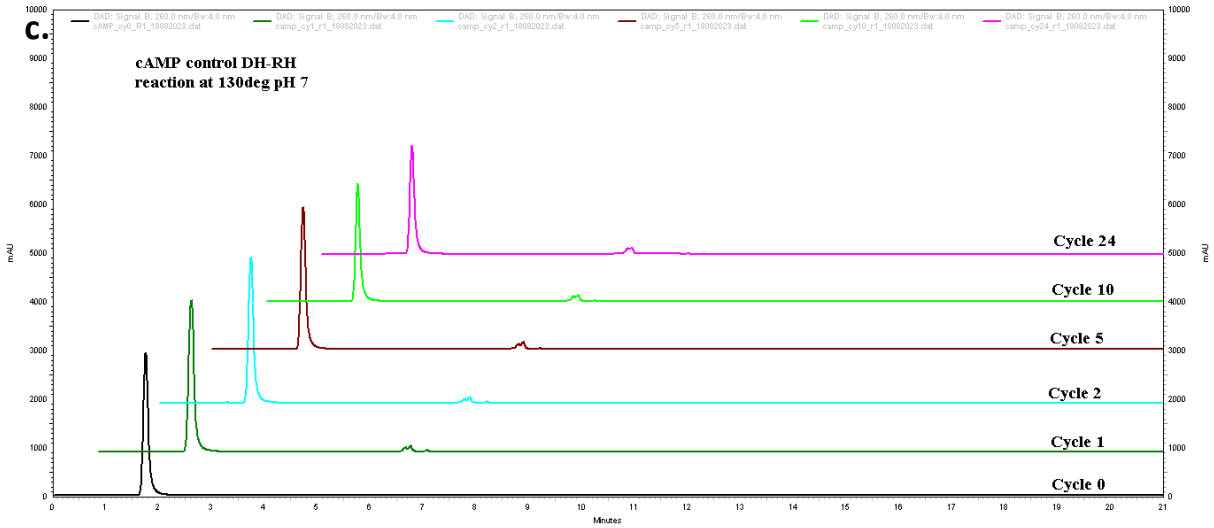

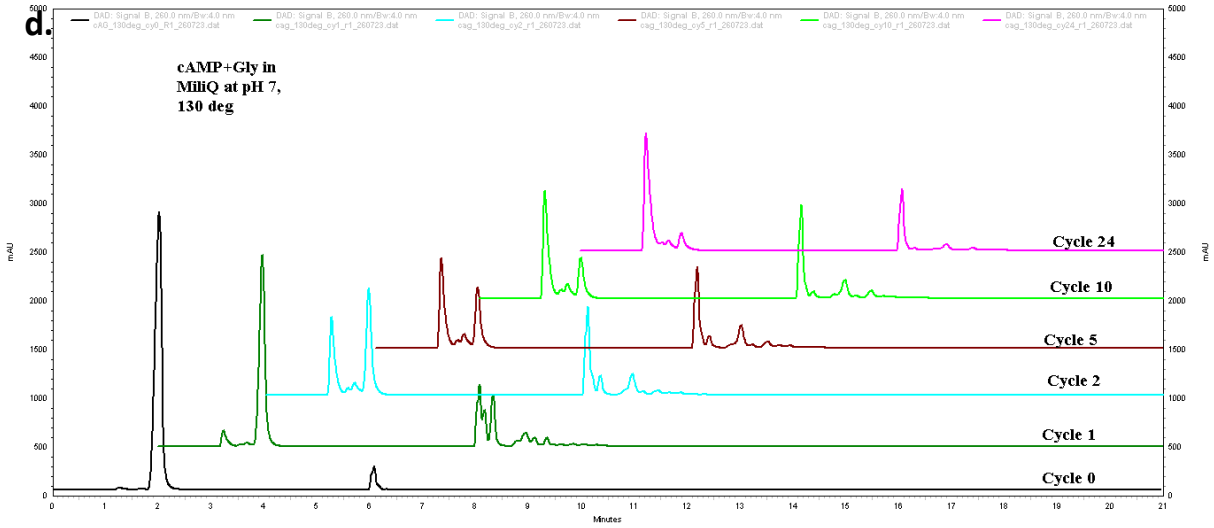

Figure S13: Overlays of HPLC chromatograms of cAMP reactions through different time points in **a.** without Gly at 90°C, **b.** with Gly at 90°C, **c.** without Gly at 130°C, **d.** with Gly at 130°C reactions. Y-axes (left and right) represent absorbance in mAU while X-axis represents retention time (RT) in minutes. An offset of 1 minute has been used from Cycle 1 onwards for better visualization.

TOF MS spectra of cyclic-ending pentamer and hexamer as obtained in cAG 130˚C reactions

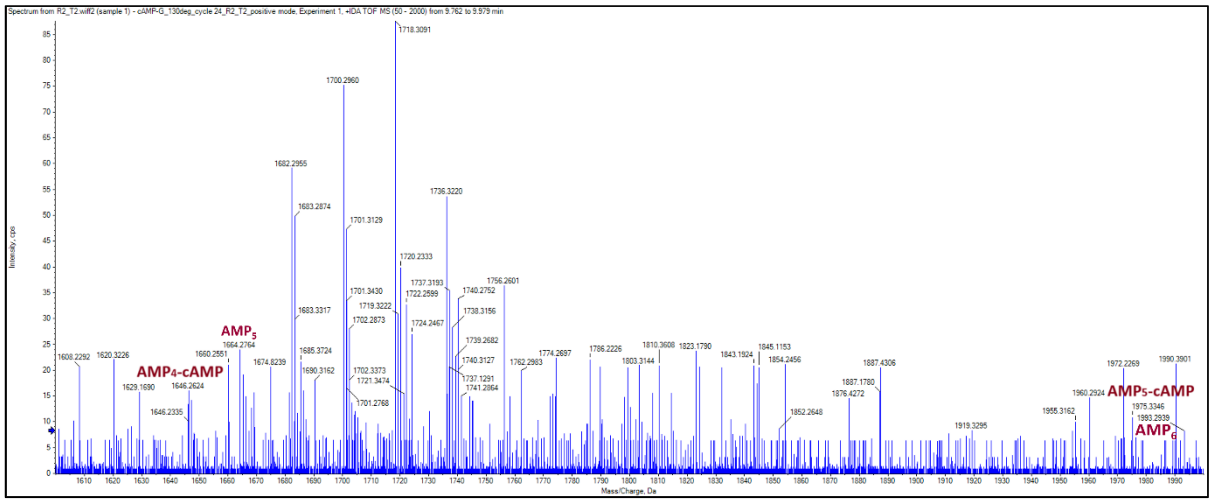

Figure S14: LC-MS spectra obtained for different length cyclic-ending pentamer (AMP_4-cAMP) [Theoretical m/z: 1646.2699 Observed m/z: 1646.2624 ppm error: 4.55] and hexamer (AMP_5-cAMP) [Theoretical m/z: 1975.3324 Observed m/z: 1975.3346ppm error: 1.11] that formed in the 2',3' cAMP + Gly (cAG 130) reaction at 130°C. The specific length oligonucleotide is denoted by the name over the masses observed for the oligonucleotides in the spectra.

TOF MS-MS spectra of oligonucleotides found in the cAMP-based reactions

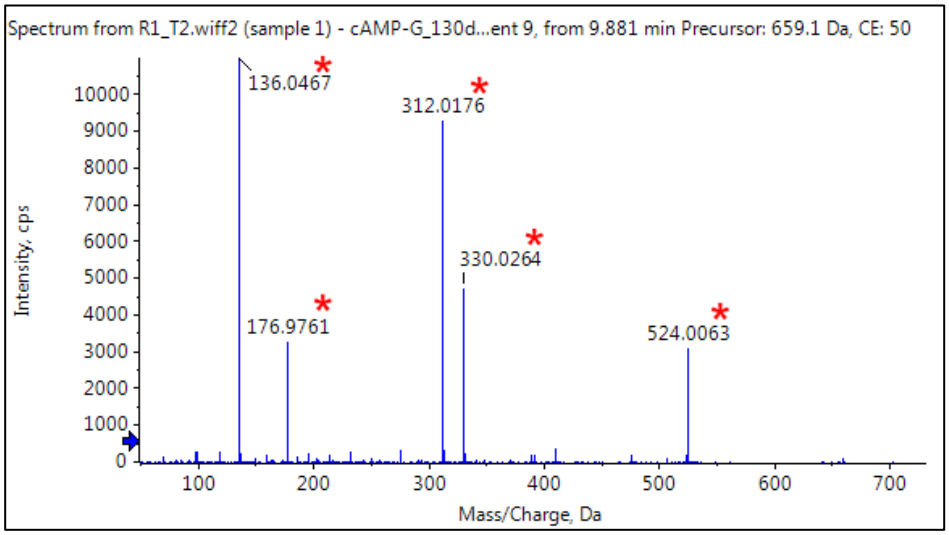

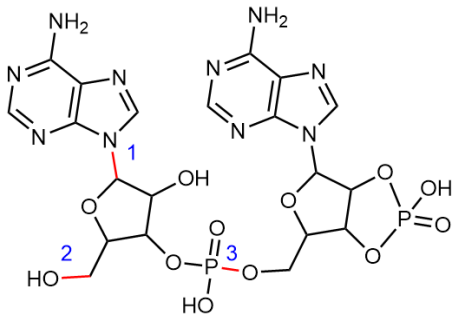

AMP-cAMP

1

Chemical Formula: $C_5H_5N_5$
Exact Mass: 135.0545

1

Chemical Formula: $C_{15}H_{20}N_5O_{12}P_2^{\bullet}$
Exact Mass: 524.0584

3

Chemical Formula: $C_{10}H_{13}N_5O_6P^{\bullet 2+}$
Exact Mass: 330.0592

2 & 3

Chemical Formula: $C_{10}H_{11}N_5O_5P^{\bullet +}$
Exact Mass: 312.0492

1, 2 & 3

Chemical Formula: $C_5H_6O_5P_5^{\bullet}$
Exact Mass: 176.9953

Figure S15a: TOF MS-MS spectra and fragmentation pattern of AMP dimer [Precursor mass: 659.1124 (M+H)+] formed in the cAMP-based reaction. Expected masses corresponding to the fragmented ions of AMP dimer are observed in the spectra. Experimental data matches with the predicted fragmentation pattern of AMP-cAMP sequence. The theoretically calculated masses and structures of molecules obtained post fragmentation were derived using ChemDraw Version 21.0.0. The fragmented bonds are highlighted in red. CE used was 50 eV. The red asterisk denotes the observed masses within 20 ppm error of the calculated fragmented mass.

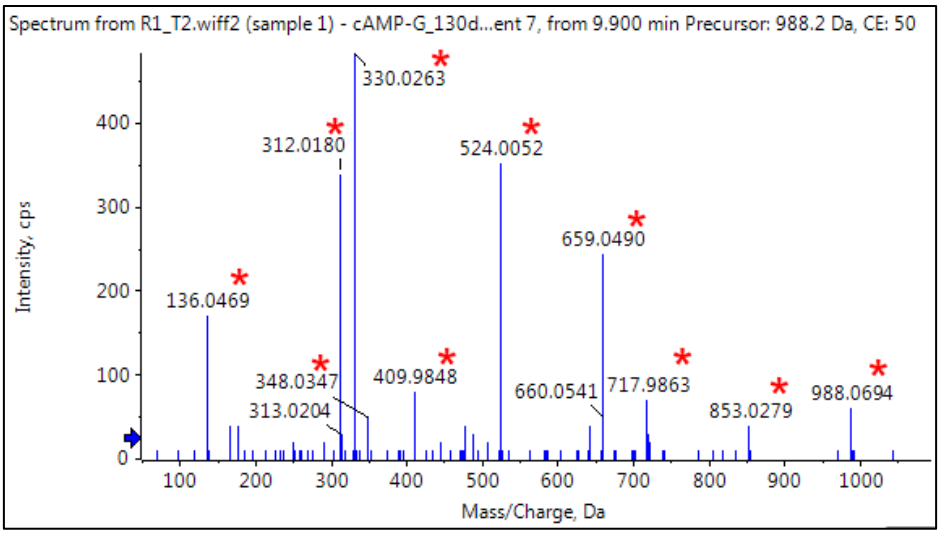

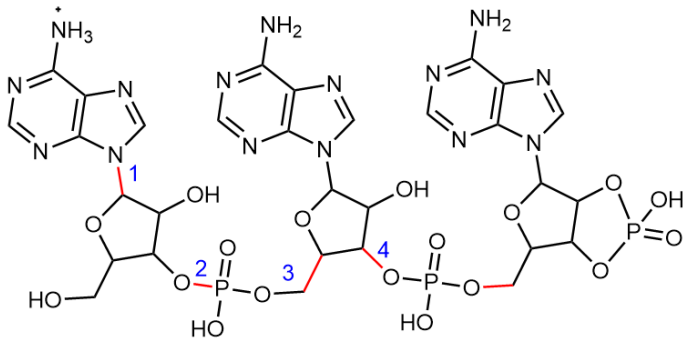

AMP-AMP-cAMP

1
Chemical Formula: $C_{25}H_{32}N_{10}O_{18}P_3^{\bullet}$
Exact Mass: 853.1109

3
Chemical Formula: $C_{11}H_{17}N_4O_7P_2^{+}$
Exact Mass: 348.0824

4
Chemical Formula: $C_{10}H_{13}N_5O_9P_2$
Exact Mass: 409.0189

5
Chemical Formula: $C_{20}H_{23}N_9O_{13}P_{22}^{\bullet}$
Exact Mass: 659.0891

2
Chemical Formula: $C_{20}H_{20}N_{10}O_{14}P_{35}^{\bullet}$
Exact Mass: 717.0373

Figure S15b: TOF MS-MS spectra and fragmentation pattern of AMP trimer [Precursor mass: 988.1649 (M+H)+] formed in the cAMP-based reaction. Expected masses corresponding to the fragmented ions of AMP trimer are observed in the spectra. Experimental data matches with the predicted fragmentation pattern of AMP-AMP-cAMP sequence. The theoretically calculated masses and structures of molecules obtained post fragmentation were derived using ChemDraw Version 21.0.0. The fragmented bonds are highlighted in red. The fragmented masses which have appeared in earlier images have not been shown for the sake of brevity. CE used was 50 eV. The red asterisk denotes the observed masses within 20 ppm error of the calculated fragmented mass.

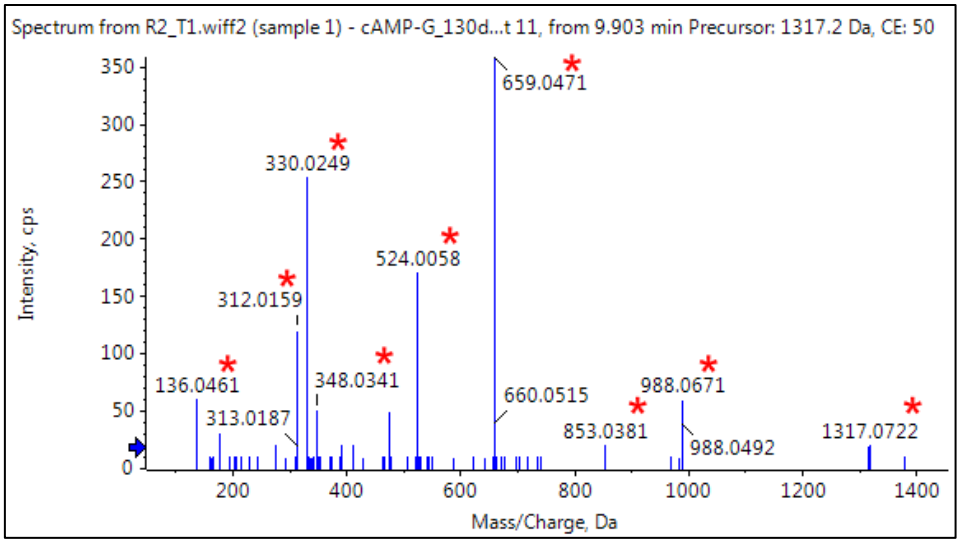

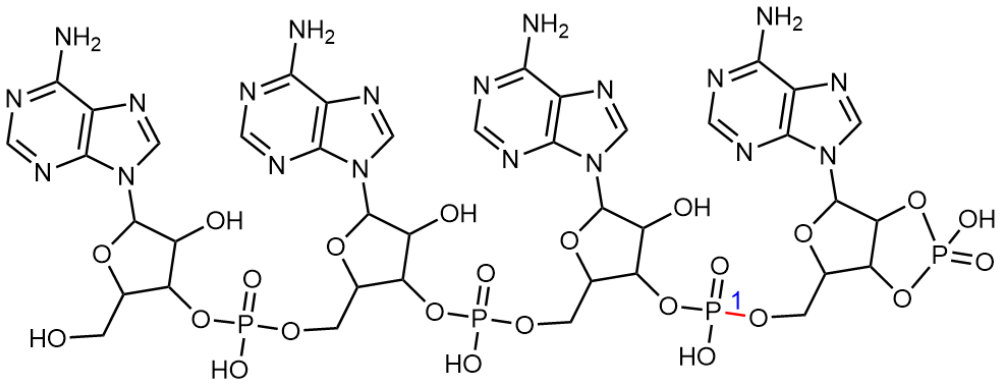

AMP-AMP-AMP-cAMP

1

Chemical Formula: $C_{30}H_{37}N_{15}O_{18}P_3$

Exact Mass: 988.1654

Figure S15c: TOF MS-MS spectra and fragmentation pattern of AMP tetramer [Precursor mass: 1316.2101 (M+H)+] formed in the cAMP-based reaction. Expected masses corresponding to the fragmented ions of AMP trimer are observed in the spectra. Experimental data matches with the predicted fragmentation pattern of AMP-AMP-AMP-cAMP sequence. The theoretically calculated masses and structures of molecules obtained post fragmentation were derived using ChemDraw Version 21.0.0. The fragmented bonds are highlighted in red. The fragmented masses which have appeared in earlier images have not been shown for the sake of brevity. CE used was 50 eV. The red asterisk denotes the observed masses within 20 ppm error of the calculated fragmented mass.

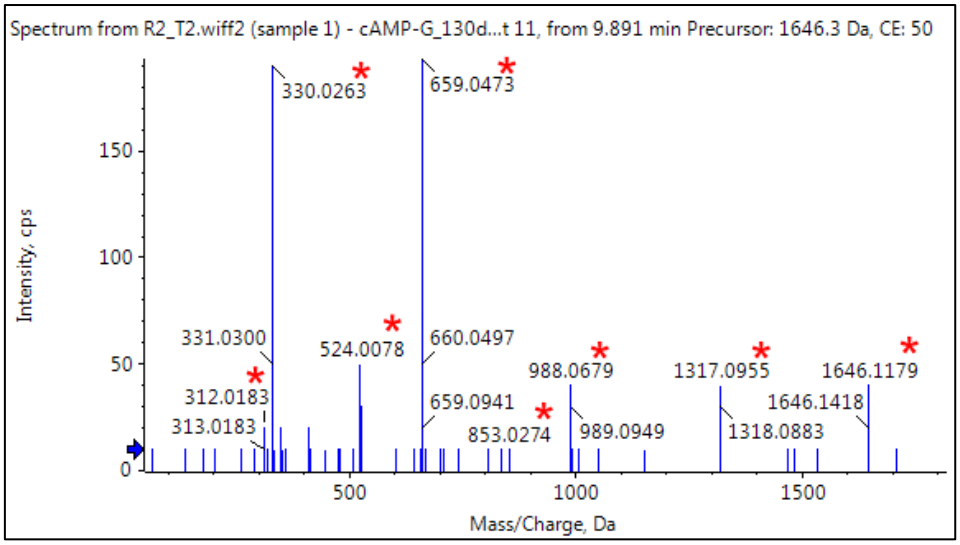

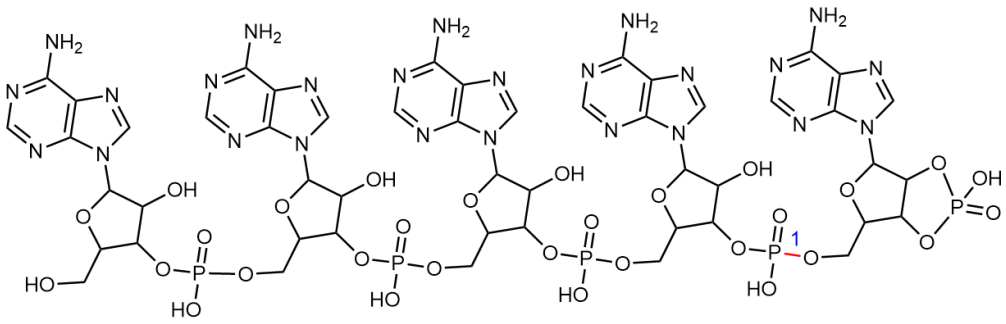

AMP-AMP-AMP-AMP-cAMP

Chemical Formula: $C_{40}H_{49}N_{20}O_{24}P_4$
Exact Mass: 1317.2179

Figure S15d: TOF MS-MS spectra and fragmentation pattern of AMP pentamer [Precursor mass: 1646.2699 (M+H)+] formed in the cAMP-based reaction. Expected masses corresponding to the fragmented ions of AMP trimer are observed in the spectra. Experimental data matches with the predicted fragmentation pattern of AMP-AMP-AMP-AMP-cAMP sequence. The theoretically calculated masses and structures of molecules obtained post fragmentation were derived using ChemDraw Version 21.0.0. The fragmented bonds are highlighted in red. The fragmented masses which have appeared in earlier images have not been shown for the sake of brevity. CE used was 50 eV. The red asterisk denotes the observed masses within 20 ppm error of the calculated fragmented mass.

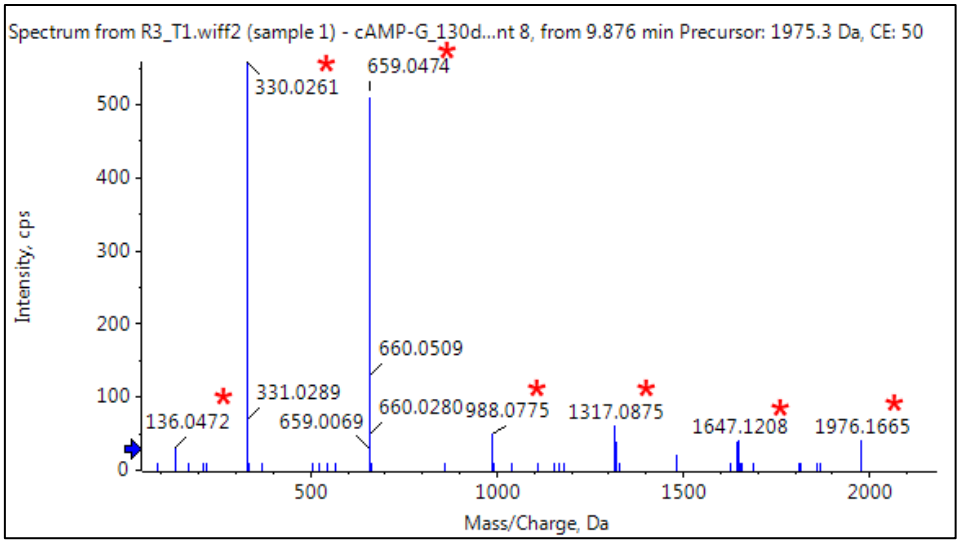

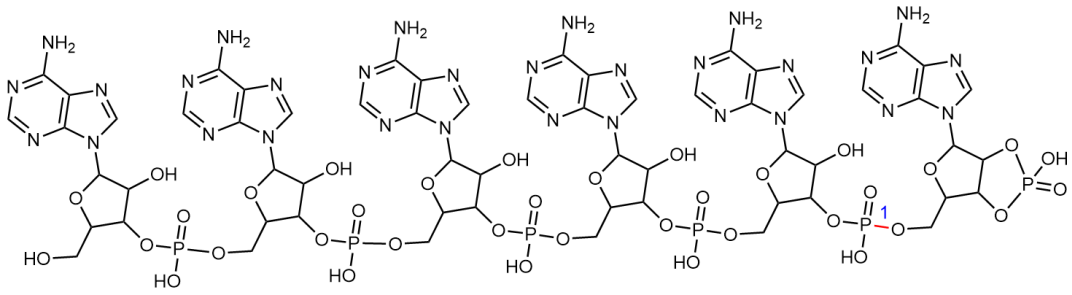

AMP-AMP-AMP-AMP-AMP-cAMP

1
Chemical Formula: $C_{50}H_{62}N_{25}O_{30}P_5^+$
Exact Mass: 1647.2777

Figure S15e: TOF MS-MS spectra and fragmentation pattern of AMP hexamer [Precursor mass: 1975.3224 (M+H)+] formed in the cAMP-based reaction. Expected masses corresponding to the fragmented ions of AMP trimer are observed in the spectra. Experimental data matches with the predicted fragmentation pattern of AMP-AMP-AMP-AMP-AMP-cAMP sequence. The theoretically calculated masses and structures of molecules obtained post fragmentation were derived using ChemDraw Version 21.0.0. The fragmented bonds are highlighted in red. The fragmented masses which have appeared in earlier images have not been shown for the sake of brevity. CE used was 50 eV. The red asterisk denotes the observed masses within 20 ppm error of the calculated fragmented mass.

Different plausibly linked AMP-Gly compounds can occur in the reaction

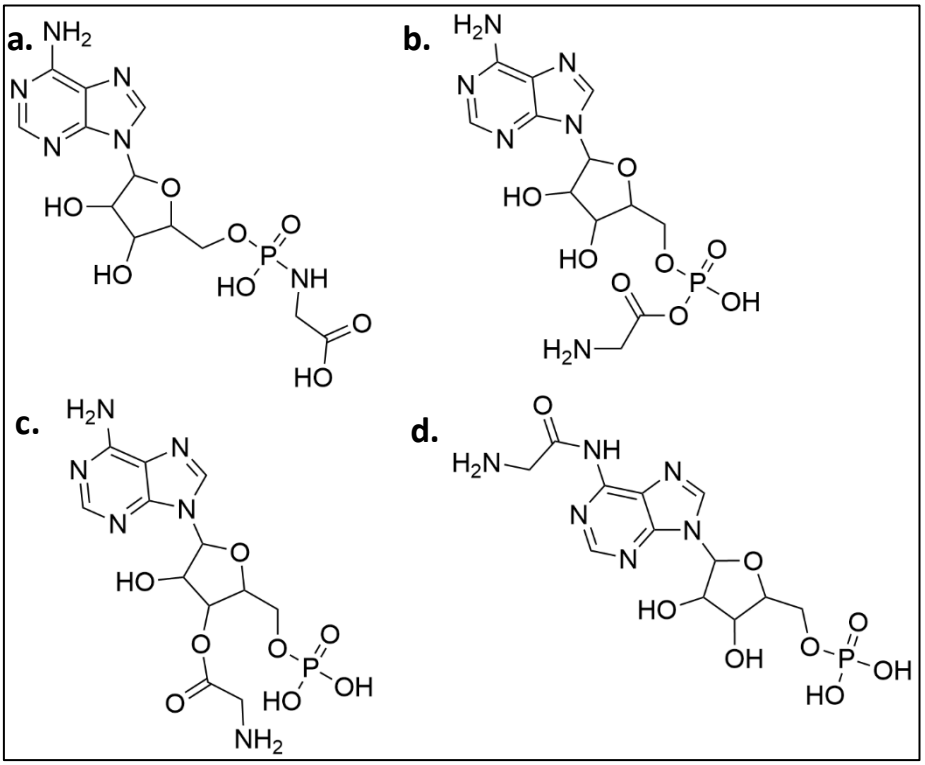

Figure S16: Different plausibly linked AMP-Gly compounds can occur in the reaction. Gly and AMP linked via **a**. phosphoramidate (P-N) bond, **b.** anhydride bond (P-O-C), **c.** ester bond (CO-OR) and **d.** amide bond (CO-NH). TOF MS-MS fragmentation spectra (Fig: S17) demonstrates the formation of all these compounds. The structures of molecules were derived using ChemDraw Version 21.0.0 and all have similar precursor mass of 405.0919 (M+H)+.

TOF MS/MS spectra of differently linked AMP-Gly formed in the AGM reactions

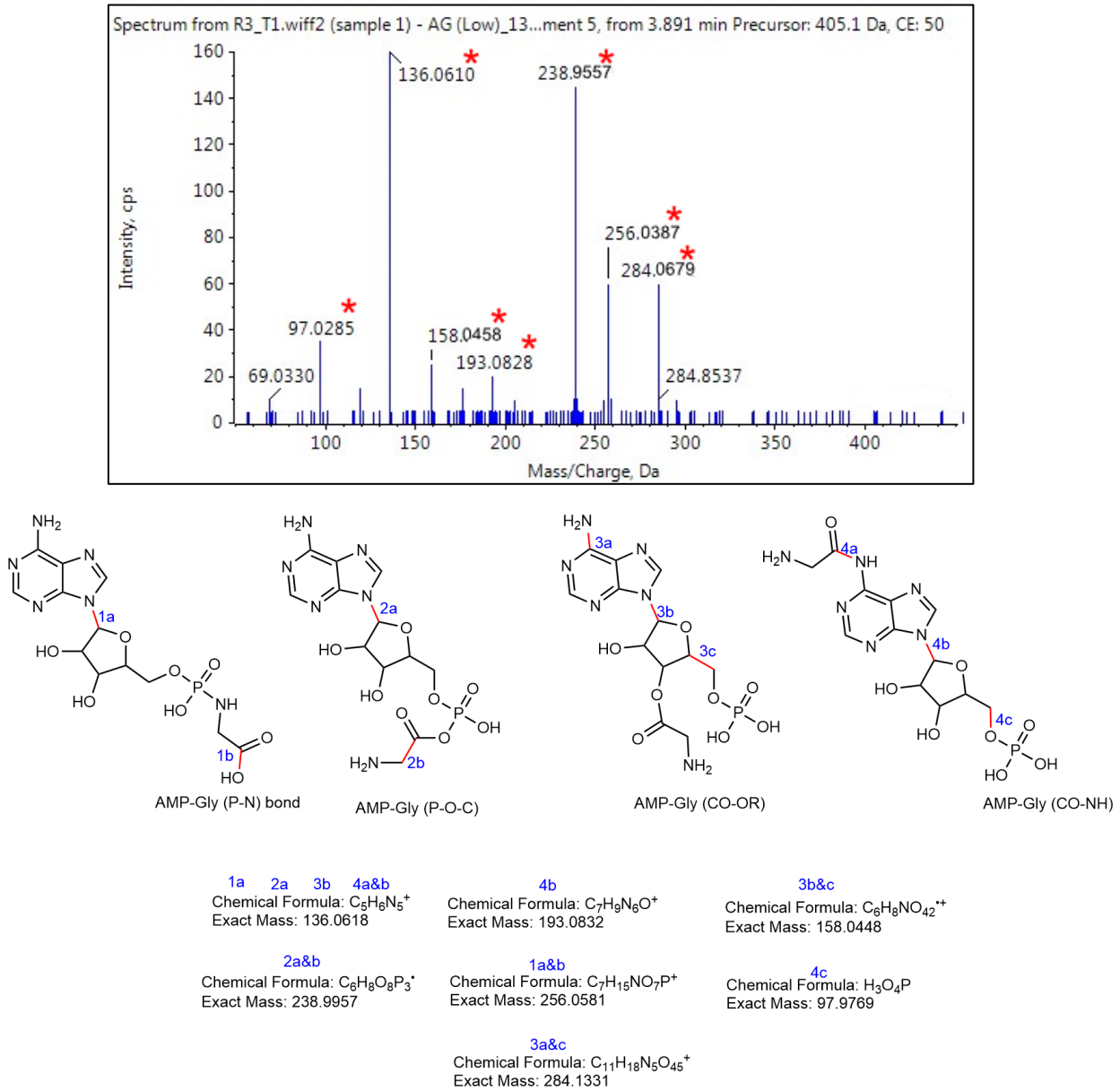

Figure S17: TOF MS-MS spectra and fragmentation pattern of plausibly linked AMP-Gly [Precursor mass: 405.0919 (M+H)+] formed in the AGM reaction. Expected masses corresponding to the fragmented7 ions of AMP-Gly are observed in the spectra. Experimental data matches with the predicted fragmentation pattern of AMP-Gly sequence. The theoretically calculated masses and structures of molecules obtained post fragmentation were derived using ChemDraw Version 21.0.0. The fragmented bonds are highlighted in red. CE used was 50 eV. The red asterisk denotes the observed masses within 20 ppm error of the calculated fragmented mass.

HPLC chromatogram of purification of AMP-Gly phosphoramidate (P-N) linkage

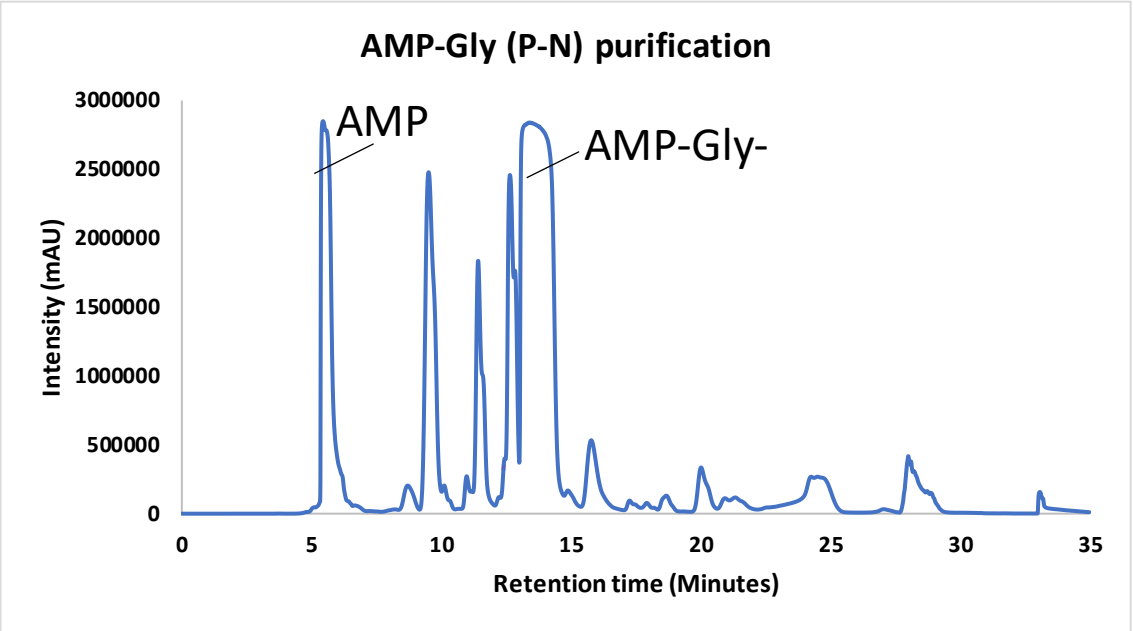

Figure S18: HPLC chromatogram of purification of chemically synthesised AMP-Gly (P-N): The purification chromatogram of the crude reaction mixture. The peak are labelled AMP and Methyl protected AMP-Gly as which were further confirmed with HRMS [**Fig S19**] and NMR [**Fig S20**]. All the other peaks following the peak for AMP-Gly were left uncharacterised.

HRMS spectra of Methyl- Gly-AMP and Boc- Gly-AMP

a.

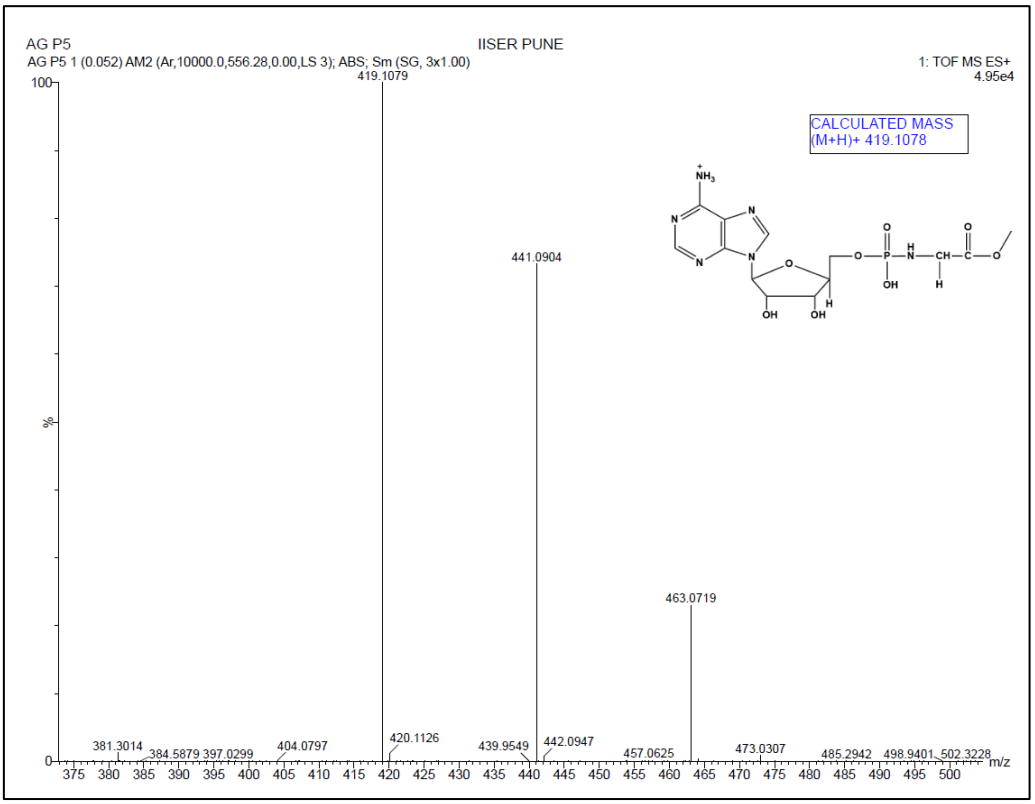

b.

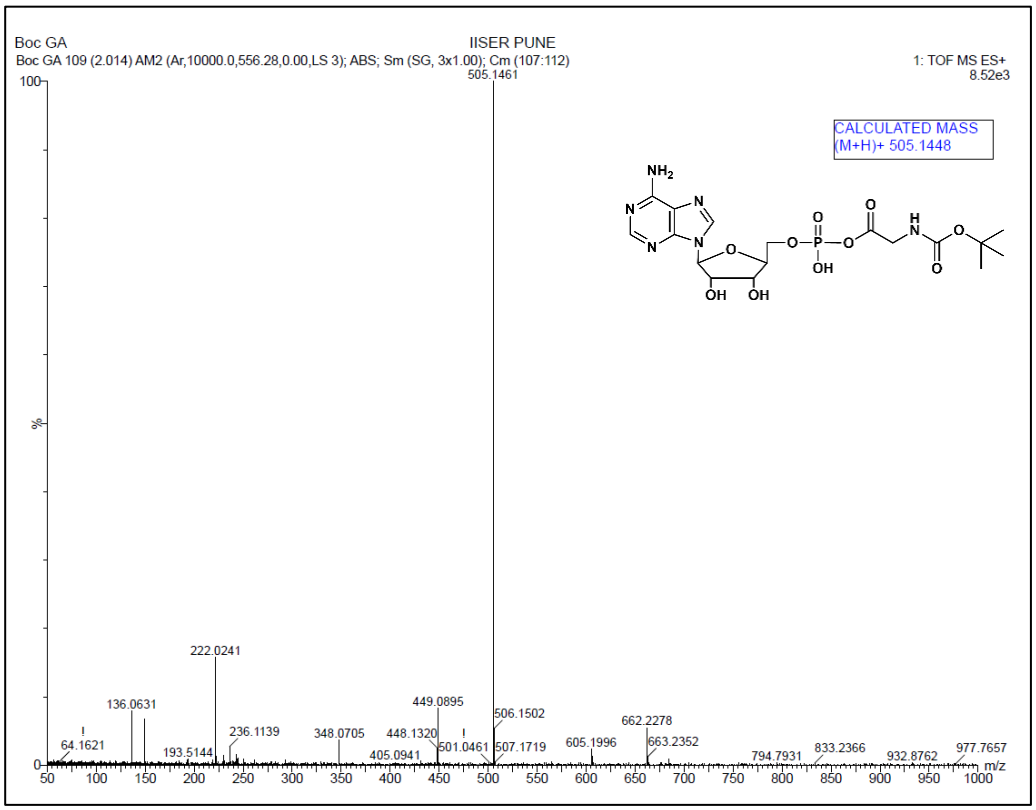

Figure S19: HR-MS profile of purification of chemically synthesised AMP-Gly intermediates: a. The peak with m/z 419.1079 corresponds to AMP-Gly (P-N) intermediate. **b.** The peak with m/z 505.1461 corresponds to Methyl protected AMP-Gly (P-O-C).

NMR analysis of chemically synthesized AMP-Gly

a.

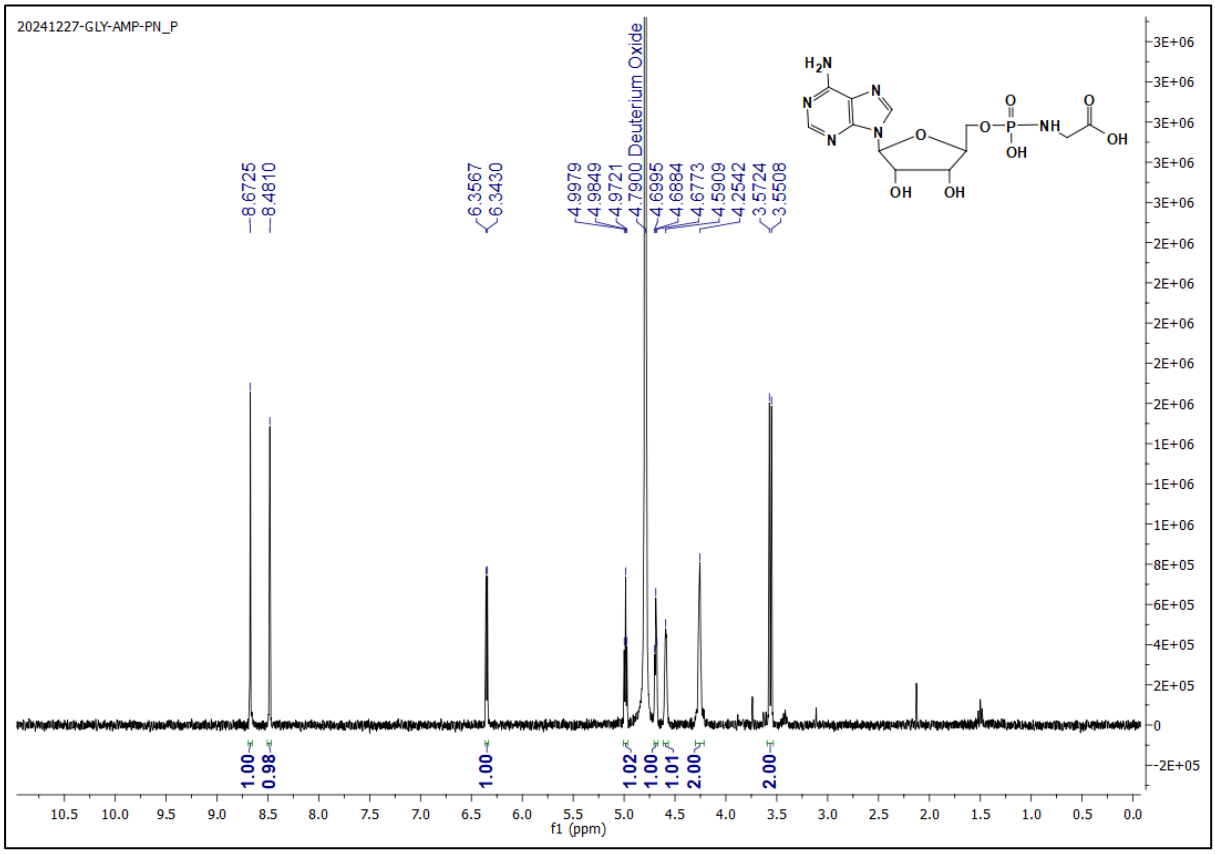

b.

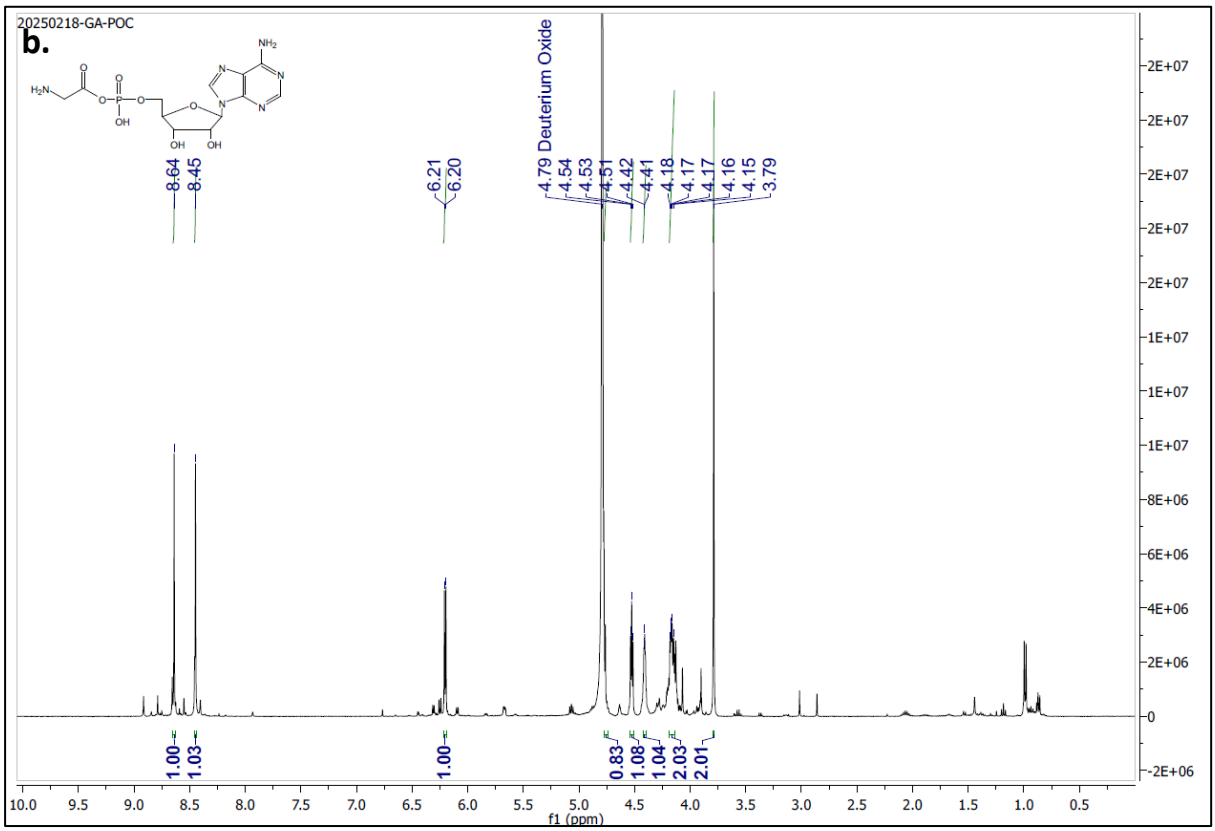

Figure S20: NMR analysis of chemically synthesized AMP-Gly a. ^{1}H NMR of AMP-Gly (P-N) (401 MHz, D_2O) δ 8.67 (s, 1H), 8.48 (s, 1H), 6.35 (d, *J* = 5.5 Hz, 1H), 4.98 (t, *J* = 5.2 Hz, 1H), 4.69 (t, *J* = 4.4 Hz, 1H),

4.59 (s, 1H), 4.25 (s, 2H), 3.56 (d, *J* = 8.7 Hz, 2H). **b.** ^{1}H NMR of AMP-Gly (P-O-C) (401 MHz, D_2O) δ 8.64 (s, 1H), 8.45 (s, 1H), 6.20 (d, *J* = 5.3 Hz, 1H), 4.75 (d, *J* = 5.7 Hz, 1H), 4.54 – 4.51 (m, 1H), 4.41 (d, *J* = 2.5 Hz, 1H), 4.19 – 4.14 (m, 2H), 3.79 (s, 2H) in Deuterium Oxide.

TOF-MS spectra of reaction with AMP-Gly (P-N and P-O-C) intermediates

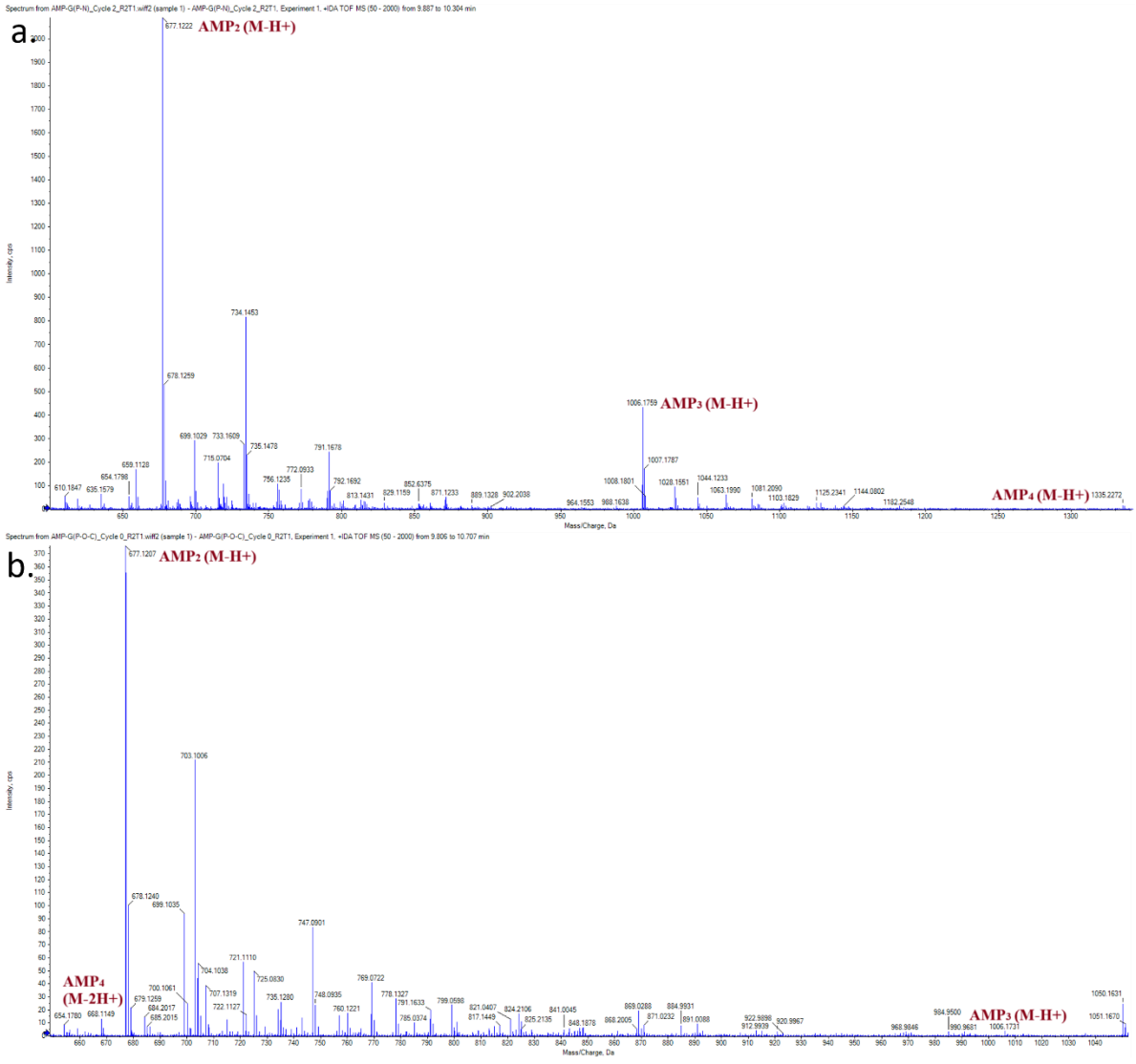

Figure S21: LC-MS spectra obtained for reactions with **a. AMP-G (P-N)** and **b. AMP-G (P-O-C)** intermediates. We can observe the masses for AMP-AMP [Precursor mass: 677.1229 (M+H)+], AMP-AMP-AMP [Precursor mass: 1006.1754 (M+H)+], AMP-AMP-AMP-AMP [Precursor mass: 668.1150 (M-2H+), inset] and AMP-G (P-N) [Precursor mass: 405.0919 (M+H)+].

TOF MS Spectra observed for reaction with β-Ala

a.

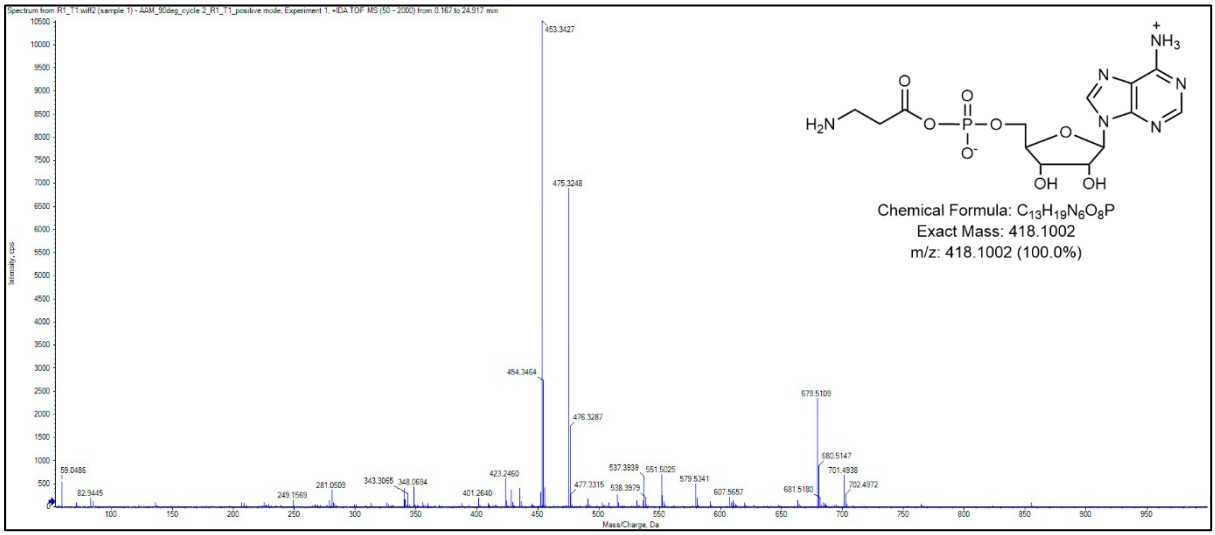

b.

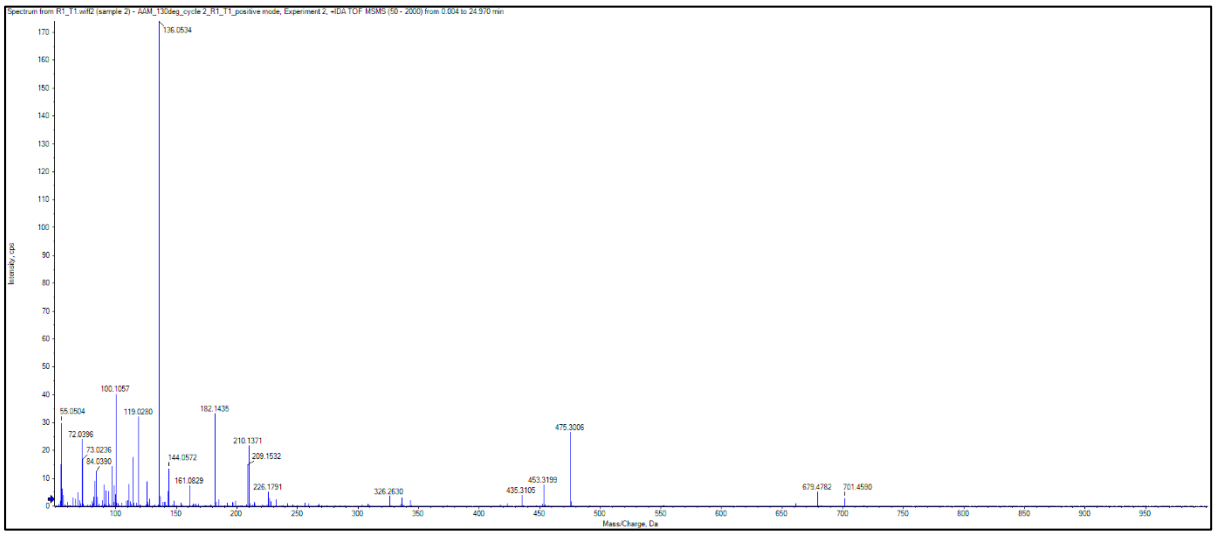

Figure S22: TOF MS-MS spectra observed for reaction with β-Ala: Targeted mass for AMP β-Ala (theoretical m/z has been shown in the inset) was not observed in the spectra for reactions containing β-Ala in **a.** AAM 90°C and **b.** AAM 130°C.

TOF MS/MS spectra of other AMP-aa formed in DH-RH reactions

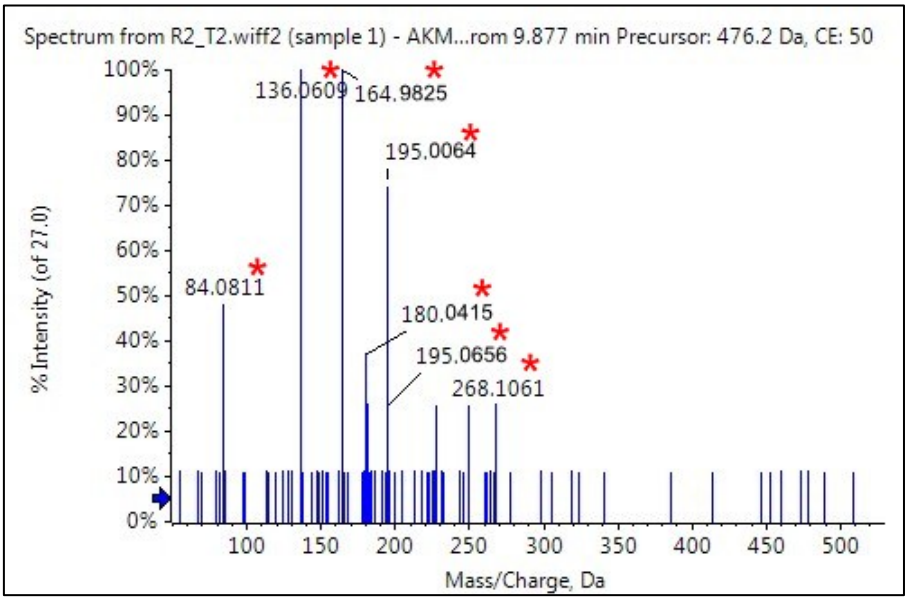

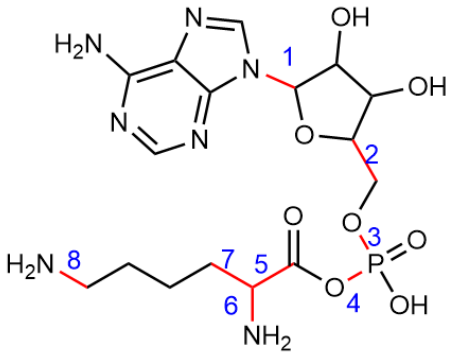

AMP-Lys

5 & 6
Chemical Formula: $C_5H_{10}N_2^{\bullet+}$
Exact Mass: 84.0808

1
Chemical Formula: $C_5H_6N_5^+$
Exact Mass: 136.0618

3 & 8
Chemical Formula: $C_6H_{14}NO_4P^{\bullet3+}$
Exact Mass: 195.0644

3
Chemical Formula: $C_{10}H_{14}N_5O_4^{\bullet2+}$
Exact Mass: 268.1035

2 & 7
Chemical Formula: $C_3H_4NO_5P_2^{\bullet2+}$
Exact Mass: 164.9816

1 & 4
Chemical Formula: $C_5H_8O_6P_2^{\bullet+}$
Exact Mass: 195.0053

Figure S23a: TOF MS-MS spectra and fragmentation pattern of AMP-Lys [Precursor mass: 476.1654 (M+H)+] formed in the AKM reaction. Expected masses corresponding to the fragmented ions of AMP-Lys are observed in the spectra. Experimental data matches with the predicted fragmentation pattern of AMP-Lys sequence. The theoretically calculated masses and structures of molecules obtained post fragmentation were derived using ChemDraw Version 21.0.0. The fragmented bonds are highlighted in red. CE used was 50 eV. The red asterisk denotes the observed masses within 20 ppm error of the calculated fragmented mass.

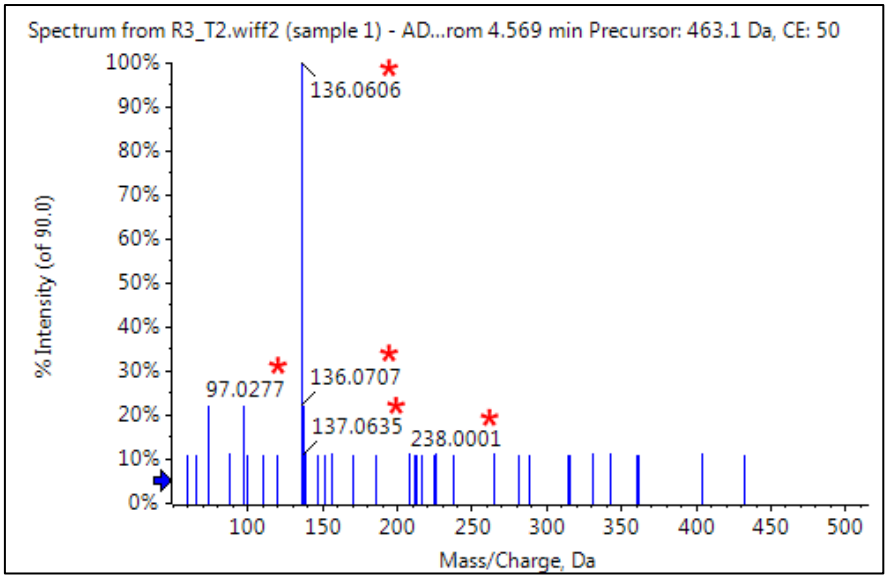

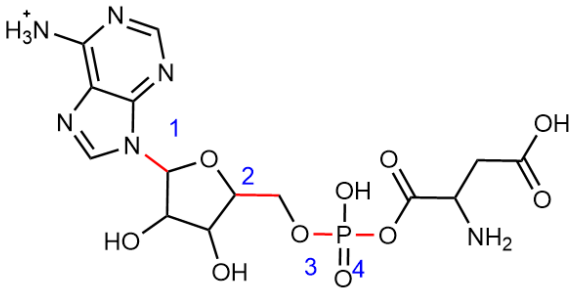

AMP-Asp

1
Chemical Formula: $C_5H_6N_5^+$
Exact Mass: 136.0618

2
Chemical Formula: $C_9H_{12}N_5O_3^+$
Exact Mass: 238.0935

4
Chemical Formula: $C_4H_{11}NO_{44}^+$
Exact Mass: 137.0666

2 & 4
Chemical Formula: $CH_6O_3P^+$
Exact Mass: 97.0049

1 & 3
Chemical Formula: $C_5H_{12}O_4^{\bullet 2+}$
Exact Mass: 136.0725

Figure S23b: TOF MS-MS spectra and fragmentation pattern of AMP-Asp [Precursor mass: 463.0097 (M+H)+] formed in the ADM reaction. Expected masses corresponding to the fragmented ions of AMP-Asp are observed in the spectra. Experimental data matches with the predicted fragmentation pattern of AMP-Asp sequence. The theoretically calculated masses and structures of molecules obtained post fragmentation were derived using ChemDraw Version 21.0.0. The fragmented bonds are highlighted in red. CE used was 50 eV. The red asterisk denotes the observed masses within 20 ppm error of the calculated fragmented mass.

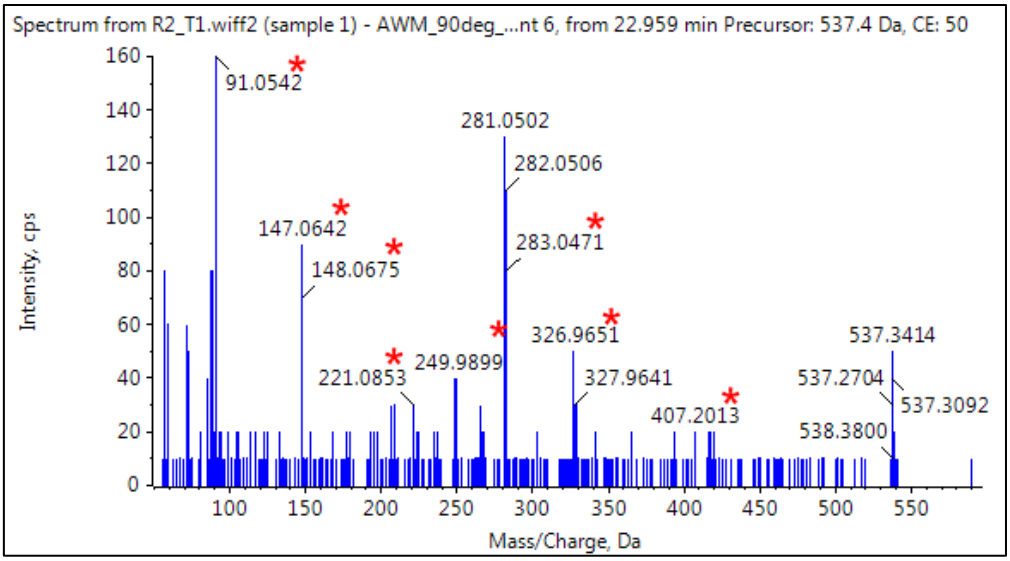

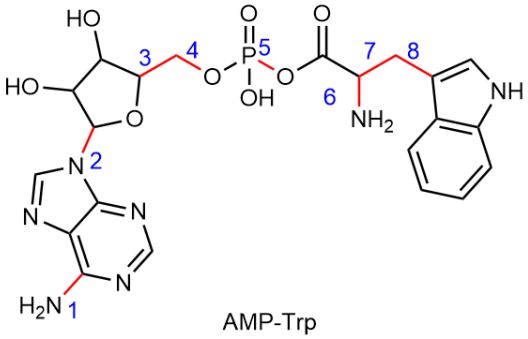

AMP-Trp

1 & 3
Chemical Formula: $C_9H_9N_4O_3^{\bullet}$
Exact Mass: 221.0675

4
Chemical Formula: $C_8H_{14}NO_8P_2^{\bullet}$
Exact Mass: 283.0457

4
Chemical Formula: $C_8H_{13}NO_8P_2^{\bullet+}$
Exact Mass: 282.0373

4
Chemical Formula: $C_8H_{12}NO_8P_2^{\bullet 2+}$
Exact Mass: 281.0290

2,6 & 7
Chemical Formula: $C_7H_7O_8P_4^{\bullet 2+}$
Exact Mass: 249.9868

5
Chemical Formula: $C_{10}H_{12}N_5O_6P^{\bullet}$
Exact Mass: 329.0525

7
Chemical Formula: $C_{10}H_{12}N^{+}$
Exact Mass: 147.0964

Figure S23c: TOF MS-MS spectra and fragmentation pattern of AMP-Trp [Precursor mass: 534.1497 (M+H)+] formed in the AWM reaction. Expected masses corresponding to the fragmented ions of AMP-Trp are observed in the spectra. Experimental data matches with the predicted fragmentation pattern of AMP-Trp sequence. The theoretically calculated masses and structures of molecules obtained post fragmentation were derived using ChemDraw Version 21.0.0. The fragmented bonds are highlighted in red. CE used was 50 eV. The red asterisk denotes the observed masses within 20 ppm error of the calculated fragmented mass.

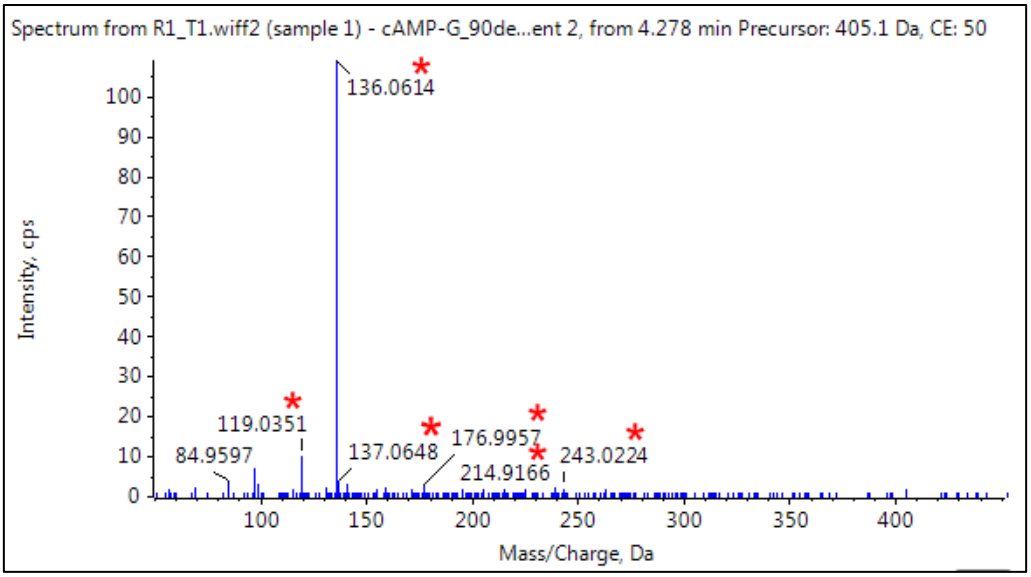

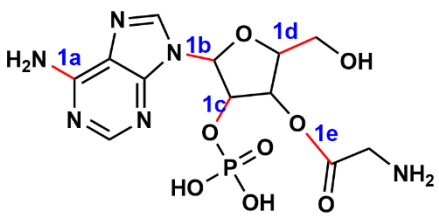

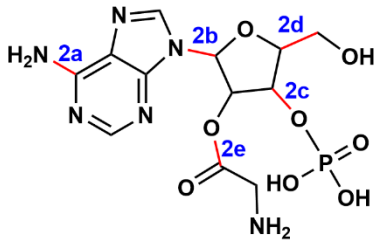

1a/2a
Chemical Formula: $C_5H_6N_5^+$
Exact Mass: 136.0618

1a,1b/2a,2b
Chemical Formula: $C_5H_3N_4$
Exact Mass: 119.0358

1e,1b/2e,2b
Chemical Formula: $C_5H_{11}O_7P$
Exact Mass: 214.0242

1d,1b/2d,2b
Chemical Formula: $C_6H_{14}NO_7P^{2+}$
Exact Mass: 243.0497

1c,1b/2c,2b
Chemical Formula: $C_7H_{14}NO_4^+$
Exact Mass: 176.0917

1a/2a
Chemical Formula: $C_5H_7N_5^{2+}$
Exact Mass: 137.0690

Figure S23d: TOF MS-MS spectra and fragmentation pattern of plausibly linked AMP-Gly [Precursor mass: 405.0919 (M+H)+] formed in the cAG reaction. Expected masses corresponding to the fragmented ions of AMP-Gly are observed in the spectra. Experimental data matches with the predicted fragmentation pattern of AMP-Gly sequence. The theoretically calculated masses and structures of molecules obtained post fragmentation were derived using ChemDraw Version 21.0.0. The fragmented bonds are highlighted in red. CE used was 50 eV. The red asterisk denotes the observed masses within 20 ppm error of the calculated fragmented mass.

^{31}P NMR overlay of AMP-aa observed in AWM ADM and AKM reactions at 130°C

a.

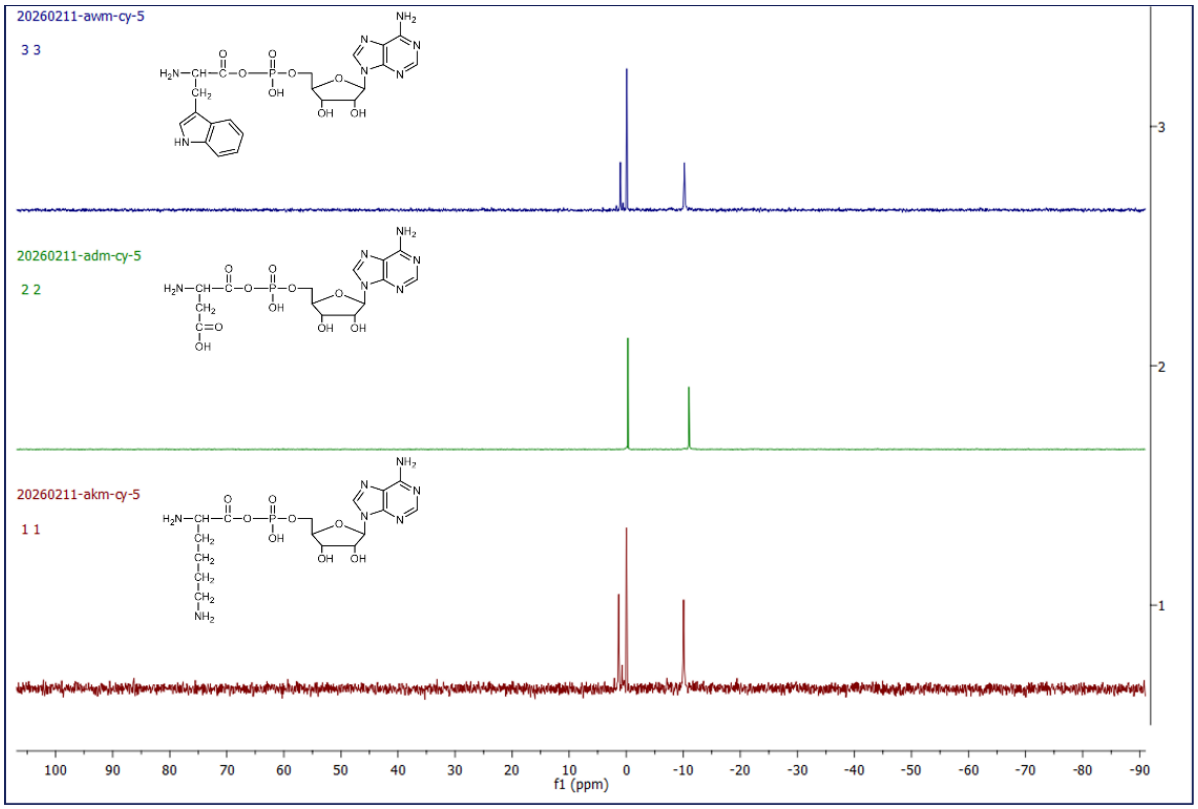

b.

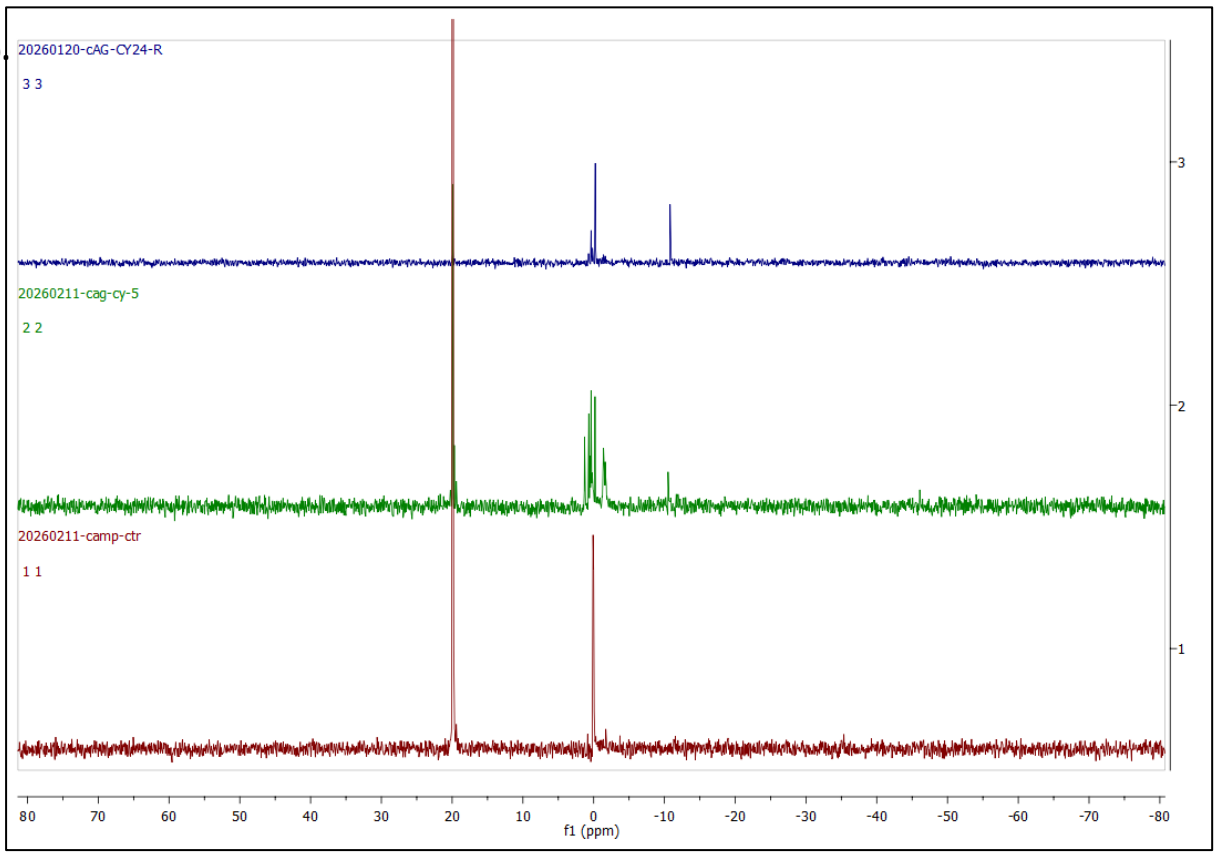

Fig 24 a demonstrates ^{31}P NMR analysis of AMP–Trp, AMP–Asp, and AMP–Lys, with intermediate peaks observed at −10 ppm during cycle 5 of the AWM 130, ADM 130, and AKM 130 reactions,

respectively. The upper blue trace is for AWM 130 cycle 5, the middle green trace is for ADM 130 cycle 5 and the lower maroon trace is for AKM 130 cycle 5. **Fig b** demonstrates ^{31}P NMR analysis of cAG 130 reactions depicting the peak at -11 ppm to be the peak for the intermediate formed in cycle 5 (green trace) and cycle 24 (blue trace) when compared with synthetic control.

TOF MS Spectra observed for reaction with (S)-3-Amino-4-methoxy-oxobutanoic acid

a.

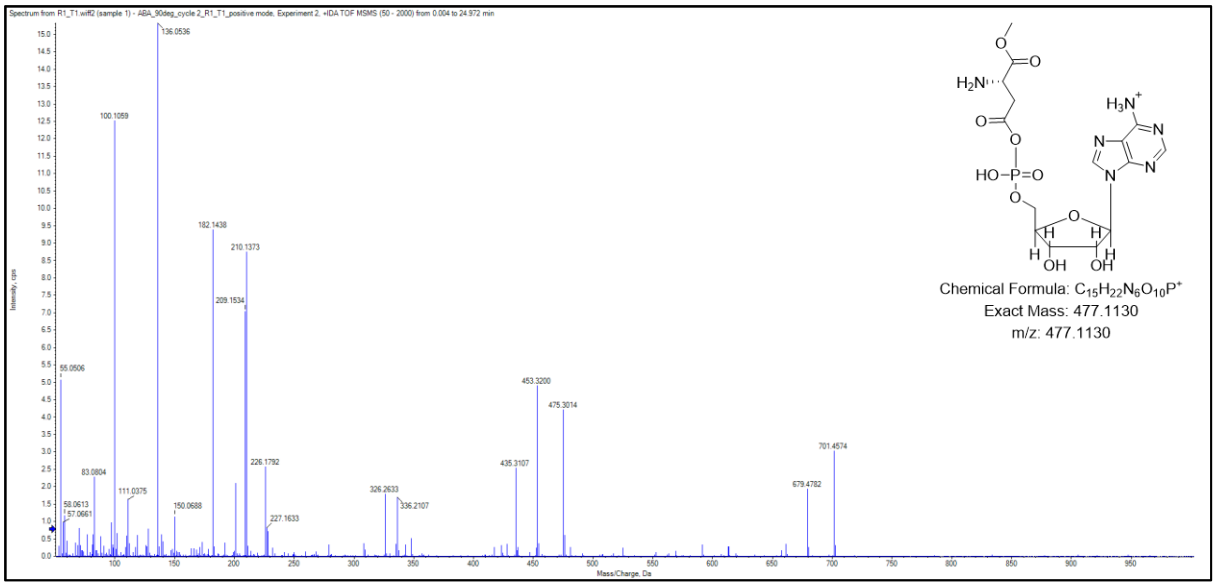

b.

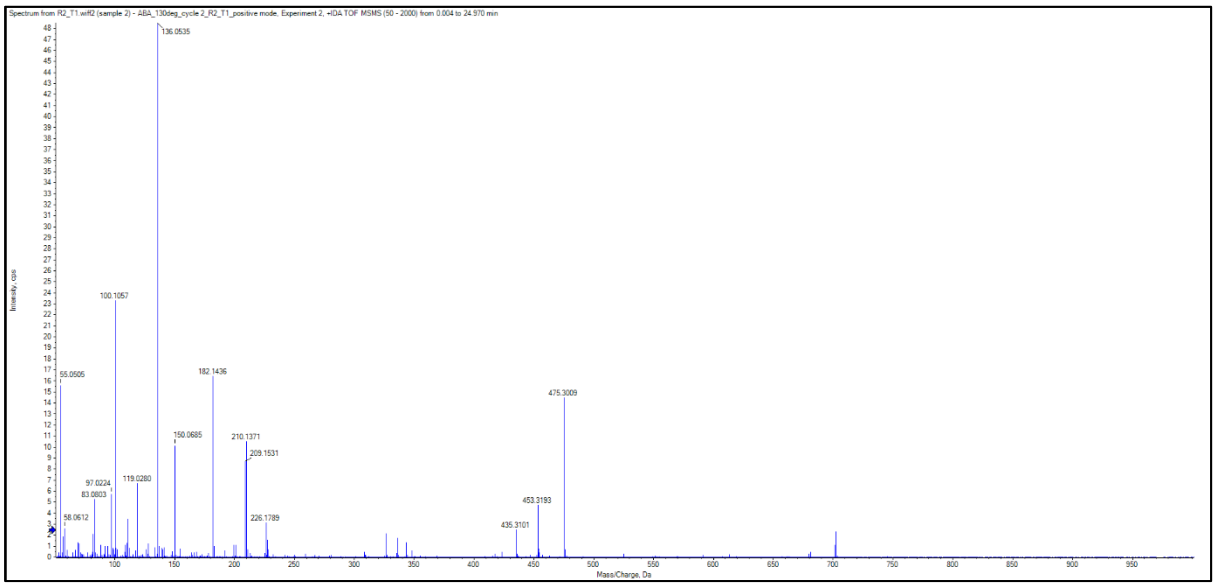

Figure S25: TOF MS-MS spectra observed for reaction with (S)-3-Amino-4-methoxy-oxobutanoic acid: Targeted mass for AMP-Asp-CH_3 (theoretical m/z has been shown in the inset) was not observed in the spectra for reactions containing (S)-3-Amino-4-methoxy-oxobutanoic acid in **a.** ABM 90°C and **b.** ABM 130°C.

TOF MS-MS spectra of AMP tetramer as obtained in AKM, ADM and AWM reactions

a.

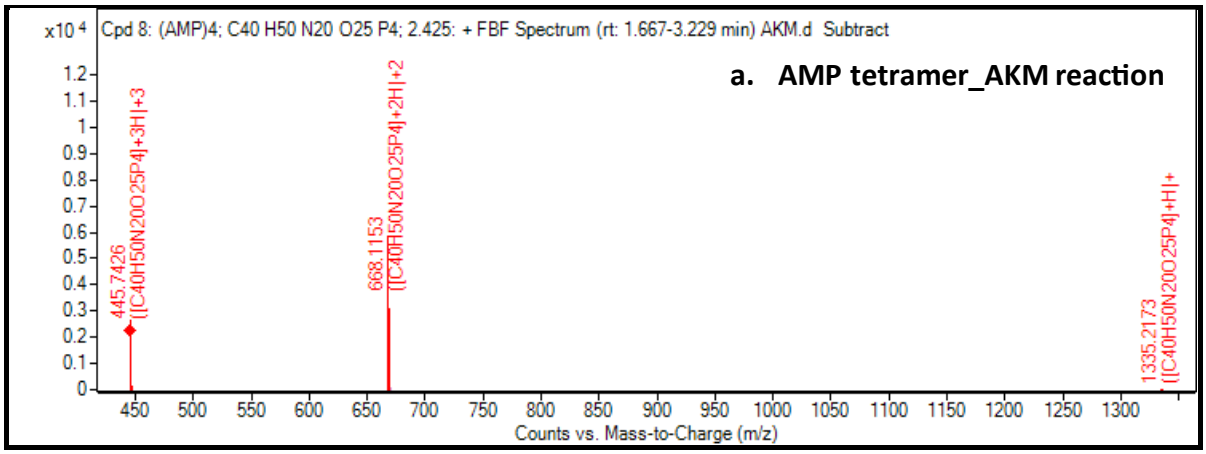

b.

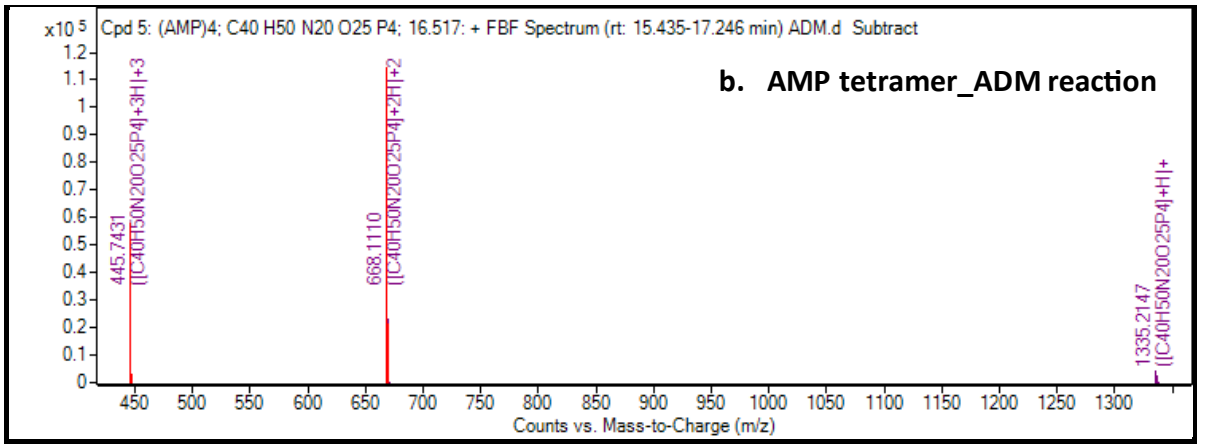

c.

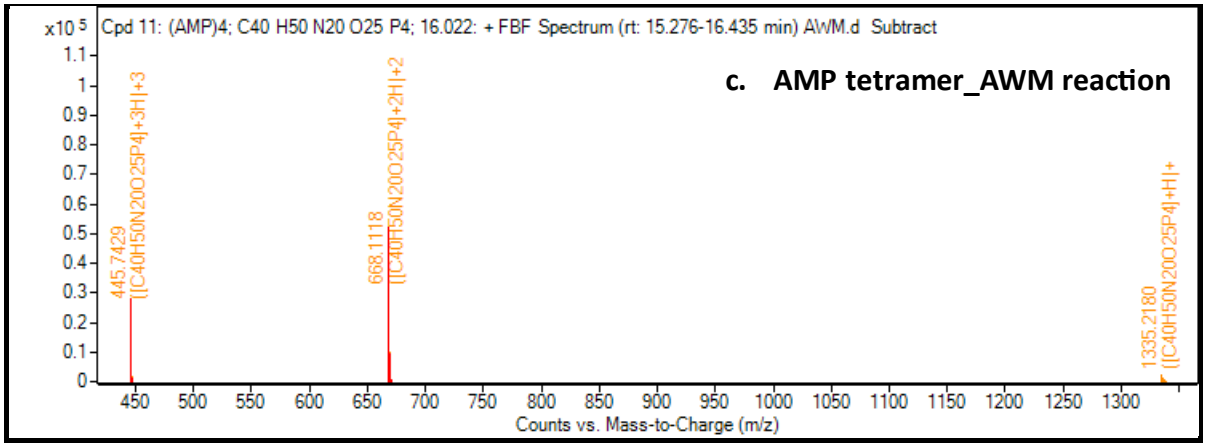

Figure S26: TOF MS-MS spectra of AMP tetramer observed: TOF MS-MS spectra of AMP tetramer $(AMP)_4$ formed in the AKM (**26a**), ADM (**26b**) and AWM (**26c**) reactions were found to be concurrent with the spectra of AMP tetramer control peak (**S12a**). X-axis denotes Intensity (cps) and Y axis denotes Counts vs Mass to charge (m/z ratio). Fragmentation pattern of AMP-AMP-AMP-AMP sequence was found to be within the 10-ppm error range across all the four reactions wrt the control peak [**Fig S12a**]. CE used was set at slope 2 with an offset of 5 and Fragmentor voltage 80 V.

TOF MS-MS spectra of the longest oligopeptide obtained in the AKM, AWM and ADM reactions

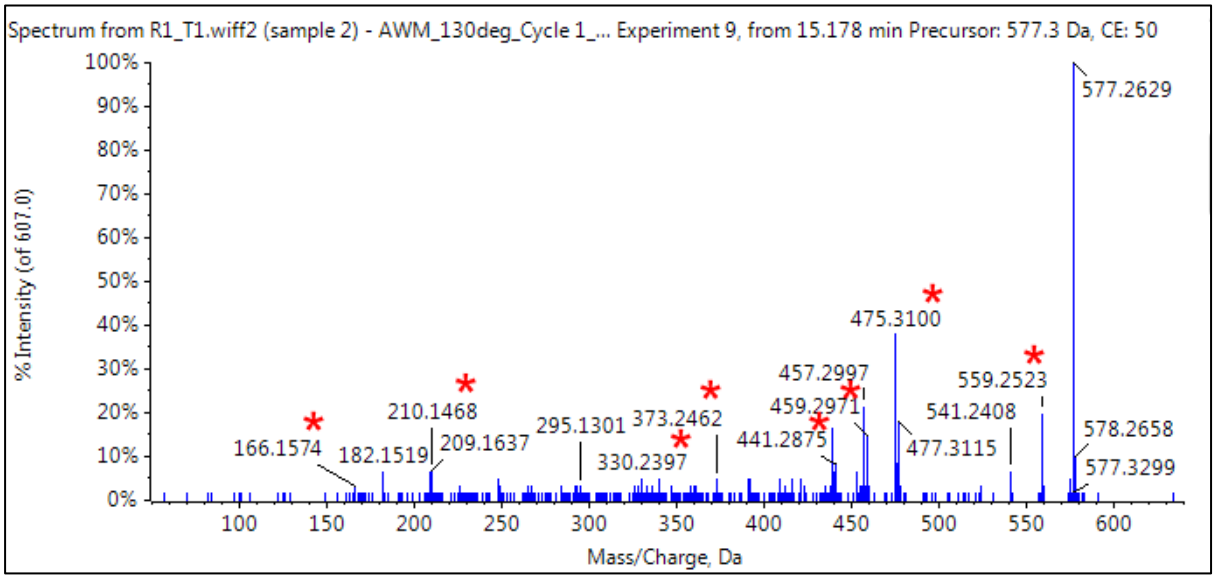

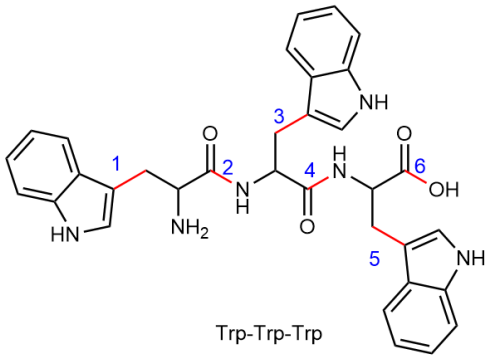

1, 3 & 5
Chemical Formula: $C_6H_{18}N_2O_{36}^+$
Exact Mass: 166.1285

1, 5 & 6
Chemical Formula: $C_{17}H_{22}N_4O_3$
Exact Mass: 330.1692

4
Chemical Formula: $C_{11}H_{17}N_2O_{25}^+$
Exact Mass: 209.1263

4
Chemical Formula: $C_{22}H_{21}N_4O_{22}^{\bullet}$
Exact Mass: 373.1665

5 & 6
Chemical Formula: $C_{25}H_{23}N_5O_{34}^{\bullet}$
Exact Mass: 441.1801

5
Chemical Formula: $C_{25}H_{25}N_5O_4^{\bullet+}$
Exact Mass: 459.1901

6
Chemical Formula: $C_{33}H_{31}N_6O_3^{\bullet}$
Exact Mass: 559.2458

Figure S27a: TOF MS-MS spectra and fragmentation pattern of Trp trimer [Precursor mass: 577.2558 (M+H)+] formed in the AWM. Expected masses corresponding to the fragmented ions of Trp trimer are observed in the spectra. Experimental data matches with the predicted fragmentation pattern of Trp-Trp-Trp sequence. The theoretically calculated masses and structures of molecules obtained post fragmentation were derived using ChemDraw Version 21.0.0. CE used was 50 eV. The fragmented bonds are highlighted in red. The red asterisk denotes the observed masses within 20 ppm error of the calculated fragmented mass.

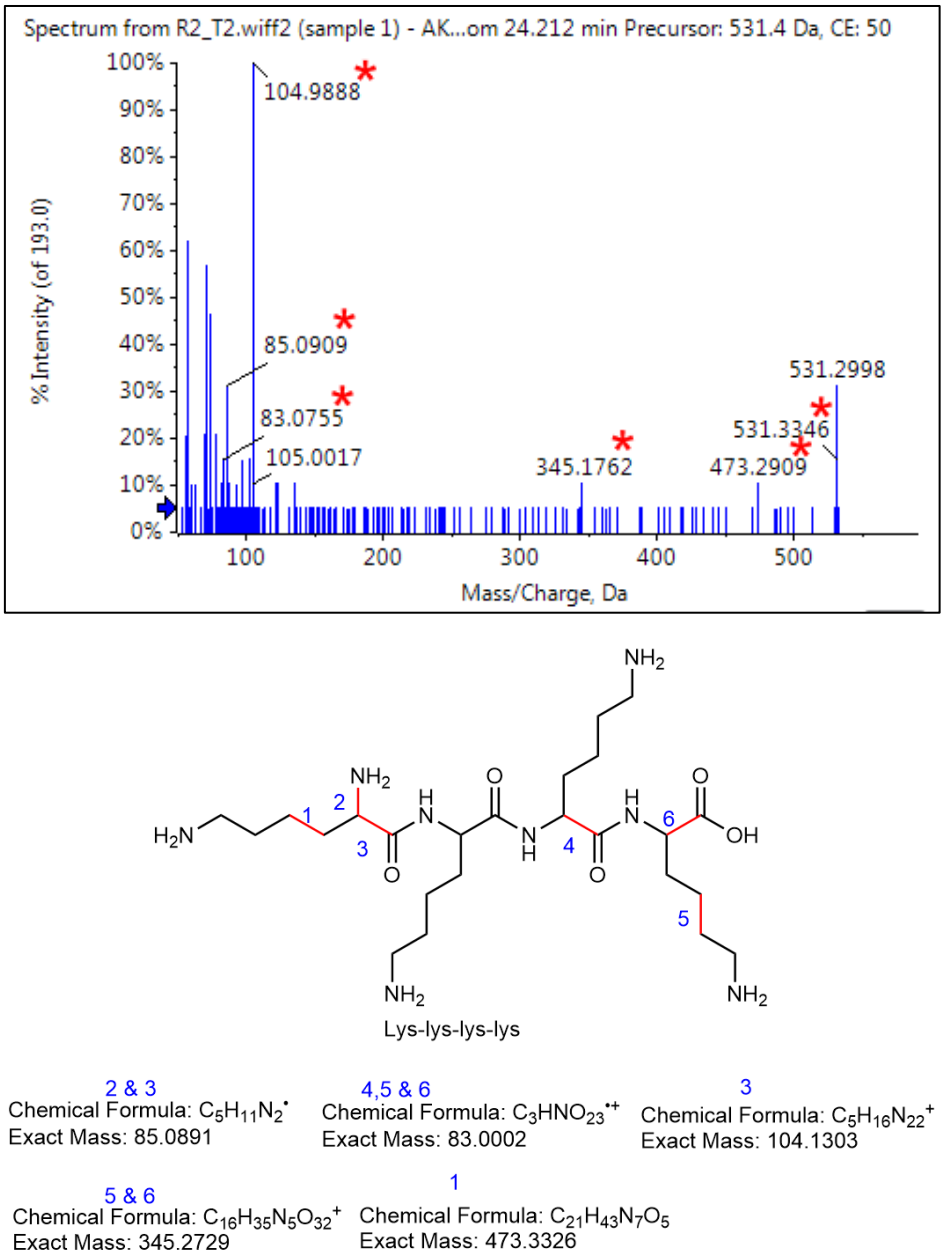

Figure S27b: TOF MS-MS spectra and fragmentation pattern of Lys tetramer [Precursor mass: 531.3977 (M+H)+] formed in the AKM. Expected masses corresponding to the fragmented ions of Lys tetramer are observed in the spectra. Experimental data matches with the predicted fragmentation pattern of Lys-Lys-Lys-Lys sequence. The theoretically calculated masses and structures of molecules obtained post fragmentation were derived using ChemDraw Version 21.0.0. The fragmented bonds are highlighted in red. CE used was 50 eV. The red asterisk denotes the observed masses within 20 ppm error of the calculated fragmented mass.

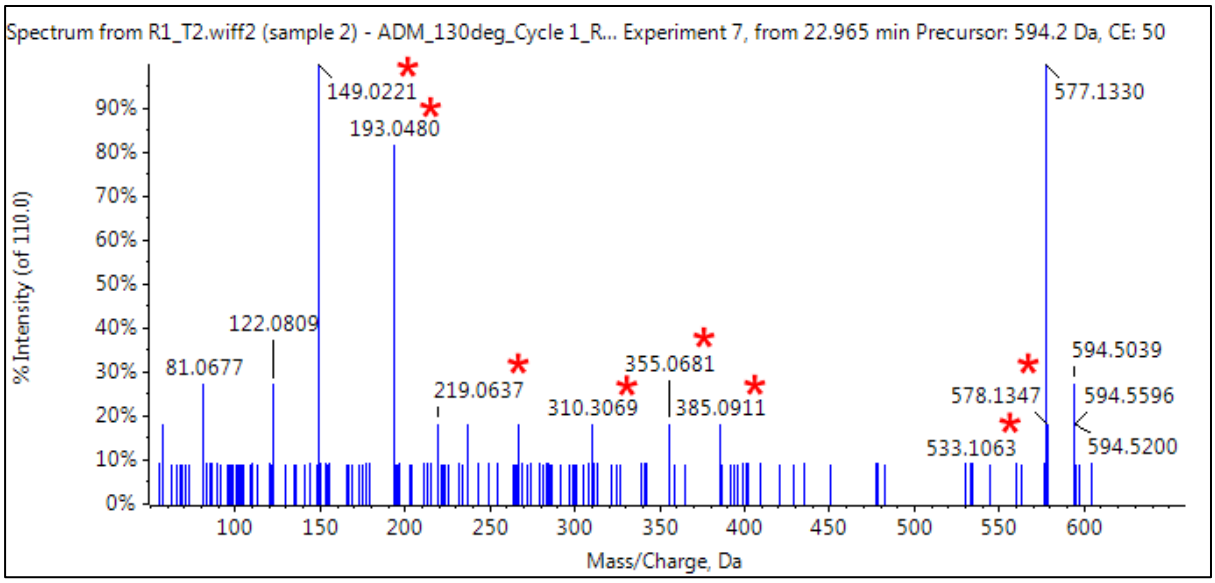

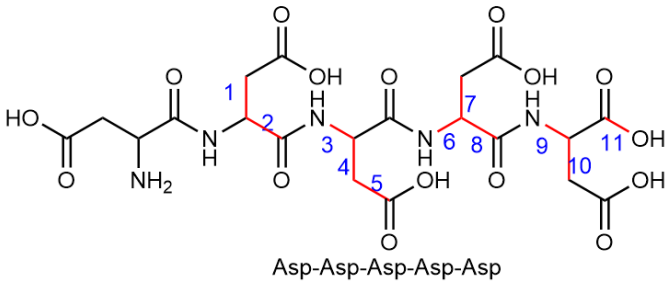

Asp-Asp-Asp-Asp-Asp

1 & 2
Chemical Formula: $C_5H_{13}N_2O_{33}^+$
Exact Mass: 149.0910

1, 4, 7 & 10
Chemical Formula: $C_{12}H_{13}N_5O_{84}^{\bullet 2+}$
Exact Mass: 355.0753

9
Chemical Formula: $C_4H_{10}O_{44}^+$
Exact Mass: 122.0557

4
Chemical Formula: $C_{18}H_{23}N_5O_{14}^{\bullet +}$
Exact Mass: 533.1236

8
Chemical Formula: $C_{14}H_{17}N_4O_{95}^{\bullet}$
Exact Mass: 385.0996

3, 7, 8 & 5
Chemical Formula: $C_4H_3NO_4^{\bullet 2+}$
Exact Mass: 81.0204

11
Chemical Formula: $C_{20}H_{28}N_5O_{15}^+$
Exact Mass: 578.1576

6 & 11
Chemical Formula: $C_8H_{13}NO_{62}^+$
Exact Mass: 219.0732

11
Chemical Formula: $C_{20}H_{27}N_5O_{15}$
Exact Mass: 577.1504

Figure S27c: TOF MS-MS spectra and fragmentation pattern of Asp pentamer [Precursor mass: 594.1977 (M+H)+] formed in the ADM. Expected masses corresponding to the fragmented ions of Lys tetramer are observed in the spectra. Experimental data matches with the predicted fragmentation pattern of Asp-Asp-Asp-Asp-Asp sequence. The theoretically calculated masses and structures of molecules obtained post fragmentation were derived using ChemDraw Version 21.0.0. CE used was 50 eV. The red asterisk denotes the observed masses within 20 ppm error of the calculated fragmented mass.

Relative abundance of peptides, oligonucleotides and intermediates formed

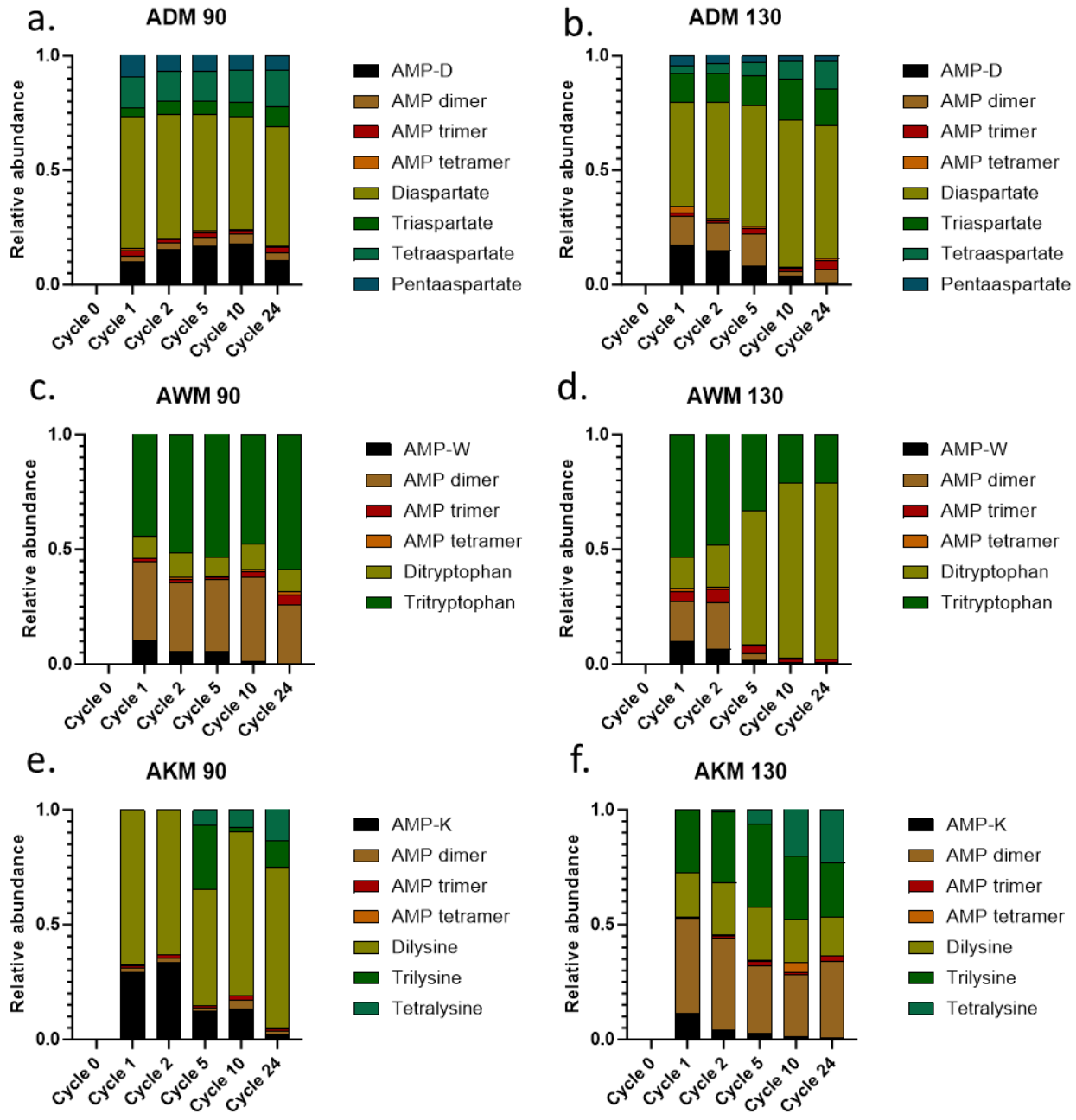

Figure S28: Relative abundance of peptides, oligonucleotides and intermediates formed under wet-dry cycling conditions at 90°C (**a.** ADM; **c.** AWM; **e.** AKM) and 130°C (**b.** ADM; **d.** AWM; **f.** AKM) of aspartic acid, tryptophan and lysine-based reactions through different cycles in the various reactions studied. The Y-axis indicates the relative abundancesdifferent length products formed in each reaction. The representation is based on the observation for N = 6 replicates.

TOF MS spectra of precursor masses found of complex compounds formed in the AGM, AKM, ADM and AWM reactions

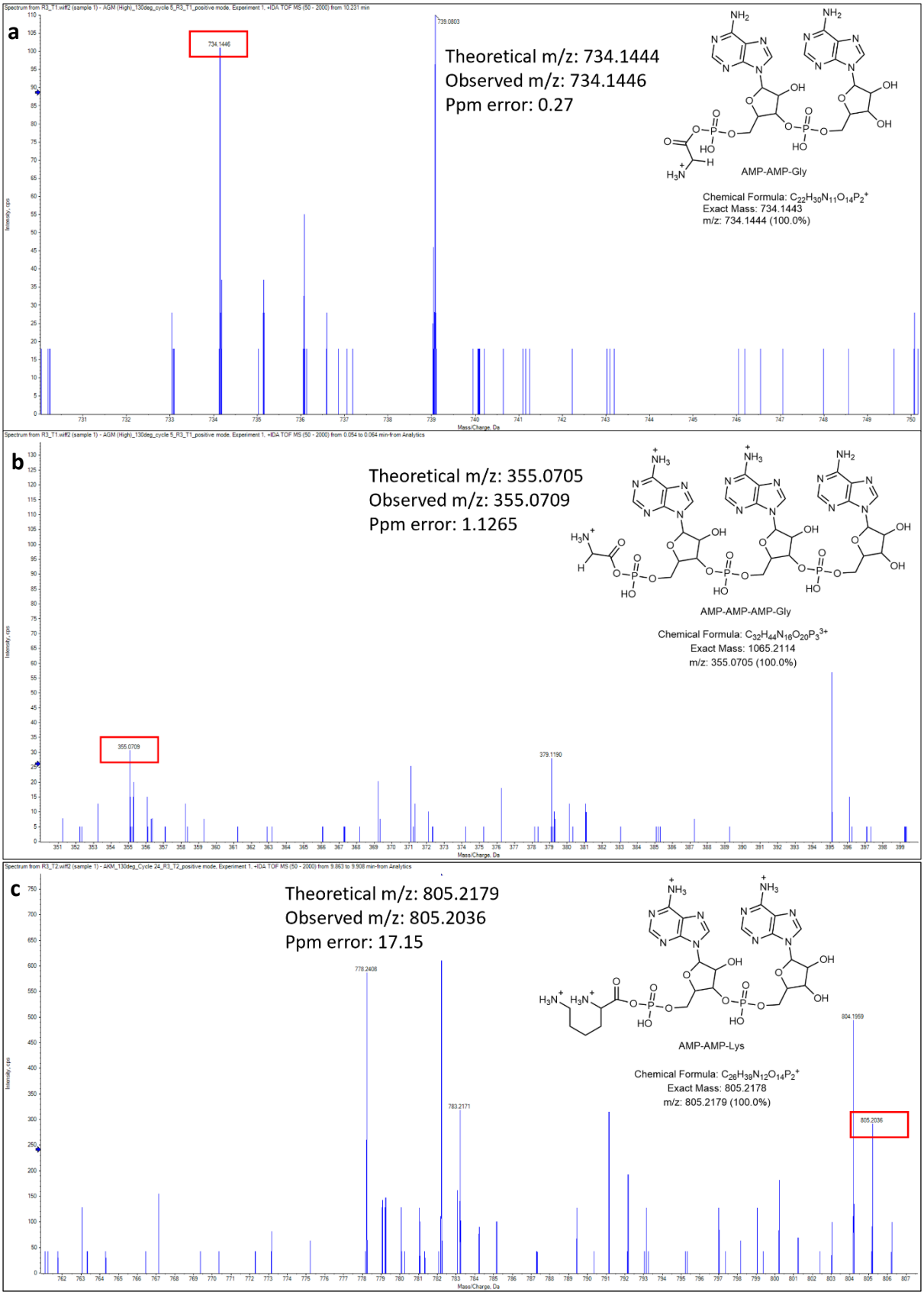

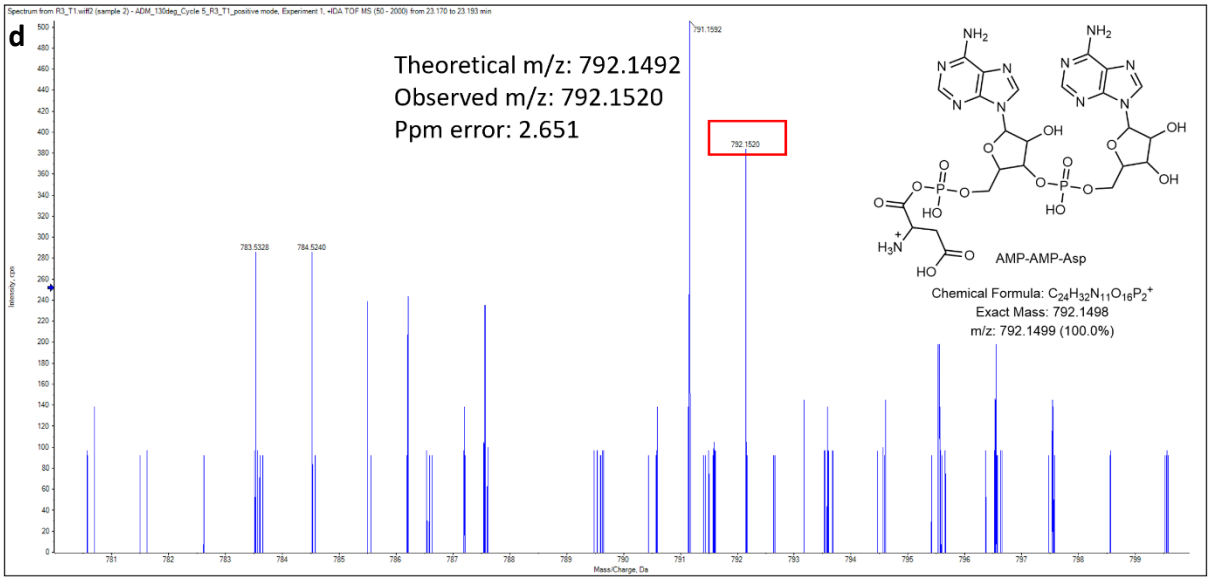
d
Theoretical m/z: 792.1492
Observed m/z: 792.1520
Ppm error: 2.651
AMP-AMP-Asp
Chemical Formula: $C_{24}H_{32}N_{11}O_{16}P_2^+$
Exact Mass: 792.1498
m/z: 792.1499 (100.0%)

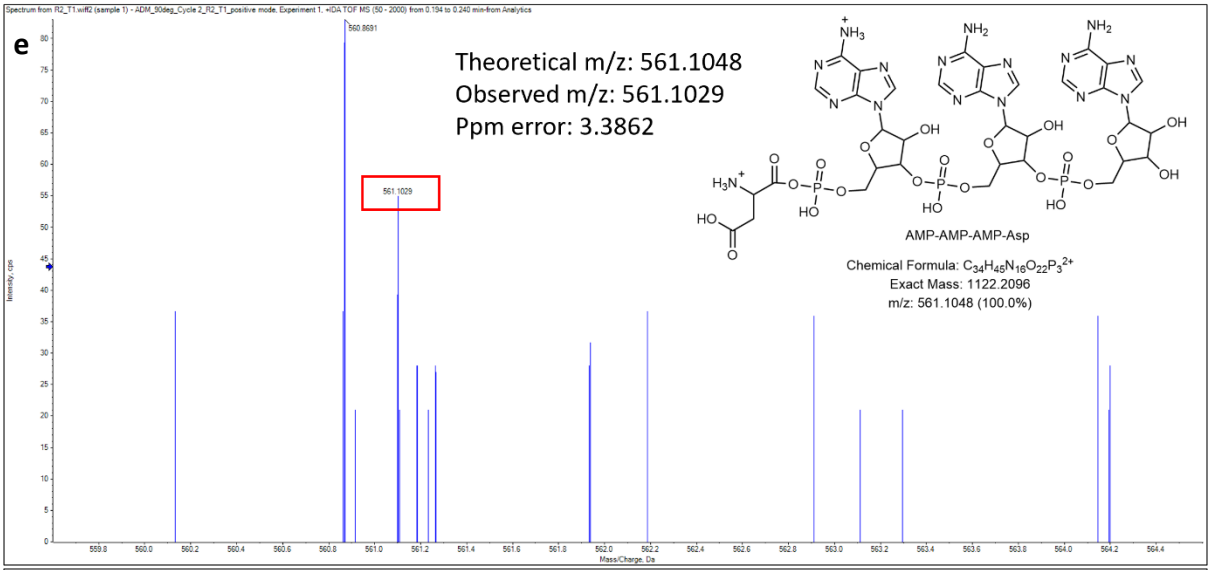
e
Theoretical m/z: 561.1048
Observed m/z: 561.1029
Ppm error: 3.3862
AMP-AMP-AMP-Asp
Chemical Formula: $C_{34}H_{45}N_{16}O_{22}P_3^{2+}$
Exact Mass: 1122.2096
m/z: 561.1048 (100.0%)

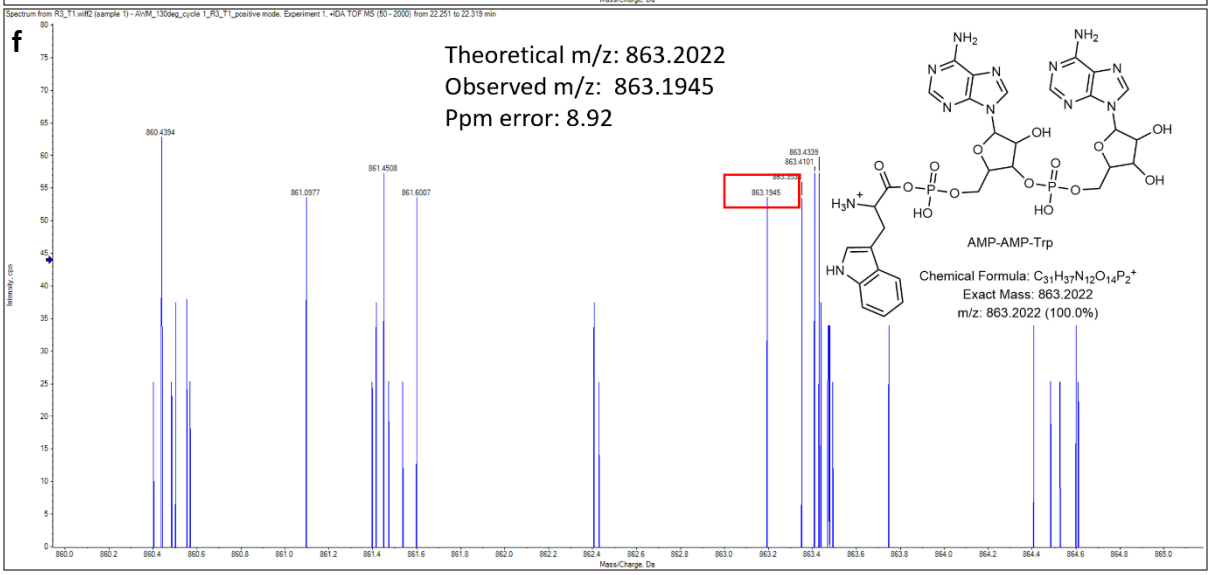
f
Theoretical m/z: 863.2022
Observed m/z: 863.1945
Ppm error: 8.92
AMP-AMP-Trp
Chemical Formula: $C_{31}H_{37}N_{12}O_{14}P_2^+$
Exact Mass: 863.2022
m/z: 863.2022 (100.0%)

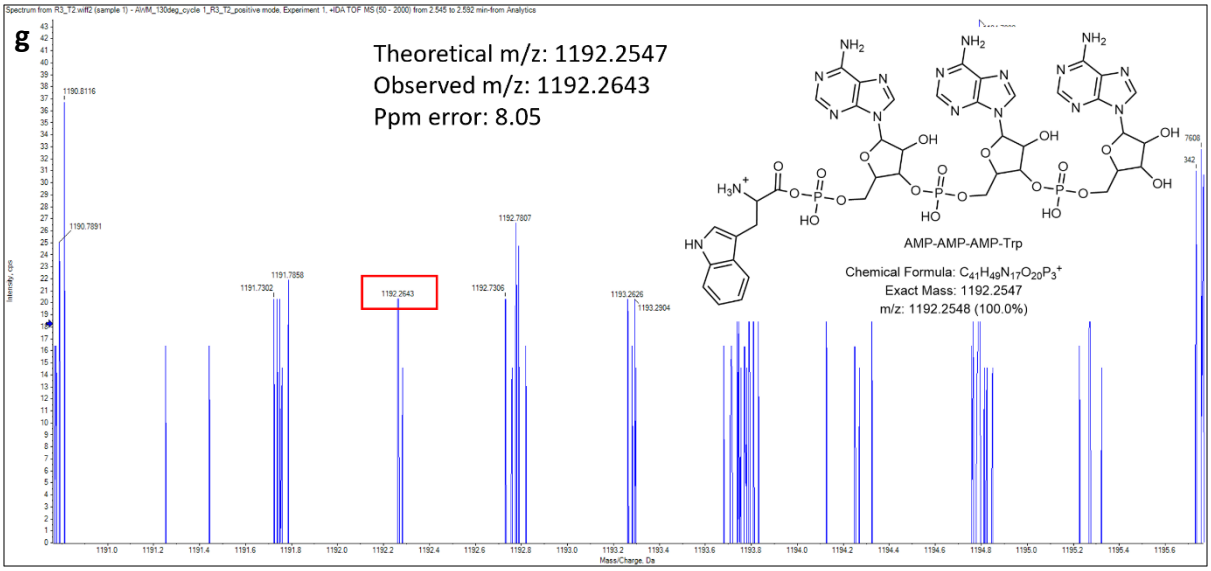

Figure S29: TOF MS spectra of various compounds formed in respective reactions detailed in materials and methods **a.** AMP-AMP-G, **b**. AMP-AMP-AMP-G, **c.** AMP-AMP-K, **d.** AMP-AMP-D, **e.** AMP-AMP-AMP-D, **f.** AMP-AMP-W, **g.** AMP-AMP-AMP-W. The red box has been used to highlight the masses observed for the molecules in the spectra. The insets details compound's chemical formula and m/z ratios as obtained from ChemDraw Version 21.0.0. The theoretical m/z, observed m/z and the ppm for each of the molecules has been calculated.

TOF-MS spectra observed in K 130, D 130 & W 130 reactions at 130°C in 24 hours cycle

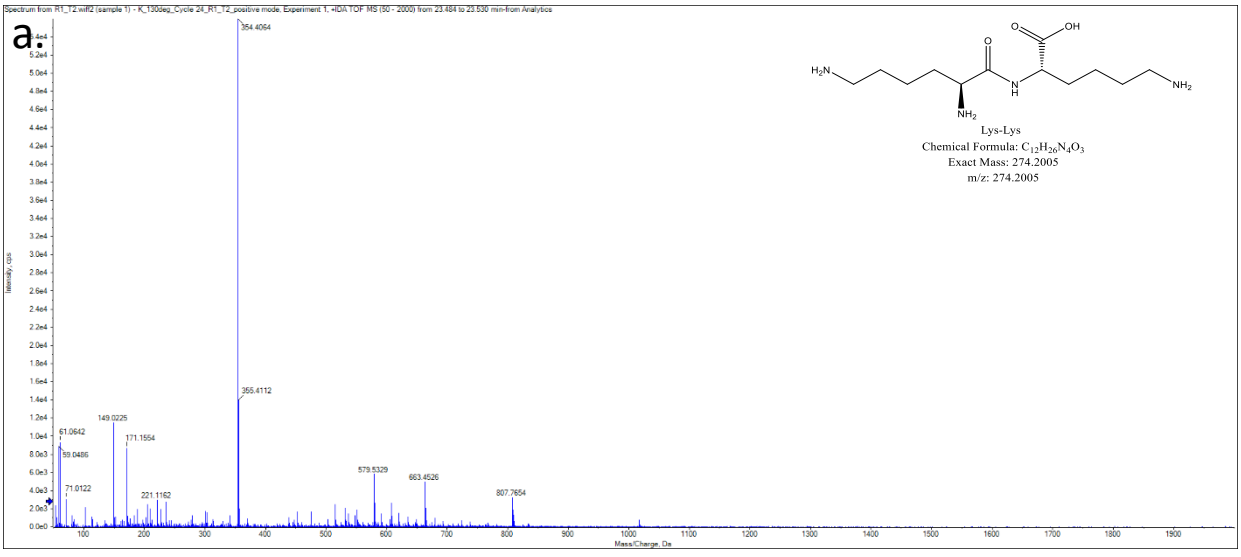

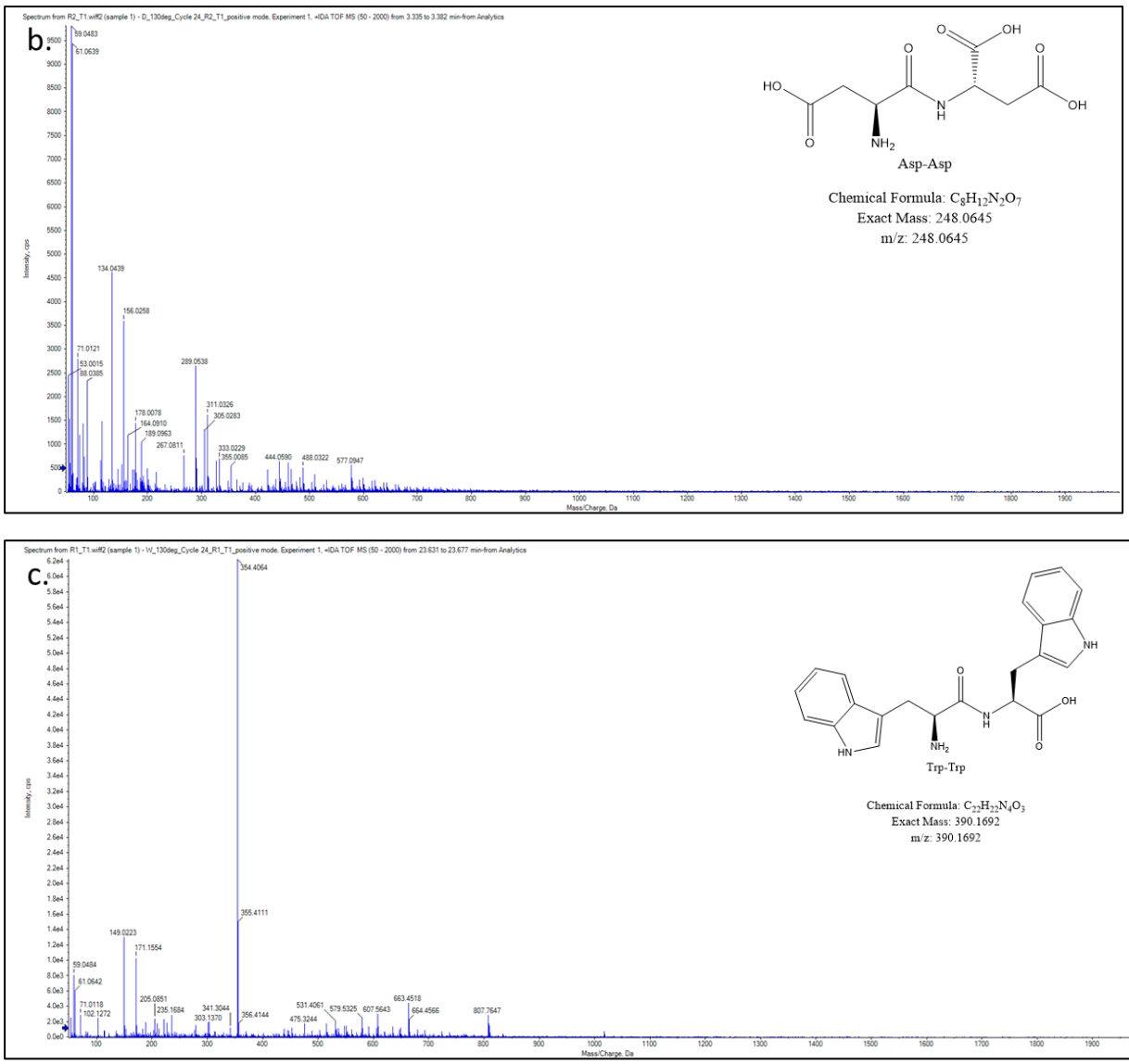

Figure S30: TOF MS spectra observed for AKM, ADM & AWM reactions at 130°C in 24 hours cycle: Targeted mass for Lys_2, Asp_2 and Trp_2 (theoretical m/z has been shown in the insets) onwards was not observed in the spectra for **a.** K 130°C, **b.** D 130°C and **c.** W 130°C reactions at 24 hours.

Supplementary Table S3: Studies that demonstrated the formation of oligopeptides.

Paper (Citation)	Reactants	pH Conditions	Temperature Conditions	Longest Peptide/Oligomer Observed
Peptide formation in the prebiotic era: thermal condensation of glycine. Lahav, White & Chang, Science 1978	Glycine + clay minerals (e.g., bentonite/kaolin) with water	Not specifically pH-buffered (likely near neutral/ambient)	Cyclic variations in temperature & hydration (thermal fluctuations, dehydration/rehydration)	Oligoglycine formation upto pentamer is seen;
Effects of pH and temperature on dimerization rate of glycine. — Sakata et al., Geochim. Cosmochim. Acta 2010	Glycine in aqueous solution	pH 3.1–10.9 explored; optimum around pH ~9.8 for dimerization	Temperatures 120–180 °C examined	Primarily glycine dimer (Gly_2) formation & DKP kinetics;
Ester Formation & Hydrolysis during Wet–Dry Cycles — Mamajanov et al., Macromolecules 2014	α-Hydroxy acids (e.g., malic acid) forming model oligoesters; peptide formation not primary focus	Not explicitly controlled; generally reactions studied across broad conditions	60–95 °C wet/dry cycling conditions (model polymer system)	Oligoesters observed; peptides not specifically quantified in this polymer context
Formation of oligopeptides in high yield… — Rodriguez-Garcia et al., Nat. Commun. 2015	Glycine (± other AAs: Ala, Asp, Glu, His, Lys, Pro, Thr, Val)	pH conditions varied highest yield at pH ~9.75; low yield at ~pH 6.1-7.5	90–130 °C dehydration/rehydration cycles; typical ~130 °C	~Gly_{12} in a soluble fraction
Ester-Mediated Amide Bond Formation… — Forsythe et al., Angew. Chem. 2015	Mixture of α-hydroxy acids (e.g., lactic acid) + amino acids (glycine/alanine) → depsipeptides	Unadjusted mixtures start acidic (~pH ~3); pH adjusted experiments at pH 7 with base	Wet phase ~65 °C (≈5.5 h), dry phase ~85 °C (≈18 h) across cycles	Depsipeptides with amino acids observed up to ~10 residues (mixed ester/amide)

Paper (Citation)	Reactants	pH Conditions	Temperature Conditions	Longest Peptide/Oligomer Observed
		re-added each cycle		containing lactic acid
Prebiotic condensation through wet–dry cycling… — Campbell et al., Nat. Commun. 2019	Glycine + salts (KCl, NaCl, OH^- mixtures; phosphate salts)	Implicit pH changes via salt composition; no fixed bulk pH but hydration phase aqueous	Hot phases at 100–120 °C (dry) with cool ~40 °C (wet, varying %RH)	Primarily to Gly_3 and up to Gly_{13} upon complete dehydration oligomers observed by HPLC after 10 cycles
Prebiotic environments with Mg^2 (ACS Earth & Space Chem. 2020)	This article examines peptide stability but also reports on condensation conditions (glycine + environment)	Typically near neutral to mildly basic (contextual studies)	Often 60–90 °C in Earth-simulated settings	Glycine condensation outcomes for small peptides (e.g., up to trimer/pentamer) depending on conditions
Proline Behavior in Model Prebiotic Peptides — ACS Earth & Space Chem. 2020	Mixtures of proline + glycine + alanine + valine in wet–dry cycling	Not strictly buffered; likely near neutral with reaction medium effect	Wet–dry cycles (specific T not in abstract; typical ~60–100 °C for such studies)	Linear oligomers including Pro and small cyclic species of dimeric or trimeric length was observed

Supplementary Table S4: Studies that demonstrated the formation of oligonucleotides.

Paper (Citation)	Reactants	pH Conditions	Temperature Conditions	Longest Oligomer Observed (Reported)
Sawai & Orgel, JACS 1975	Activated nucleotides + Zn^{2+} catalyst	Slightly acidic to neutral	Ambient temperature	Dimers and trimers
Kawamura & Ferris, JACS 1994	5′-Phosphorimidazolide of adenosine (ImpA) + Na^+-montmorillonite	Near-neutral to mildly basic (≈ pH 7–8)	Ambient to ~40 °C	Up to 7-mer oligoadenylates (quantified kinetically; longer chains not reported in this study)

Paper (Citation)	Reactants	pH Conditions	Temperature Conditions	Longest Oligomer Observed (Reported)
Prabahar, Cole & Ferris, JACS 1994	Activated adenosine phosphates + montmorillonite	Near-neutral	Ambient to moderate	Up to ~4-mer oligoadenylates, predominantly 3′,5′-linked
Crowe & Sutherland, ChemBioChem 2006	Cytidine nucleotides + cyanoacetylene	Mild aqueous conditions	Ambient to moderate	2′,3′-cyclic phosphate intermediates
Powner et al., ChemBioChem 2007	Cytosine nucleosides/nucleotides (photochemical synthesis)	Controlled lab pH	UV + low/moderate temperature	Monomers / activated nucleotides only (no oligomers reported)
Costanzo et al., PLOS ONE 2016	3′,5′-cyclic AMP	Slightly acidic to neutral	~80–90 °C (drying)	Tetramer (4-mer) only for cAMP
Costanzo et al., ChemBioChem 2017	3′,5′-cyclic CMP + protons / UV	Acidic	UV irradiation with moderate heating (~60–80 °C)	Dimers and trimers (2–3-mers)
Dagar et al., RNA 2020	2′,3′- and 3′,5′-cyclic nucleotides (cAMP, cCMP) ± salts/minerals	Broad; effective under mildly alkaline conditions	~40–90 °C; wet–dry cycling	Up to ~4mers, condition-dependent
Braun et al., Preprint 2024	Ribonucleotides + amino acids (as catalysts)	Alkaline (≈ pH 9–10)	Ambient temperature	Up to ~6–10-mers for cGMP (~3 for other cNMPs)

Supplementary references:

1. Mungi, C. V., & Rajamani, S. (2015). Characterization of RNA-like oligomers from lipid-assisted nonenzymatic synthesis: implications for origin of informational molecules on early earth. *Life*, *5*(1), 65-84.
2. Griesser, H., Tremmel, P., Kervio, E., Pfeffer, C., Steiner, U. E., & Richert, C. (2017). Ribonucleotides and RNA promote peptide chain growth. *Angewandte Chemie International Edition*, *56*(5), 1219-1223.
3. Armstrong, D. W., Seguin, R., Saburi, M., & Fendler, J. H. (1979). Synthesis of amino acyl adenylates using the tert-butoxycarbonyl protecting group. *Journal of Molecular Evolution*, *13*, 103-113.

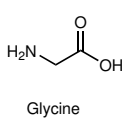

Glycine

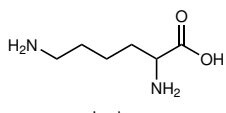

Lysine

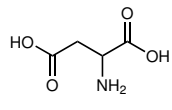

Aspartic acid

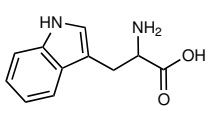

Tryptophan

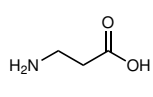

ß-alanine,

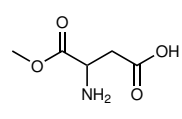

(S)-3-Amino-4-methoxy-4-oxobutanoic acid

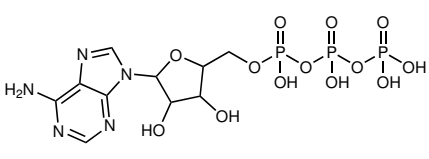

Adenosine 5' triphosphate

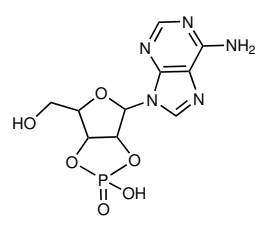

Adenosine 2',3'-cyclic phosphate

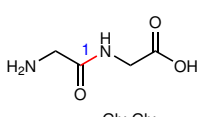

Gly-Gly

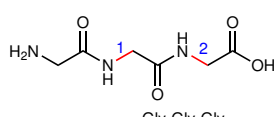

Gly-Gly-Gly

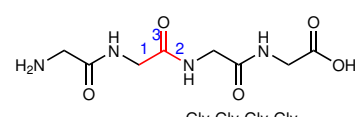

Gly-Gly-Gly-Gly

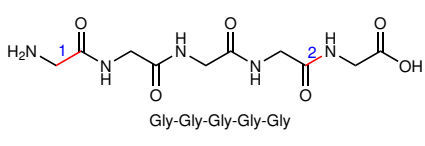

Gly-Gly-Gly-Gly-Gly

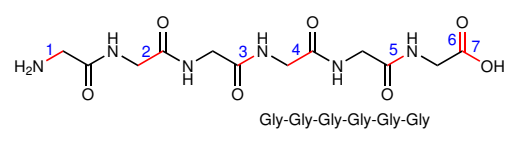

Gly-Gly-Gly-Gly-Gly-Gly

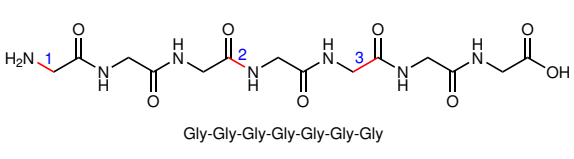

Gly-Gly-Gly-Gly-Gly-Gly-Gly

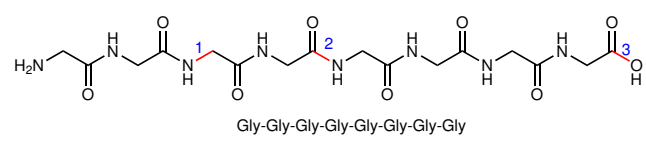

Gly-Gly-Gly-Gly-Gly-Gly-Gly-Gly

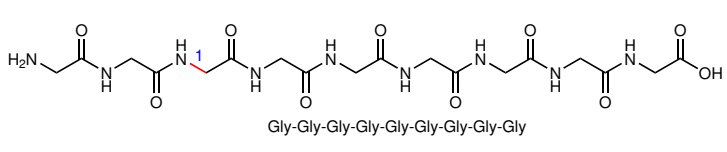

Gly-Gly-Gly-Gly-Gly-Gly-Gly-Gly-Gly

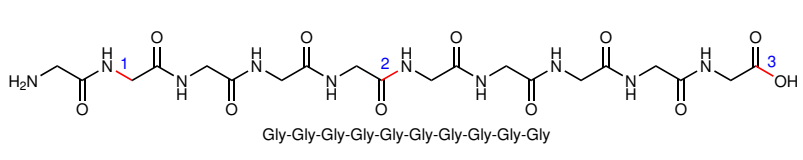

Gly-Gly-Gly-Gly-Gly-Gly-Gly-Gly-Gly-Gly

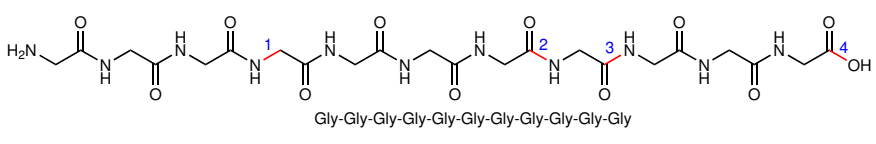

Gly-Gly-Gly-Gly-Gly-Gly-Gly-Gly-Gly-Gly-Gly

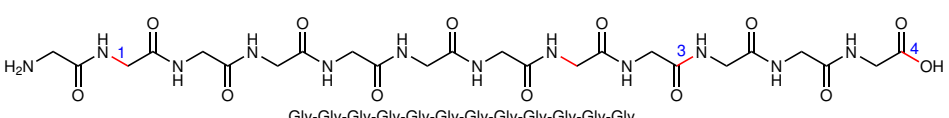

Gly-Gly-Gly-Gly-Gly-Gly-Gly-Gly-Gly-Gly-Gly-Gly

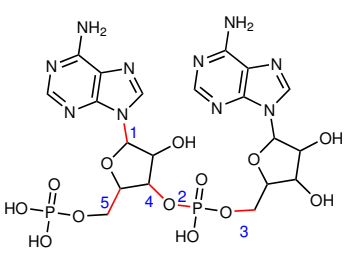

AMP-AMP

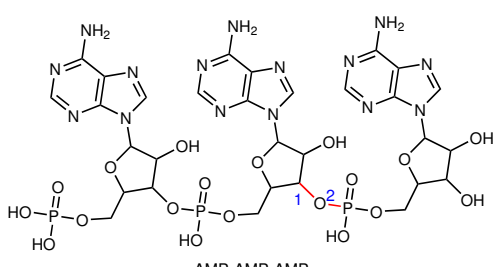

AMP-AMP-AMP

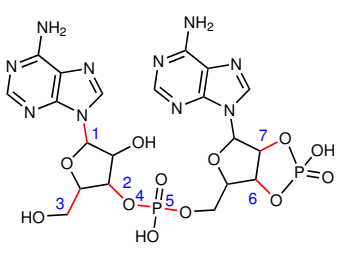

AMP-cAMP

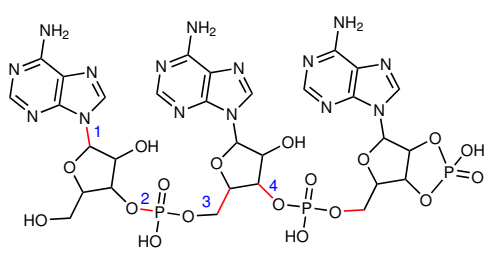

AMP-AMP-cAMP

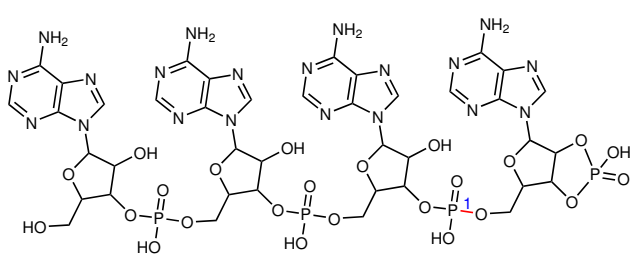

AMP-AMP-AMP-cAMP

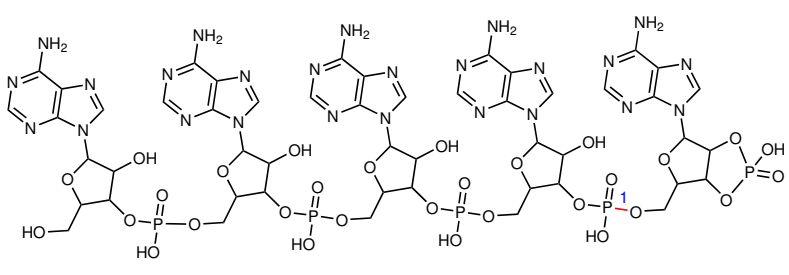

AMP-AMP-AMP-AMP-cAMP

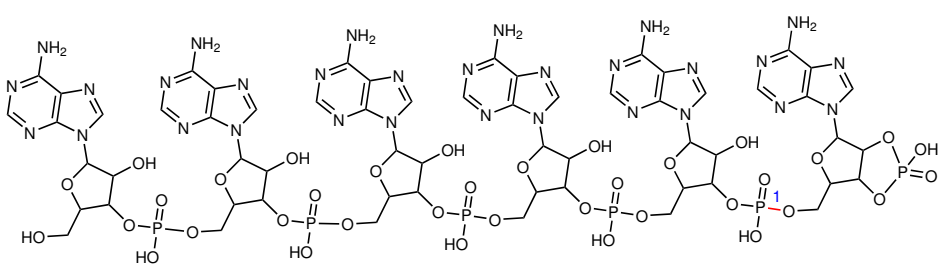

AMP-AMP-AMP-AMP-AMP-cAMP

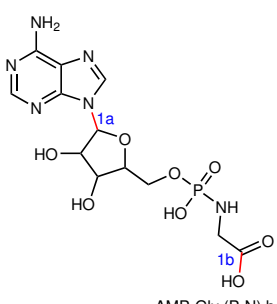

AMP-Gly (P-N) bond

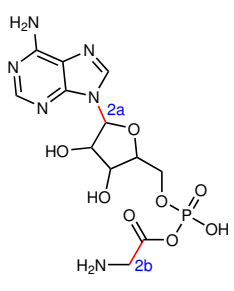

AMP-Gly (P-O-C)

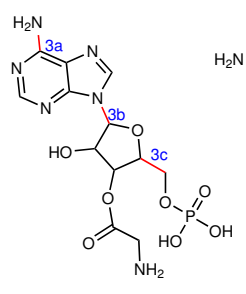

AMP-Gly (CO-OR)

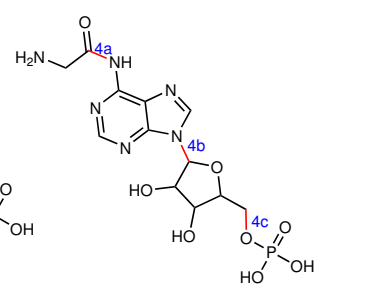

AMP-Gly (CO-NH)

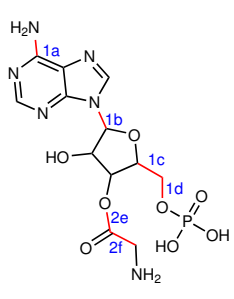

3' AMP-Gly (CO-OR)

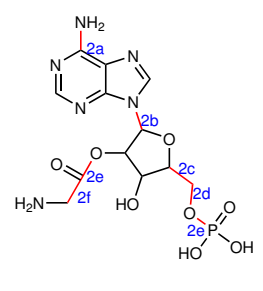

2'AMP-Gly (CO-OR)

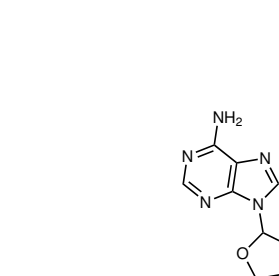

AMP-Lys

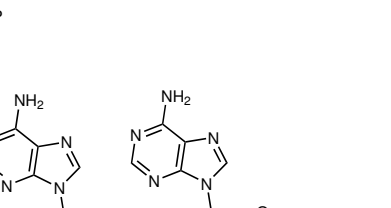

AMP-Asp

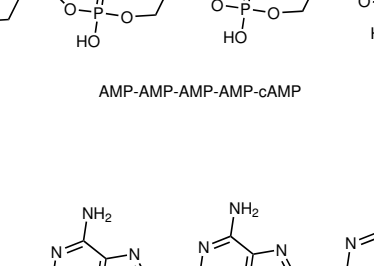

AMP-Trp

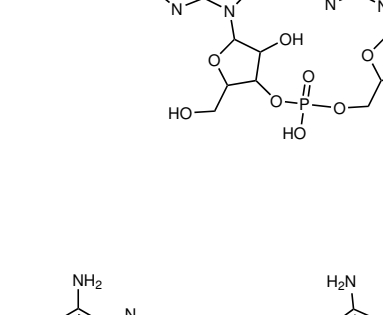

Trp-Trp-Trp

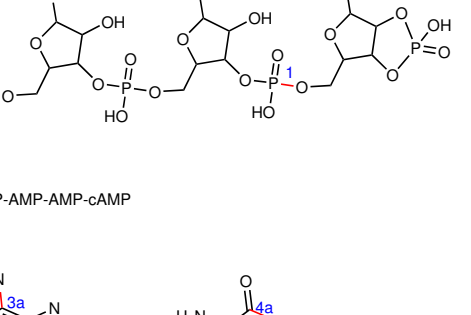

Lys-lys-lys-lys

Asp-Asp-Asp-Asp-Asp

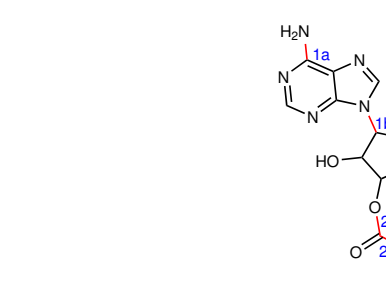

AMP-AMP-Gly

AMP-AMP-AMP-Gly

AMP-AMP-Lys

AMP-AMP-AMP-Lys

AMP-AMP-Asp

AMP-AMP-AMP-Asp

AMP-AMP-Trp

AMP-AMP-AMP-Trp